AWARD NUMBER: W81XWH-15-1-0551

TITLE:
The impact of PERK on post-traumatic tauopathy in Alzheimer's disease

PRINCIPAL INVESTIGATOR: Jose Francisco Abisambra, PhD

CONTRACTING ORGANIZATION: University of Kentucky
Lexington, KY 40526

REPORT DATE: October 2017

TYPE OF REPORT: Annual

PREPARED FOR: U.S. Army Medical Research and Materiel Command
Fort Detrick, Maryland 21702-5012

REPORT DOCUMENTATION PAGE

Form Approved
OMB No. 0704-0188

1. REPORT DATE	2. REPORT TYPE	3. DATES COVERED
October 2017	Annual	15Sep16 - 14Sep17

4. TITLE AND SUBTITLE

The impact of PERK on post-traumatic tauopathy in Alzheimer's disease

5a. CONTRACT NUMBER

5b. GRANT NUMBER
W81XWH-15-1-0551

5c. PROGRAM ELEMENT NUMBER

6. AUTHOR(S)

Jose F. Abisambra, PhD

E-Mail: joe.abisambra@uky.edu

5d. PROJECT NUMBER

5e. TASK NUMBER

5f. WORK UNIT NUMBER

7. PERFORMING ORGANIZATION NAME(S) AND ADDRESS(ES)

University of Kentucky
800 S Limestone Street
Lexington, KY 40536-0230

8. PERFORMING ORGANIZATION REPORT NUMBER

9. SPONSORING / MONITORING AGENCY NAME(S) AND ADDRESS(ES)

U.S. Army Medical Research and Materiel Command
Fort Detrick, Maryland 21702-5012

10. SPONSOR/MONITOR'S ACRONYM(S)

11. SPONSOR/MONITOR'S REPORT NUMBER(S)

12. DISTRIBUTION / AVAILABILITY STATEMENT

Approved for Public Release; Distribution Unlimited

13. SUPPLEMENTARY NOTES

14. ABSTRACT

Risk for AD is one of the most imminent threats to military personnel sustaining TBI. A major challenge in the field of TBI/AD research is elucidation of the molecular mechanisms linking TBI with tau pathogenesis that is associated with AD. This critical and urgently needed information will identify novel therapeutic targets that will benefit both military personnel and civilian population. Our recent data indicate that TBI induces sustained and dramatic endoplasmic reticulum stress, and that there is a pathological relationship between AD tau species and the ER stress sensor PERK. For the first time, we directly address the role PERK activity as a molecular mediator of TBI-induced *tau pathology* and provide unique understanding of the association between TBI and AD. Therapies aiming to interrupt the molecular events identified by this work will be monitored using our imaging technology known as MEMRI. Finally, our work will test the therapeutic value of inhibiting the PERK, which is involved in several neurodegenerative disorders.

15. SUBJECT TERMS

PERK, tauopathies, Alzheimer's disease, traumatic brain injury, controlled cortical impact

16. SECURITY CLASSIFICATION OF:			17. LIMITATION OF ABSTRACT	18. NUMBER OF PAGES	19a. NAME OF RESPONSIBLE PERSON
a. REPORT	b. ABSTRACT	c. THIS PAGE			USAMRMC
Unclassified	Unclassified	Unclassified	Unclassified	74	19b. TELEPHONE NUMBER *(include area code)*

Table of Contents

Page

INTRODUCTION:
Risk for AD is one of the most imminent threats to military personnel sustaining TBI. A major challenge in the field of TBI/AD research is elucidation of the molecular mechanisms linking TBI with tau pathogenesis that is associated with AD. This critical and urgently needed information will identify novel therapeutic targets that will benefit both military personnel and civilian population. Our recent data indicate that TBI induces sustained and dramatic endoplasmic reticulum stress, and that there is a pathological relationship between AD tau species and the ER stress sensor PERK. In this proposal we aim to establish for the first time the impact of PERK on tau-mediated pathogenesis as a means by which TBI confers risk for AD. We will directly address the role PERK activity as a molecular mediator of TBI-induced *tau pathology* and provide unique understanding of the association between TBI and AD. This understanding is *critical and urgent* to develop novel therapeutic strategies. This work will further develop a novel imaging *technology* (ME-MRI) that will identify a course of functional deficits in the brain after injury and monitor the magnitude at which these phenomena persist over time. This technology will set a standard of disease course imaging from TBI to AD onset. Therapies aiming to interrupt the molecular events identified by this work will be monitored using our imaging technology. Finally, our work will test the therapeutic value of inhibiting the PERK, which is involved in several neurodegenerative disorders.

KEYWORDS:
PERK, tau, tauopathies, Alzheimer's disease, traumatic brain injury, controlled cortical impact, neurodegeneration, UPR, ER stress

ACCOMPLISHMENTS:

What were the major goals of this project?

Annual Report 1

AIM1

1. Establish mouse colony and validate anatomical and volumetric damage caused by CCI
    - *ACURO protocol approved*
    - *Wild type mouse colony established*
    - *Training to perform controlled cortical impact injury model complete*
2. Determine immunohistochemical changes in the brain (and complete all MRI analyses)
    - *Early timeline of PERK activation complete*
    - *Established which cell types show PERK activation*
3. Complete imaging analyses (this work is completed continuously as injuries are performed)

AIM2

4. Establish mouse cohorts for Aim 2
    - *rTg4510 transgenic colony established*
    - *PERK conditional knockout colony backcrossed: estimated completion date: Dec 2016*
5. Perform genetic manipulation to activate and inhibit PERK function
    - *Establishment of the PERK conditional knockout colony: estimated completion date: Dec 2016*
    - *Viral particles are continuously produced by the University of Kentucky Viral Core*
6. Perform chemical manipulations to modulate PERK
    - *Currently underway*
7. Complete data collections and analysis for all functional measurements (this work is completed continuously as injuries are performed)
    - *Cohort 1 of chemical PERK inhibition following injury data collection – MEMRI, behavioral analyses (novel object recognition, radial arm water maze)*
    - *Data collection for first four cohorts of PERK inhibition following injury (MEMRI, behavior, immunohistochemical staining) will be complete by January 1, 2017*
8. Complete data analysis (this work is completed continuously as injuries are performed)

Annual Report 2

Aim 2

1. Chemical inhibition of PERK in WT and rTg4510 mice after injury.
    - Multiple cohorts of animals that underwent severe injury and were treated with GSK2606414 for 30 days after injury

- IHC and MRI performed
- IHC analyzed (almost complete)
- MRI – T1 MEMRI analyzed
- MRI – T2 volumetric analyses completed

What was accomplished under these goals?

Annual Report 1

During the first year, we established the mouse colony for experiments in Aim 1 and Aim 2, we successfully performed controlled cortical impact injuries to characterize PERK activation following traumatic brain injury, we performed MEMRI and analyses following injury, we established an early timeline of PERK activation using immunohistochemical staining, and we began to investigate the impact of chemical PERK inhibition following injury on cognition and neuronal function. We are continuing to complete the goals as cohorts of mice become available.

Using immunohistochemical analyses in our initial studies with a small sample group, we found that PERK is more robustly activated in the contralateral hemisphere compared to the ipsilateral hemisphere at early time points following injury. However, upon completion of the larger cohorts, we identified that early activation is even between contralateral and ipsilateral brain hemispheres (Fig. 1 and 2). We also found that PERK is active in neurons (Fig. 3) but not glia as evidenced by counterstains with GFAP (Fig. 4) or Iba1 (Fig. 5). Using the non-radioactive, puromycin-based translation assay we also determined, in a small cohort, that protein synthesis is increased at early time points in neurons (Fig. 6).

Injuries were performed as previously described in the proposal; briefly, mice were anesthetized using isoflurane and a midline incision was made. A 3mm in diameter craniotomy was performed and mice were injured using the electromagnetic CCI machine at 1.5m/s with 500msec dwell time. A cranioplasty was then placed over the injury site and the incision was sutured. Mouse brains were collected following cardiac perfusion using 0.9% saline. Tissue was sectioned using a microtome and stained using immunofluorescence.

Annual Report 2

The *major activities* in the last year were to complete Sub-Aim 2.2b (chemical inhibition) and establish the mice for Sub-Aim 2.2a (genetic inhibition). These two objectives were met. The *specific objectives* were to perform severe CCI (3.5m/s, 1.0mm depth, 500ms dwell) on WT and rTg4510 animals. One hour post-injury animals were treated with PERK inhibitor GSK2606414 (414) or vehicle (VEH). Treatment continued once a day for 30 days. Outcome measurements taken for these animals included immunohistochemical analyses

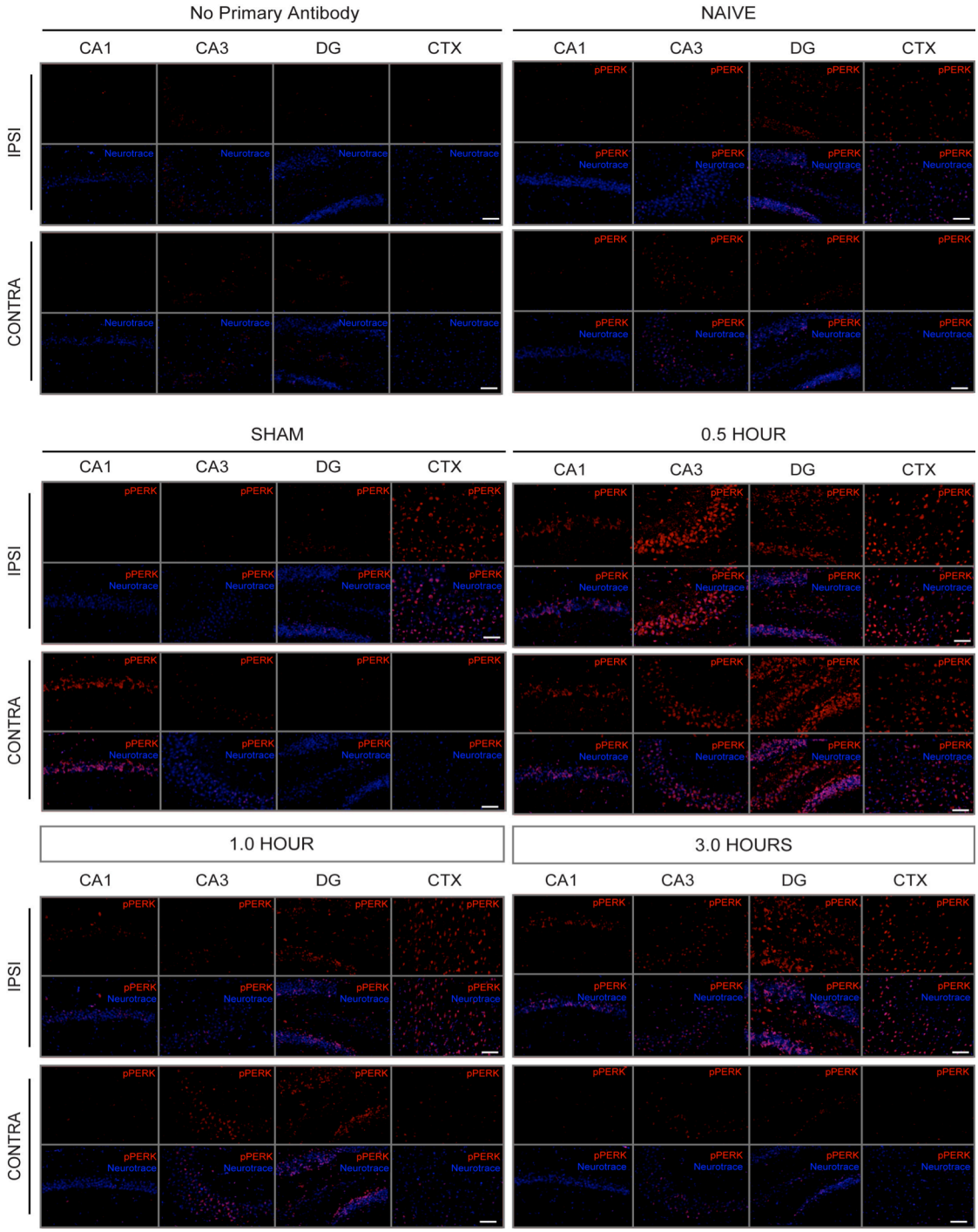

Fig. 1: Early time course of PERK activation after injury. pPERK levels (red) were measured in CA1, CA3, dentate gyrus, and cortex of ipsilateral and contralateral hemispheres to the injury.

of specific stains, behavioral analyses, and MRI analyses.

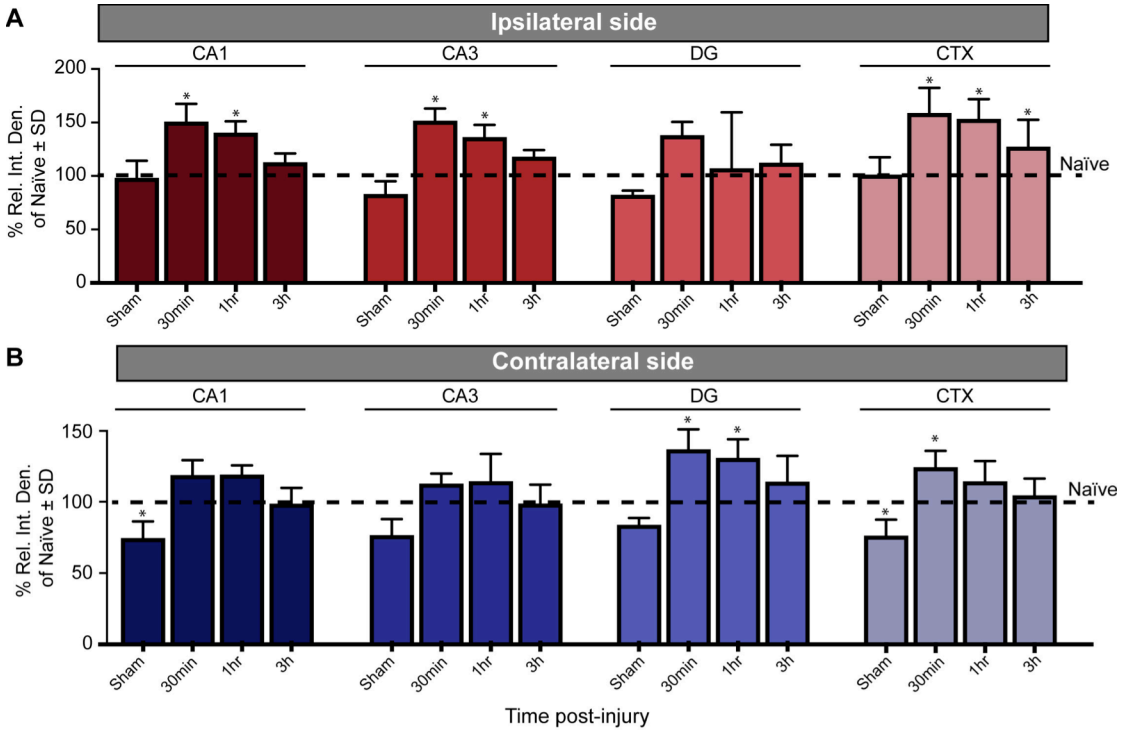

Fig. 2: Quantification of pPERK levels in different brain regions (CA1, CA3, dentate gyrus, and cortex) in ipsilateral (A) and contralateral (B) hemispheres to the injury. pPERK levels were measured at 30, 60, and 360 min after injury.

Our *significant findings* are that PERK inhibition for 30 days effectively reduced PERK activity, as expected. Moreover, its downstream target, eIF2a, was also inhibited. Surprisingly, we found that GFAP, a marker of astrocytic activation, was also decreased when treated with the PERK inhibitor. These data are surprising because, as we determined in year 1, PERK is only activated in neurons; co-localization immunofluorescence with cell markers demonstrated that PERK did not co-localize with GFAP or Iba1 (Fig. 3-5). Therefore, we suspect the compound inhibits neuronal signaling to astrocytes. This hypothesis would uncover a remarkable mechanism of intercellular communication, which we plan to explore in the future. Finally, and also counter to our expectations, brain volume was decreased in animals that were injured and treated with the compound. These data suggest that treatment with the inhibitor is either not beneficial (promotes atrophy post-injury) or reduces inflammation. The former would lead us to establish an earlier time course because we anticipate that inhibiting self-regulation of the UPR for 30d might improve short-term outcomes, which would be shadowed by overall tissue damage. The latter would suggest that 414 has an anti-inflammatory effect, but whether this is beneficial remains to be determined.

Other significant findings are the extent of PERK activation after injury. Per our recent preliminary results, PERK activity is increased throughout the 30d of treatment. Therefore, we are hesitant to genetically activate PERK since inactive PERK levels will be depleted. However, as mentioned above, we are on

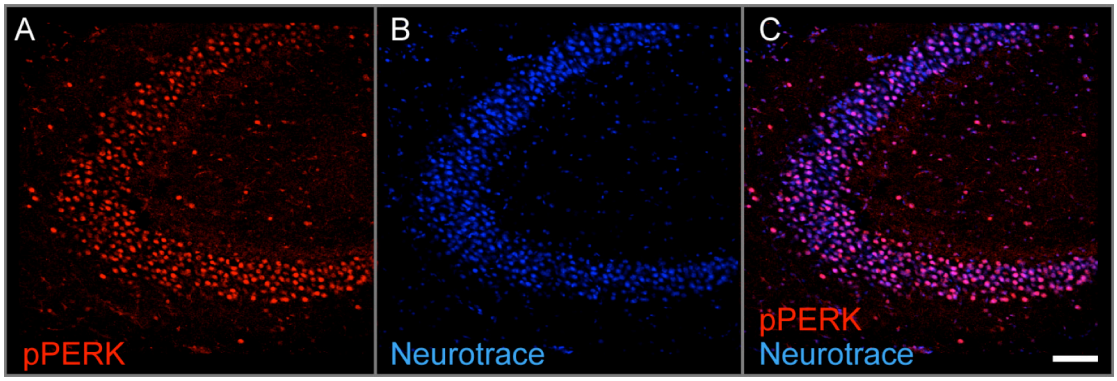

Fig. 3: pPERK signal coincides in cells positive for the neuronal marker neurotrace. Mice were injured using CCI. Brains were prepared for immunohistochemistry staining of pPERK and neurotrace 3h post injury.

our way to genetically inhibit PERK with the ongoing establishment of PERK-cKO mice.

Key to these findings is the context of functional outcomes. We had proposed to perform cognitive testing (Fig. 7-8). Preliminary data showed that the injured mice did not display the cognitive defects that should have been evident. This puzzling and *negative* result was disconcerting. Similar to other concurrent studies in my lab, mice did not display cognitive alterations as predicted in the literature. We attribute this phenomenon to the construction of a new research building in a lot adjacent to where our animals are housed. We believe construction of the foundations have affected the mice such that they all perform poorly in the novel object recognition test. We are currently evaluating which would be the best strategy to obtain functional data and truly test if the compound offers benefits. Nonetheless, since the end of construction of the foundation

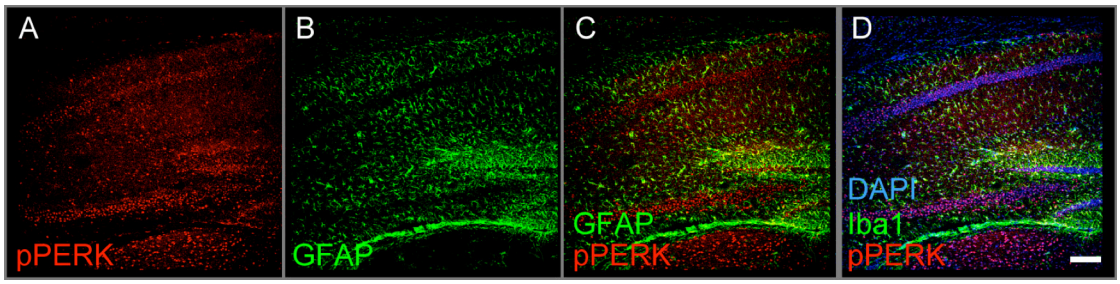

Fig. 4: pPERK signal is not in GFAP-positive cells. Mice were injured using CCI. Brains were prepared for immunohistochemistry staining of pPERK and neurotrace 3h post injury.

coincides with the establishment of our new colony of PERK knockout mice, we should have cohorts born in a more “stress free” environment. We will be able to test changes in cognitive outcomes with this new cohort.

What opportunities for training and professional development has the project provided?

This project provided the opportunity to become proficient in the CCI

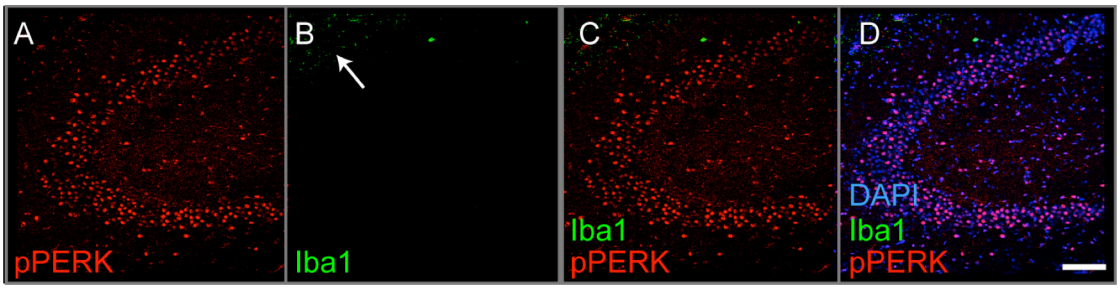

Fig. 5: pPERK signal is not in Iba1-positive cells. Mice were injured using CCI. Brains were prepared for immunohistochemistry staining of pPERK and neurotrace 3h post injury. Arrowhead posints at Iba1-positive stain

models of injury. One graduate student successfully completed training from Dr. Kathryn Saatman, and she is working to train other students in our lab. She recently passed her qualifying exam to become a PhD candidate. This award has also allowed for professional development in allowing us to expand our knowledge and relationships with TBI experts at the National Neurotrauma Society annual meeting and the Alzheimer's Association International Conference. One graduate student presented her work at both meetings and received feedback to aid in data interpretation. These meetings greatly expanded our knowledge on the most recent findings in the TBI field.

This project also enhanced professional development in my lab by allowing work to be presented at the Alzheimer's Disease/Parkinson's Disease (ADPD) 2017 and Alzheimer's Association International Conference 2017. One graduate student presented her work at both meetings and received feedback to aid in data interpretation. These meetings greatly expanded our knowledge on the most recent findings in the TBI field. Importantly, I presented these data in the 2017 IPR Briefing where I obtained critical insight from Roderick Corriveau (NIH/NINDS), Heather Snyder (Alzheimer's Association), and Eliezer Masliah (NIA). Unfortunately, I was unable to physically attend the briefing; however, our impactful results encouraged a conversation via email and during ADPD 2017.

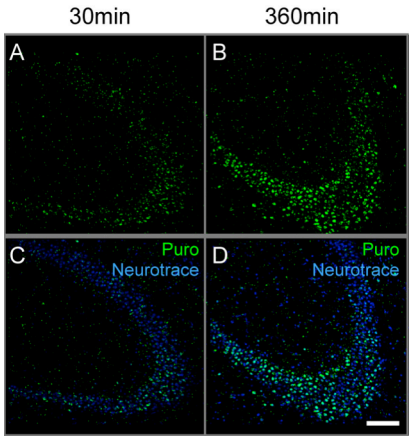

Fig. 6: Puromycinylated proteins are increased in hippocampus after CCI. Puromycin tags newly-synthesized proteins. Brains were prepared for staining 3h post-injury. Puromycin was injected 30min before harvesting brains.

How were the results disseminated to communities of interest?

Annual Report 1

Data collected from this project was presented at two separate meetings and in department level seminars. We anticipate submitting a manuscript within the next few weeks to the Journal of Neurotrauma. Two other manuscripts are in preparation; they focus on the impact of PERK inhibition on

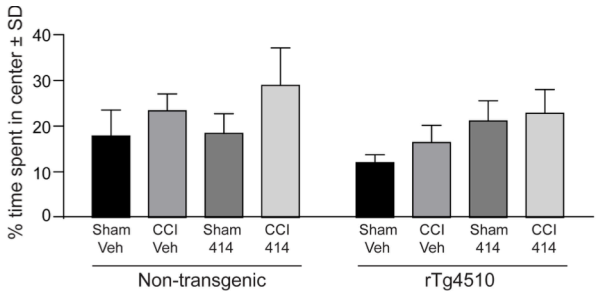

Fig. 7: Open field preliminary results. Sham: not injured. CCI: controlled cortical injury. Veh: vehicle treated. 414: PERK inhibitor GSK2606414. rTg4510: tau transgenic mice.

tau and the impact of genetic PERK inhibition on adverse consequences of TBI.

Annual Report 2

Data collected from this project was presented at two separate meetings and has been presented at multiple department level seminars. The anticipated manuscript submission was delayed after further critical analysis of the data collected. We currently have the manuscript drafted and a preparing to send it to the Journal of Neurotrauma by the end of the month.

What do you plan to do during the next reporting period to accomplish the goals?

During the next reporting period, we plan to complete all Major Tasks. Considering that construction may have hampered our ability to measure changes in cognition, we might have to alter our plan in order to realistically complete the aims by the time of the end of the project. We will begin surgeries on the PERK knockout mice that will be injected with tau virus. We also plan to begin injuries in wildtype animals to parse out the most beneficial window of treatment following injury.

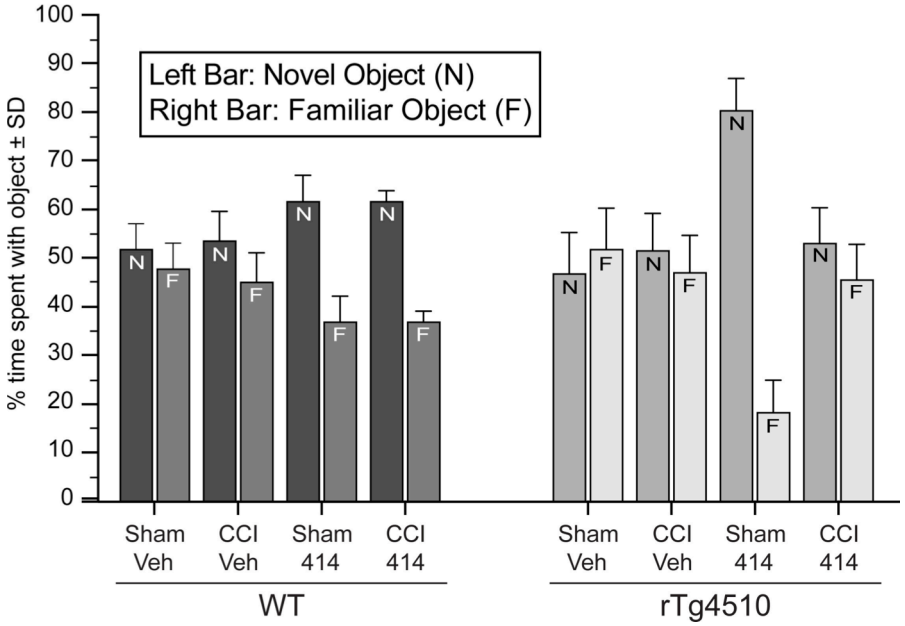

Fig. 8: Novel Object Recognition preliminary results. Sham: not injured. CCI: controlled cortical injury. Veh: vehicle treated. 414: PERK inhibitor GSK2606414. rTg4510: tau transgenic mice.

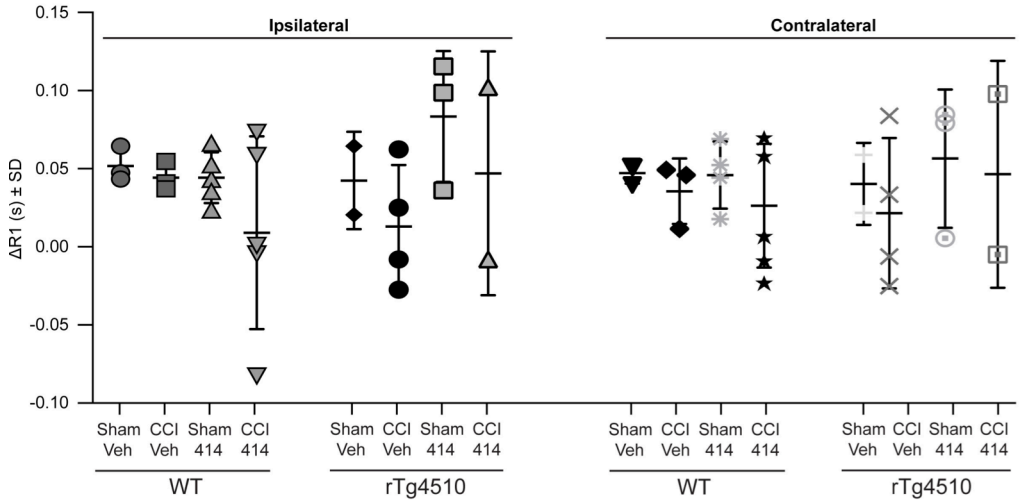

Fig. 9: MEMRI results. MEMRI did not detect defects in hippocampus as a result of injury.

IMPACT:

What was the impact on the development of the principal discipline(s) of the project?

Annual Report 1

Although we are continuously working on increasing our sample size for each experimental group, our preliminary data suggest that CCI impacts neurons before glia. This is a surprising finding considering that previous data in related fields of neurodegeneration suggest that inflammatory responses would be more prevalent. In addition, it would explain why cognition is the first faculty to be impacted immediately after injury. Another surprising finding is that injured neurons are the primary cell type that increases protein synthesis. The identity of these proteins is unknown, and we hypothesize that they correspond to stress proteins, such as PERK, and not synaptic proteins.

Annual Report 2

So far our data have shown that PERK plays a critical role in the brain's response to head injury, but the exact nature of that role is still unclear. Shortly after injury and despite acute PERK activation, the hippocampus increases protein synthesis as evidenced by puromycin uptake (Fig. 6). Moreover, PERK inhibition for 30d decreases brain volume. These are two examples of unexpected results that make the next steps of this project fascinating.

From a technical perspective, progress in the project has enhanced our ability to use MRI for careful and accurate measurement of brain volume (Fig. 10). These approaches are now being used in other animal studies in my lab. I have also been approach by another local lab after presenting our volumetric MRI results for a collaborative project. In addition, we used the in vivo puromycin technique for another major project in my lab. The goal of the experiment is to identify changes in the synthesis of new proteins as a consequence of tau pathology. We received our first set of results where puromycinylated proteins

from tau transgenic mouse brains were identified using LC-MS/MS.

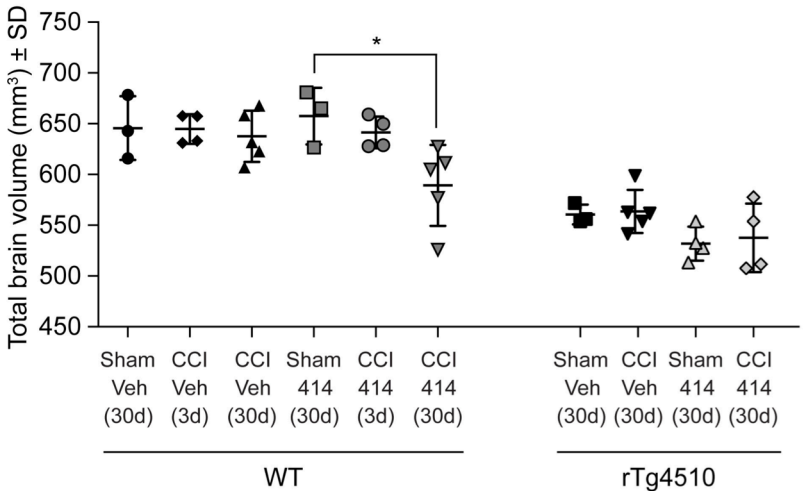

Fig. 9: T2 volumetric measurements. 414 decreased brain volume after injury. No change was detected in tau transgenic mice; this is likely because brain atrophy that is characteristic of rTg4510 mice reached the limit. Prevention of atrophy would have likely been detectable.

What was the impact on other disciplines?

Annual Report 1

Nothing to report

Annual Report 2

Nothing to report

What was the impact on technology transfer?

Annual Report 1

Nothing to report

Annual Report 2

Nothing to report

What was the impact on society beyond science and technology?

Annual Report 1

Nothing to report

Annual Report 2

Nothing to report

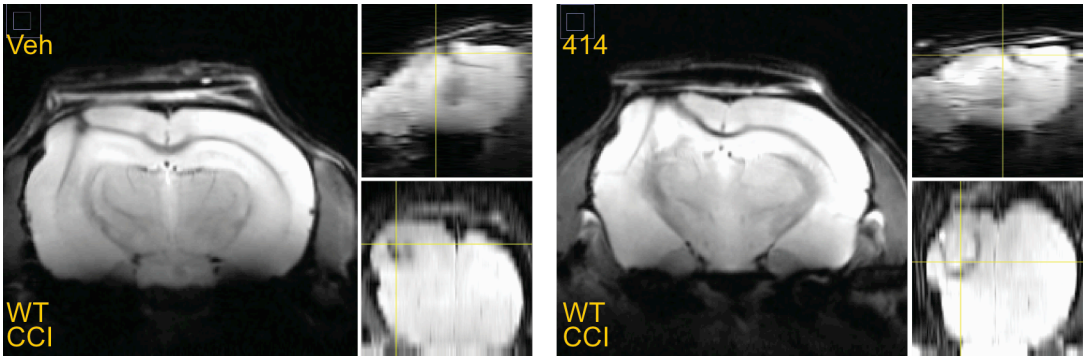

Fig. 10: Orthogonal views for T2 volumetric analysis. 414-treated mice show changes in the injury phenotype.

CHANGES/PROBLEMS:

Changes in approach and reasons for change

Annual Report 1

We injured mice and analyzed PERK activation at earlier time points than originally suggested to optimize the timing of the drug delivery for chemical PERK inhibition. We wanted to make sure we were targeting an appropriate window. Now that we have a clear therapeutic window, we will continue our time points as established in the proposal.

Annual Report 2

We included experiments with altered length of chemical PERK inhibition. PERK inhibition for 30 days promotes brain atrophy, which would be considered detrimental. However, 30d inhibition abrogated tau pathology. We altered the length of treatment to investigate the effects on TBI outcomes and tau outcomes.

Actual or anticipated problems or delays and actions or plans to resolve them

Annual Report 1

Currently, our major delay comes from establishing the PERK conditional knockout colony. The animals have been backcrossed, but now we must have the appropriate parental cross to ensure maximal usable offspring for future experiments. This requires the animals to age to appropriate breeding age before we can perform any experiments.

Annual Report 2

Two major problems we observed were in the behavioral studies and the MEMRI outcomes. For behavior, the first cohorts of animals (n=6-8 per group) showed that the tests were not sensitive enough to detect changes; we think this is due to construction occurring on campus. Additionally, our measurements on MEMRI (in multiple regions) show that this test is not sensitive enough to detect changes between sham and injured animals.

Changes that had a significant impact on expenditures
Annual Report 1
No changes that have had significant impact on expenditures

Annual Report 2
No changes that have had significant impact on expenditures

Significant changes in use or care of human subjects, vertebrate animals, biohazards, and/or select agents
Annual Report 1
Nothing to report

Annual Report 2
Nothing to report

Significant changes in use or care of human subjects
Annual Report 1
Not applicable

Annual Report 2
Not applicable

Significant changes in use or care of vertebrate animals.
Annual Report 1
Nothing to report

Annual Report 2
Nothing to report

Significant changes in use of biohazards and/or select agents
Annual Report 1
Nothing to report

Annual Report 2
Nothing to report

PRODUCTS:

Publications, conference papers, and presentations *Report only the major publication(s) resulting from the work under this award.*

Journal publications.
Nothing to report
Books or other non-periodical, one-time publications.
Nothing to report
Other publications, conference papers, and presentations.

Conferences and Symposia

1. Meier, S. **Abisambra, JF**. PERK activation in controlled cortical impact model of TBI National Neurotrauma Society Annual Meeting. Lexington, KY. 2016. Poster

2. Meier S, Bell M, Lyons DN, Rodriguez-Rivera J, Ingram A, Fontaine SN, Mechas E, Chen J, Wolozin B, LeVine H 3rd, Zhu H, **Abisambra JF**. Pathological Tau Promotes Neuronal Damage by Impairing Ribosomal Function and Decreasing Protein Synthesis. Alzheimer's Association International Conference. Toronto, Canada. July 2016. Podium.
   Received travel award from Alzheimer's Association

3. Meier S, Boychuk J, Smith B, Saatman K, **Abisambra J.** Post-injury PERK inhibition in a mouse model of tauopathy. International Conference on Alzheimer's and Parkinson's Diseases (AD/PD). Vienna, Austria. March 2017. Poster.

4. Meier S, Lanzillotta, C., Galvis S., Saatman K., Boychuk J., Smith B., **Abisambra J.** Post-injury PERK inhibition in a mouse model of tauopathy. Alzheimer's Association International Conference. London, UK. July 2017. Poster.
   Received travel award from UK COM

Invited talks:

	University of Rochester
	Rochester, NY
11/2016	Department of Pharmacology Seminar Series: "Lost in translation: mechanisms of tau-mediated neurotoxicity."
	University of Florida
	Gainesville, FL
04/2017	PSP/LBD Think Tank VI: "Novel molecular mechanisms of tauopathies involving PERK and ribosomal function."

	VA Think Tank Clearwater, FL
04/2017	"TBI, ER stress, and Tauopathies"
	International Clinical Research Center (FNUSA-ICRC)
09/2017	Brno, Czech Republic "Altered RNA translation as an essential pathogenic event in tauopathies."
	University of Florida
09/2017	Gainesville, FL "Lost in Translation: ER stress and ribosomal damage in tauopathies."

Website(s) or other Internet site(s)
Nothing to report

Technologies or techniques
Nothing to report

Inventions, patent applications, and/or licenses
Nothing to report

Other Products
Nothing to report

PARTICIPANTS & OTHER COLLABORATING ORGANIZATIONS

What individuals have worked on the project? *Provide the following information for: (1) PDs/PIs; and (2) each person who has worked at least one person month per year on the project during the reporting period, regardless of the source of compensation (a person month equals approximately 160 hours of effort). If information is unchanged from a previous submission, provide the name only and indicate "no change."* ***Example****:*

Name:	Joe Abisambra
Project Role:	PI
Researcher Identifier (e.g. ORCID ID):	
Nearest person month worked:	
Contribution to Project:	
Funding Support:	No change

Name:	Kathryn Saatman, PhD
Project Role:	Collaborator
Researcher Identifier (e.g. ORCID ID):	
Nearest person month worked:	1
Contribution to Project:	Dr. Saatman trained Shelby Meier in the CCI model of injury
Funding Support:	No change

Name:	Shelby Meier
Project Role:	Graduate Student
Researcher Identifier (e.g. ORCID ID):	0000-0003-1946-9004
Nearest person month worked:	6
Contribution to Project:	Shelby has performed all CCI injuries, the majority of the MEMRI scans and analyses, all immunohistochemical staining and analyses, and all behavioral studies.
Funding Support:	University of Kentucky IBS program

Name:	Grant Nation
Project Role:	Colony manager

Researcher Identifier (e.g. ORCID ID):	
Nearest person month worked:	10
Contribution to Project:	Grant takes care of all the animals for this project and ensures proper genotype.
Funding Support:	R01 NS091329-01A1

Name:	Bret Smith
Project Role:	Collaborator
Researcher Identifier (e.g. ORCID ID):	
Nearest person month worked:	1
Contribution to Project:	Dr. Smith offered feedback and expertise in interpreting results.
Funding Support:	Collaborator

Has there been a change in the active other support of the PD/PI(s) or senior/key personnel since the last reporting period?
Nothing to report

What other organizations were involved as partners?

Organization Name: GlaxoSmithKline
Location of Organization: Collegeville, PA
Partner's contribution to the project: GSK developed the chemical PERK inhibitor used for this project, and supplies it for us.

The Impact of PERK on Posttraumatic Tauopathy in Alzheimer's Disease

AZ140097 Task Title Here

W81XWH-15-1-0551

PI: Jose Abisambra, PhD **Org:** University of Kentucky **Award Amount:** $500,000 (direct)

Study/Product Aim(s)

- Aim 1: Determine the extent to which TBI severity induces PERK activation in mice over time.
- Aim 2: Determine the effect of PERK modulation on tau pathology and brain function after TBI.

Approach

Mouse cohorts will undergo a sham (control), mild (0.4mm depth), moderate (0.7mm depth), or severe (1.0mm depth) cortical contusion injury (CCI). Throughout a 90-day period (days 1, 7, 14, 30, 45, 60, 75, and 90) we will measure the distribution and intensity of PERK activity using MRI. We also seek to 1) establish which cell types harbor active PERK signal, 2) determine changes in the downstream effectors of the PERK pathway, 3) determine the rate of new protein synthesis as a functional consequence of PERK activation, and 4) determine changes in spare tissue as a consequence of CCI. We will test this aim in two sub-aims. *Sub-Aim 2.1* will determine how PERK activation increases tau pathology and brain dysfunction in TBI mice compared to controls. PERK activation will be induced by two means: 1) genetically altering mice using adeno-associated viral particles containing PERK cDNA and 2) using a chemical compound to induce PERK activation. *Sub-Aim 2.2* will determine how PERK inhibition will attenuate the tau pathology and brain dysfunction that occurred in the TBI mice. The *primary outcomes* of Aim 2 are to measure changes in brain function (using cognitive testing, ME-MRI, and electrophysiology) and tau pathology. Secondarily, we will measure changes in activation of the PERK pathway, brain volume, cell types affected, and changes in protein synthesis.

2 major activities since last report:

1) Begin CCI
2) Begin MRI

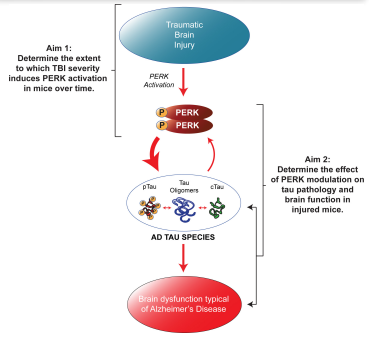

Timeline and Cost

TIMETABLE	YEAR 1				YEAR 2				YEAR 3			
AIMS / TASKS	1st Qrtr	2nd Qrtr	3rd Qrtr	4th Qrtr	1st Qrtr	2nd Qrtr	3rd Qrtr	4th Qrtr	1st Qrtr	2nd Qrtr	3rd Qrtr	4th Qrtr
AIM 1: Determine the extent to which TBI severity induces PERK activation in mice over time.												
Task 1: Establish the mouse colony and validate anatomical and volumetric damage caused by CCI												
Approval of animal protocol (ACURO)												
Establish mouse cohort and perform CCI												
MRI scans (25% complete)												
Task 2: Determine immunohistochemical changes in the brain (and complete all MRI analyses)												
Harvest brains from all time points and prepare brains for IHC												
Perform SUnSET: inject puromycin, prepare brains, and stain for puromycin												
Begin Aperio imaging												
Task 3: Complete imaging analyses												
Complete Aperio Imaging Analysis												
Complete volumetric analyses												
AIM 2: Determine the effect of PERK modulation on tau pathology and brain function after TBI.												
Task 4: Establish mouse cohorts for Aim 2												
Breed mice												
Task 5: Perform genetic manipulation to activate and inhibit PERK function												
Obtain viral particles												
Inject viral particles												
Perform CCI												
Perform primary outcome measures: ME-MRI, begin cognitive testing, electrophysiological experiments												
Task 6: Perform chemical manipulations to modulate PERK												
Deliver PERK activator / inhibitor												
Perform CCI												
Task 7: Complete data collections and analysis for all functional measurements												
Complete all functional measurements												
Complete all MRI												
Task 8: Complete data analysis												
Complete analysis of all pathological data												

Updated: 10/10/17

Goals/Milestones Task 1 and 5 (deliverables relevant to 1st and 2nd quarters)

Task 1 – Establish mouse colony and validate anatomical damage by CCI

☑ ACURO approval

☑ Establish mouse cohort and perform CCI: in progress

☑ MRI scans began

Task 5 –Perform genetic manipulation to activate/inhibit PERK function

☑ Obtain viral particles

Comments/Challenges/Issues/Concerns

- No issues/concerns to report

Budget Expenditure to Date

Projected Expenditure:

Actual Expenditure:

Published in final edited form as:

J Alzheimers Dis. 2015 ; 48(3): 687–702. doi:10.3233/JAD-150298.

Identification of Novel Tau Interactions with Endoplasmic Reticulum Proteins in Alzheimer's Disease Brain

Shelby Meier[a], **Michelle Bell**[a], **Danielle N. Lyons**[a], **Alexandria Ingram**[a], **Jing Chen**[b], **John C. Gensel**[c,e], **Haining Zhu**[b], **Peter T. Nelson**[a,d], and **Jose F. Abisambra**[a,e,*]

[a]Sanders Brown Center on Aging, University of Kentucky, Lexington, KY, USA

[b]Department of Molecular and Cellular Biochemistry, University of Kentucky, Lexington, KY, USA

[c]Spinal Cord and Brain Injury Research Center, University of Kentucky, Lexington, KY, USA

[d]Department of Pathology, Division of Neuropathology, University of Kentucky, Lexington, KY, USA

[e]Department of Physiology, College of Medicine, University of Kentucky, Lexington, KY, USA

Abstract

Alzheimer's disease (AD) is a progressive neurodegenerative disorder that is pathologically characterized by the formation of extracellular amyloid plaques and intraneuronal tau tangles. We recently identified that tau associates with proteins known to participate in endoplasmic reticulum (ER)-associated degradation (ERAD); consequently, ERAD becomes dysfunctional and causes neurotoxicity. We hypothesized that tau associates with other ER proteins, and that this association could also lead to cellular dysfunction in AD. Portions of human AD and non-demented age matched control brains were fractionated to obtain microsomes, from which tau was co-immunoprecipitated. Samples from both conditions containing tau and its associated proteins were analyzed by mass spectrometry. In total, we identified 91 ER proteins that co-immunoprecipitated with tau; 15.4% were common between AD and control brains, and 42.9% only in the AD samples. The remainder, 41.8% of the proteins, was only seen in the control brain samples. We identified a variety of previously unreported interactions between tau and ER proteins. These proteins participate in over sixteen functional categories, the most abundant being involved in RNA translation. We then determined that association of tau with these ER proteins was different between the AD and control samples. We found that tau associated equally with the ribosomal protein L28 but more robustly with the ribosomal protein P0. These data suggest that the differential association between tau and ER proteins in disease could reveal the pathogenic processes by which tau induces cellular dysfunction.

*Correspondence to: Jose F. Abisambra, Sanders-Brown Center on Aging and Department of Physiology, College of Medicine, University of Kentucky, 800 S Limestone Street, Lexington, KY 40536-0230, USA. Tel.: +1 859 218 3852; ; Email: joe.abisambra@uky.edu

Authors' disclosures available online (http://j-alz.com/manuscript-disclosures/15-0298r2).

Keywords

Alzheimer's disease; co-immunoprecipitation; endoplasmic reticulum; mass spectrometry; microsome; ribosome; tau; tauopathies

INTRODUCTION

Alzheimer's disease (AD) is a progressive neurodegenerative disorder that affects 5.2 million Americans [1] and 36 million people worldwide [2]. This number is expected to rise to 13.8 million by 2050. The direct and indirect costs of maintaining the quality of life of AD amounts to $203 billion annually. Since there is currently no cure for AD, and therapeutic interventions are ineffective in preventing the dramatic rise of patients, expenditures are projected to reach $1.2 trillion annually by 2050.

The pathological hallmarks of AD consist of amyloid plaques and neurofibrillary tangles (NFTs). Plaques result from extracellular aggregation of a 40–42 amino acid peptide termed amyloid-β (Aβ) (reviewed in [3]). Meanwhile, NFTs are intraneuronal lesions comprised of aberrant aggregates of the microtubule-associated protein tau. Within NFTs, tau is abnormally folded, oligomerized, hyperphosphorylated, and mislocalized [4–6]. In AD, as well as in other tauopathies, tau becomes neurotoxic [7]; however, the exact mechanisms leading to tau neurotoxicity have not been identified.

As a microtubule stabilizing protein [8], tau interacts with various other proteins that are transported along microtubules. Pathogenic tau adopts a β-pleated sheet conformation [9], rendering it hydrophobic and able to bind non-specifically to other proteins and itself (reviewed in [10, 11]). In many cases, these aberrant linkages have deleterious consequences to the functions and processes in which tau-associated proteins participate [11–16]. For example, soluble, pathological tau conformers associate with endoplasmic reticulum (ER)-associated degradation (ERAD) proteins, and abrogate ERAD function [12].

Recent studies suggest that a key mechanism of neuronal dysfunction in neurodegenerative diseases is impaired protein synthesis [17]. This phenomenon could be the result of tau-mediated impairment of ribosomal function. Tau normally associates with ribosomes [18]. However, due to its intrinsically disordered conformation, which is amplified in disease, tau binds to proteins that participate in RNA translation thereby impairing translation [19]. Thusly, a mechanism of tau-mediated neurodegeneration could implicate aberrant tau-ribosomal interactions.

In the current study, we sought to identify tau-associated ER proteins with particular emphasis on proteins involved in RNA translation. We hypothesized that tau-associated ER proteins could serve as potential therapeutic targets. We identified tau-interacting ER proteins in both AD and non-AD brains with an integrated approach involving sub-cellular fractionation, co-immunoprecipitation, and mass spectrometry. We established three types of tau-associated ER proteins: those that were identified in AD brains, others that were only identified in non-AD brains, and those that were common to both. Interestingly, 85% of the proteins we identified had not been previously established as associating with tau. Among

them, were several proteins that participate in RNA translation. To validate our approach, we focused on the ribosomal proteins L28 and P0, which had not been previously identified to be associated with tau, and we found that tau associated more robustly with P0 in the AD brain. Overall, these data suggest that changes in the association between tau and ER proteins could underlie pathogenic mechanisms leading or contributing to cellular dysfunction evident in AD. Further characterization and validation of AD tau-associated ER proteins and their functions could lead to better understanding of the pathogenesis of AD and other tauopathies.

MATERIALS AND METHODS

Human brain samples

Samples were obtained from the University of Kentucky-Alzheimer's Disease Center Tissue Bank. All sample collection and experimental procedures involving human subjects were in compliance with the University of Kentucky Institutional Review board (IRB) protocols. Samples from the superior and mid-temporal gyrus (Brodmann areas 21/22) were used. AD tissues were from symptomatic individuals and they were neuropathologically scored as Braak V (female, 93 years old), VI (male, 88 years old), and VI (female, 80 years old); non-demented control samples were scored Braak I (male, 79 years old), II (female, 94 years old), and II (female, 88 years old). The average postmortem interval (between death and the tissue being snap-frozen in liquid nitrogen) was 3.0 h.

Microsome isolation

Microsomes were isolated as previously described [20, 21] and modified for brain [22]. Briefly, 200 mg of human brain samples were dounce homogenized in 0.25 M sucrose containing 1X protease inhibitor mixture (Calbiochem), 100 mM phenylmethylsulfonyl fluoride, and 1X phosphatase inhibitor II and III cocktails (Sigma). All samples were then centrifuged at 16,000 × g for 15 min at 4°C. The supernatant was transferred and centrifuged at 100,000 × g for 1 h at 4°C. The pellet, which corresponded to the microsomal protein fraction, was resuspended in RIPA buffer containing 1X protease inhibitor mixture (Calbiochem), 100 mM phenylmethylsulfonyl fluoride, and 1X phosphatase inhibitor II and III cocktails (Sigma).

Co-immunoprecipitations (co-IP) and western blotting

Co-IP was performed as previously described [23] using antibodies for tau (Tau5 EMD Millipore), actin (Sigma-Aldrich), RPL28 (GeneTex), or RPP0 (Gene-Tex). Western blots were performed as previously described [24]. Briefly, 20 μg of protein were denatured by mixing with a sample buffer (consisting of 2x Laemmli buffer with 5% β-mercaptoethanol) and subjecting to heat at 100°C for 10 min. Samples were loaded in 10% tris-glycine gels (Life Technologies). Gels were subjected to 100 mV until the dye front reached the bottom of the gel. We then performed wet transfers as indicated previously [25]. Samples were blocked in 7% non-fat dry milk (LabScientific) with 0.02% sodium azide. This milk was used to mix antibodies for incubation with the membranes. Antibodies used were anti total tau h-150 (1:1000) from Santa Cruz Biotechnology, actin (1:1000) from Sigma, RPL28 from GeneTex, RPP0 from GeneTex, and calnexin C-20 from Santa Cruz Biotechnology.

Immunofluorescence

Frozen brain samples were fixed in 4% paraformaldehyde. Fixed brains were cryoprotected in successive 24 h increments of 10%, 20%, and 30% sucrose gradients as described previously [26]. Brains were frozen on a temperature-controlled freezing stage, sectioned (25 μm) on a sliding microtome, and stored in a solution of PBS containing 0.02% sodium azide at 4°C. Immunostaining was performed following protocols described previously with minor modifications [22]. Brain sections were mounted on glass slides with medium (30% ethanol in PBS). Once dry, sections were blocked and permeabilized in blocking buffer (4% normal goat serum, 0.2% Triton X-100, and 0.02% sodium azide in TBS) for 1 h. Slides were incubated overnight at 4°C with the following antibodies: tau h-150 (1:50), PHF1 (1:50), calnexin C-20 (1:50), calnexin F-17 (1–50). Slides were then washed with TBS and incubated with Alexa Fluor 488 nm and Alexa Fluor 594 nm secondary antibodies (Life Technologies) at 1:2000 for 2 h at room temperature. Tissues were stained with Sudan black to block autofluorescence inherent to the sample. Slides were then washed again and incubated with Neurotrace (1:200) according to the manufacturer's recommendations. Slides with both AD and control were stained omitting primary antibodies in order to identify non-specific background signal.

Microscopy

All slides were imaged using a Nikon Eclipse Ti laser-scanning confocal microscope. Fields for colocalization analysis were randomly selected based upon tau immunolabeling by an investigator blinded to group inclusion. Specifically, fields were chosen that included areas of tau staining with morphological distribution in agreement with NeuN labeling; ER labeling was not considered in field selection. All immunolabeling acquisition intensities, field sizes, and microscopy settings were kept consistent across all images. Scatter plots and images for graphical representation of co-localization were prepared using the NIS Elements 4.20 (Nikon) and Photoshop Cs6 (Adobe) software programs and were based upon cells that most closely approximated the group means.

Co-localization analysis

Images were analyzed for co-localization as previously described with minor modifications [12]. Briefly, regions of interest (ROIs) corresponding to z-stack images of neurons that stained positively for calnexin and tau (either total tau or PHF1) were selected for co-localization analysis. Three to five ROIs were selected per image, and there were at least three images per brain from three AD brains. Z-stack images were analyzed according to [27] using Pearson's, Manders', and Costes' (auto-threshold and randomization control) coefficients.

Mass spectrometry (MS) and proteomics data analysis

Each lane in the gel was excised into 12 major portions and subjected to dithiothreitol reduction, iodoacetamide alkylation, and in-gel trypsin digestion using a standard protocol as previously reported [28, 29]. The resulting tryptic peptides were extracted, concentrated to 15 μl each using a SpeedVac, and 5 μl was injected for nano-LC-MS/MS analysis. LC-MS/MS data were acquired on an LTQ Velos Orbitrap mass spectrometer (Thermo Fisher

Scientific, Waltham, MA) coupled with a Nano-LC Ultra/cHiPLC-nanoflex HPLC system (Eksigent, Dublin, CA) through a nano-electrospray ionization source. The tryptic peptides sample was injected by an autosampler, desalted on a trap column, and subsequently separated by reverse phase C18 column (75 mm i.d. × 150 mm) at a flow rate of 250 nL/min. The HPLC gradient was linear from 5% to 60% mobile phase B for 30 min using mobile phase A (H_2O, 0.1% formic acid) and mobile B (90% acetonitrile, 0.1% formic acid). Eluted peptides were analyzed using data-dependent acquisition: peptide mass spectrometry was obtained by Orbitrap with a resolution of 60,000. The seven most abundant peptides were subjected to collision induced dissociation and MS/MS analysis in LTQ linear trap. The LC-MS/MS data were submitted to a local MASCOT server for MS/MS protein identification search via the ProteomeDiscoverer software. The mass error tolerance was 5 ppm for peptide MS and 0.8 Da for MS/MS. All peptides were required to have an ion score greater than 30 ($p < 0.05$). The false discovery rate in each LC-MS/MS analysis was set to be less than 1%. Proteins that were identified in the actin-IP samples were excluded from the tau-IP list. Although tau binds to actin under normal conditions this interaction occurs primarily in the growth cone [30]. Since tau tangles deposit in the soma [31], our results reflect primarily ER proteins associated with pathological tau [32].

Functional categorization of MS results

Functional descriptions for all proteins were acquired by searching for accession numbers in the UNIPROT database (http://www.uniprot.org). Proteins were categorized by function (Fig. 3B). In some cases, proteins were multifunctional, but they were only organized into one parameter as justified by their primary function.

Western blot analysis

For western blots, the relative intensity of the bands was measured using ImageJ. Bands of the protein of interest were normalized to a loading control. Statistical analysis of the bands was performed using Student's *t*-test. All graphs were prepared in Prism 6 (GraphPad).

RESULTS

Tau abnormally associates with proteins on the cytosolic surface of the ER in the rTg4510 tau transgenic model [12]. VCP and Hrd1 are two examples of tau-associated ER proteins, and both of these proteins play crucial roles in ERAD. As a result of this abnormal interaction, ERAD function becomes impaired in tau transgenic mice and in AD brain. Therefore, we hypothesized that tau associated with other ER proteins, the functions of which could similarly be altered by the abnormal association with tau.

In AD brains, tau tangle formation occurs primarily in neuronal soma [31, 33]. In fact, a large pool of tau deposits in the perinuclear region coincident with the ER [12, 34, 35]. To further characterize this interaction, we performed subcellular fractionation of three AD and three age-matched, non-demented control brains to isolate the microsomal compartment, which is predominantly composed of ER and associated proteins [36]. Tau formed high molecular weight complexes (Fig. 1A, C) in AD brains which is characteristic of hyperphosphorylated and detergent insoluble pathological tau (reviewed in [37]).

Conversely, control brains showed a typical tau smear between 48–60 kDa. We quantified the amount of tau in the 48–60 kDa range of AD and control whole brain lysates and microsomes. We determined that while tau levels did not differ between whole cell lysates of AD and control, AD microsomes contained 34% more tau than control (Fig. 1A–1D). These data suggest that tau shifts in tau distribution in AD. We then performed co-immunofluorescent staining of human AD and control brains to determine the distribution of total and hyperphosphorylated tau with the ER (Fig. 1E, L). We co-immunofluorescently labeled total tau or hyperphosphorylated tau (pS396/S404 detected with PHF1) and calnexin, an ER transmembrane protein [38]. We found that both tau and hyperphosphorylated tau decorated the ER by largely co-localizing with calnexin (Fig. 1G, K).

To reveal the identity of tau-associated ER proteins, we isolated microsomes from human AD and control brains and performed co-immunoprecipitation analyses using an anti-tau antibody (Tau5); actin was co-immunoprecipitated from the same tissues as a control. All samples were processed for liquid chromatography-tandem mass spectrometry (LC-MS/MS) (Fig. 2).

We applied robust exclusion criteria to minimize false positive results. First, each peptide matched from a MS/MS spectrum had an ion score based on the calculated probability, p, that the observed match between the experimental data and the database sequence was a random event. We set an ion score threshold to achieve $p < 0.05$. The scores in the tables (Protein Score) were mathematically derived from the ion scores of all peptides matched to this protein. Confidence in protein identification is directly proportional to the magnitude of the Protein Score. In addition, we set the false discovery rate at 1% for the MASCOT data analysis to ensure the high confidence of all proteins identified from the LC-MS/MS data. Second, proteins that were identified in the actin-IP samples were excluded from the tau-IP list. Although tau binds to actin under normal conditions this interaction occurs primarily in the growth cone [30]. Since tau tangles deposit in the soma [31], our results reflect primarily ER proteins associated with pathological tau [32].

Data were submitted to a local Mascot server for protein identification analysis. Tau was identified in both the AD and non-AD samples, indicating that the co-immunoprecipitation was successful. In addition, a total of 92 proteins were identified (Tables 1–3). Of these, 39 (42.4%) were found in AD brain (Table 1), 38 (41.3%) were only found in the non-AD brain (Table 2), and 15 (16.3%) were found in both AD and non-AD (Table 3; Fig. 3A). Interestingly, 77 of these (85%) had not been previously identified as tau-interacting proteins. Based on previous work showing that the aberrant association of tau with ERAD proteins caused ERAD impairments [12], we grouped the 92 proteins identified in our screen by functional categories (Fig. 3B). Each protein was assigned a function based on the description in the UNIPROT database. Figure 3B represents the relative abundance of proteins from each category.

Our screen showed that the ribosomal proteins L28 and P0 co-immunoprecipitated differentially with tau in both AD and control brains. More specifically, P0 did not complex with tau in control brains. To confirm these results, we co-immunoprecipitated L28 or P0 from human AD or control brain microsomes. We determined that tau formed a complex

with both L28 and P0 (Fig. 4A, B); however, the tau-P0 association was much more robust in the AD microsomes than in control, as suggested by the MS/MS data (Fig. 4C). Interestingly, the data show that P0 formed a complex with high molecular weight tau species. We also performed the reverse co-immunoprecipitation by isolating tau from AD and control microsomes and measuring the levels of P0 and L28 by western blot. We found no significant difference in the levels of P0 or L28 in the reverse co-immunoprecipitation (Fig. 4G). The input blot shows that the primary tau species that was isolated corresponded to a 50–60kDa tau band that lacks post-translational modifications. These data suggest that P0 and L28 associate normally with tau around the ER; however, in AD brains, there is a significant increase in the association of high molecular weight tau (heavily post-translationally modified and pathological) with P0.

DISCUSSION

We present a list of 92 tau-associated ER proteins. The list contains proteins that have been previously identified as disease modulators such as AD-related tau kinases and apolipoprotein E (ApoE). However, 77 proteins (85%) have not been previously linked to tau. Among the identified proteins were several that participate in ERAD thereby validating this approach with previous findings [12]. Moreover, we show that the subcellular fractionation-coIP-MS/MS approach is sufficiently sensitive to identify different affinities of tau for L28 and P0, which are closely localized in ribosomes.

The newly identified tau-associated ER proteins could reveal tau functions that have not been previously described. For instance, synaptojanin, a protein involved in the uncoating of synaptic vesicles [39], was identified as a tau-associated ER protein in normal, non-AD brain. This suggests that tau facilitates synaptojanin's function and therefore indirectly participates in endocytic processes for synaptic function. Similarly, loss of the tau-synaptojanin interaction would reduce uncoating of synaptic vesicles altering synaptic function; indeed, synaptojanin was not identified as a tau-associated ER protein in the AD brain data set. Another example is caspase-14, which had not been previously identified as a tau interacting protein but was a positive hit in the normal brain. This could be the first evidence of tau cleavage by another caspase besides caspases 3, 6, 7, 8, and 9 [40–43]. Since this association was not determined in the AD brain, it is possible that caspase-14 function is beneficial, and loss of the interaction could lead to early pathogenesis.

Ribosomal proteins constituted the largest functional category of tau-associated ER proteins. Yet, since the immunoprecipitation was performed with Tau5, an antibody that binds to the middle region of tau (aa 210–241), it is possible that the co-IP isolated both mature and nascent tau (partially translated tau beyond aa 241), the latter of which could still be attached to ribosomes while it is being translated. Identification of chaperones as tau-associated ER proteins also supports the idea that this is non-pathological nascent tau. However, some of these tau-associated ribosomal proteins are different between the AD and control brains. For instance, ribosomal proteins P0 and L28 showed differential association with pathological tau suggesting possible disease-based differences that could alter ribosomal function. Indeed, hyperphosphorylated tau associates with ribosomes in AD and tauopathy models but not in normal models but the consequences of this interaction are unknown [19, 44]. This is

critical to understand disease mechanisms since ribosomal dysfunction has been associated with AD pathogenesis [45]. Ribosomal proteins P0 and L28 are both structural proteins located in the 60 S subunit. While the individual proteins have not been studied in depth, the function of the 60 S subunit has been extensively covered. Proteins in this subunit participate in ribosome biogenesis, all phases of translation, viral transcription, and nonsense-mediated decay of mRNA [46]. The structural proteins in the 60 S ribosomal subunit play a critical part in joining the 60 S subunit with the 40 S subunit. Since P0 and L28 are structural proteins, it is possible that the association of abnormal tau with these proteins could prevent the coupling of the 60 S subunit with the 40 S subunit and would subsequently lead to a decrease in translation.

Our study further characterizes region-specific features of previously identified tau-interacting proteins. For instance, ApoE, the main cholesterol transporter in the brain, was previously identified as a tau-interacting protein [47]. Since expression of different ApoE iso-forms confer either increased risk for AD (ApoE4) or protection from AD (ApoE2), and tau is intricately involved in AD pathology, the ApoE-tau relationship should be studied in further detail. Identification of ApoE in our study highlights that this interaction occurs in proximity to the ER. Interestingly, ApoE was identified as a tau-associated ER protein in both AD and non-AD brains. Therefore, the ApoE-tau interaction plays a normal role in the brain, and aberrancy of the interaction could be a component of the AD mechanism.

Spectrin, a cytoskeletal protein that was identified in our screen, had also been reported to associate with tau [48]. However, the association occurs as a consequence of disease or trauma instead of a direct interaction [49, 50]. In AD and traumatic brain injury, axonal damage activates calpains and caspases that cleave tau and spectrin. Consequently, cleaved tau and spectrin levels increase in parenchyma and cerebrospinal fluid [37]. These cleavage products have been studied as potential biomarkers of AD diagnosis and traumatic brain injury severity.

The association of a functional category with tau is more robust than that of tau with an individual protein. Therefore, while Table 1 presents interesting leads, Figure 3B offers tantalizing support for unidentified tau functions, the disturbance of which could be linked to AD. For example, identification of complement C3 as a tau-associated ER protein is insufficient evidence to suggest involvement of tau in regulating inflammatory processes. However, identification of other proteins that participate in inflammation, such as S100A8, S100A9, and inter-alpha-trypsin inhibitor as tau-associated ER proteins, supports the possibility of a role for tau in inflammation.

Although the mass spectrometry platform maximizes the sample input and yields a high amount of data, it is limited in the characterization of protein-protein interactions. Therefore, identification of individual tau partners must be validated to establish whether both proteins associate or interact. Albeit, despite the robust exclusion criteria we applied to our data, we identified tau-associated ER proteins that were previously validated as tau-interacting proteins such as ApoE and annexin, among others (Table 1) [8, 47, 51]. Tubulin, which interacts with both tau and actin, was identified in both co-immunoprecipitates. Since our exclusion criterion to limit false positives involved eliminating proteins identified in the

actin co-IP from the tau co-IP, we excluded tubulin from the list of tau-interacting proteins. Our approach adds novelty to these findings by establishing that this interaction might occur in brain microsomes.

We utilized robust exclusion criteria that showed no association between tau and the ribosomal protein P0 in non-demented control brain. Further characterization of these interactions revealed that tau indeed associated with P0 in both the AD and control samples; these data suggest that the exclusion criteria considered the less robust tau-P0 association below the threshold of a true positive hit. Furthermore, these data underscore the importance of validating MS/MS results such as the tau-ER proteins identified herein.

AD is a complex disease that often presents other clinical and pathological signs. Considering the complexity of AD etiology, it is possible that our current results are not unique to AD. In fact, they could be a common occurrence in many and newly-characterized tauopathies [52].

In conclusion, we performed a selective identification of ER proteins that associate with tau in AD and control brains. Further characterization of the dynamic changes in the association of tau and the listed proteins could reveal novel insights into the pathogenesis and progression of AD and related tauopathies. In addition, the tau-associated ER proteins in non-AD brain could identify tau functions that have not been previously described. Future efforts involve biochemical validation of these tau-associated ER proteins as tau-interacting proteins, characterization of the role of normal tau in the functional categories (Fig. 3B), and determination of the impact of pathological tau on the function of the tau-associated ER proteins in AD brain.

Acknowledgments

We acknowledge the University of Kentucky Alzheimer's Disease Center (UK-ADC) and its Neuropathology Core NIH/NIA, which is supported by NIH/NIA P30 AG028383. We also acknowledge the University of Kentucky Proteomics Core that is partially supported by grants from the NIH/NIGMS (P20GM103486) and the NIH/NCI (P30CA177558). This work was also supported in part by NIH R01NS077284 (to H.Z.). The LC-MS/MS instrument was acquired with a High-End Instrumentation Grant S10RR029127 (to H.Z.) from the NIH. We further acknowledge NIH/NINDS P30NS051220 for support and maintenance of the microscopy core used for imaging. J.F.A., D.L., and S.M. were supported by the Alzheimer's Association NIRG-14-322441, NIH/NIMHD LRP, UK Center for Clinical and Translational Science Pilot Award supported by NIH/NCATS 5UL1TR000117-04, UK-ADC Pilot Award 8.1 supported by NIH/NIA P30 AG028383, and the UK Epilepsy Center Pilot Project. We thank Dr. Peter Davies for his generous contribution of the PHF1 antibody used for immunofluorescent staining. We thank Ms. Ela Patel and Ms. Sonya Anderson with their assistance accessing the human brain tissue. We also thank Ms. Linda Simmerman for her technical assistance with microscopy. Finally, we thank Maria Bodero for her contributions to these studies.

References

1. Alzheimer's Association. 2014 Alzheimer's disease facts and figures. Alzheimers Dement. 2014; 10:e47–e92. [PubMed: 24818261]
2. Prince M, Bryce R, Albanese E, Wimo A, Ribeiro W, Ferri CP. The global prevalence of dementia: A systematic review and metaanalysis. Alzheimers Dement. 2013; 9:63–75. e62. [PubMed: 23305823]
3. Murphy MP, LeVine H 3rd. Alzheimer's disease and the amyloid-beta peptide. J Alzheimers Dis. 2010; 19:311–323. [PubMed: 20061647]

4. Grundke-Iqbal I, Iqbal K, Tung YC, Quinlan M, Wisniewski HM, Binder LI. Abnormal phosphorylation of the microtubule-associated protein tau (tau) in Alzheimer cytoskeletal pathology. Proc Natl Acad Sci U S A. 1986; 83:4913–4917. [PubMed: 3088567]
5. Lasagna-Reeves CA, Castillo-Carranza DL, Sengupta U, Guerrero-Munoz MJ, Kiritoshi T, Neugebauer V, Jackson GR, Kayed R. Alzheimer brain-derived tau oligomers propagate pathology from endogenous tau. Sci Rep. 2012; 2:700. [PubMed: 23050084]
6. Takashima A. Tauopathies and tau oligomers. J Alzheimers Dis. 2013; 37:565–568. [PubMed: 23948895]
7. Lasagna-Reeves CA, Castillo-Carranza DL, Sengupta U, Clos AL, Jackson GR, Kayed R. Tau oligomers impair memory and induce synaptic and mitochondrial dysfunction in wild-type mice. Mol Neurodegener. 2011; 6:39. [PubMed: 21645391]
8. Weingarten MD, Lockwood AH, Hwo SY, Kirschner MW. A protein factor essential for microtubule assembly. Proc Natl Acad Sci U S A. 1975; 72:1858–1862. [PubMed: 1057175]
9. von Bergen M, Friedhoff P, Biernat J, Heberle J, Mandelkow EM, Mandelkow E. Assembly of tau protein into Alzheimer paired helical filaments depends on a local sequence motif ((306)VQIVYK(311)) forming beta structure. Proc Natl Acad Sci U S A. 2000; 97:5129–5134. [PubMed: 10805776]
10. Mandelkow EM, Mandelkow E. Biochemistry and cell biology of tau protein in neurofibrillary degeneration. Cold Spring Harb Perspect Med. 2012; 2:a006247. [PubMed: 22762014]
11. Abisambra JF, Jinwal UK, Jones JR, Blair LJ, Koren J 3rd, Dickey CA. Exploiting the diversity of the heat-shock protein family for primary and secondary tauopathy therapeutics. Curr Neuropharmacol. 2011; 9:623–631. [PubMed: 22654720]
12. Abisambra JF, Jinwal UK, Blair LJ, O'Leary JC 3rd, Li Q, Brady S, Wang L, Guidi CE, Zhang B, Nordhues BA, Cockman M, Suntharalingham A, Li P, Jin Y, Atkins CA, Dickey CA. Tau accumulation activates the unfolded protein response by impairing endoplasmic reticulum-associated degradation. J Neurosci. 2013; 33:9498–9507. [PubMed: 23719816]
13. Abisambra JF, Blair LJ, Hill SE, Jones JR, Kraft C, Rogers J, Koren J 3rd, Jinwal UK, Lawson L, Johnson AG, Wilcock D, O'Leary JC, Jansen-West K, Muschol M, Golde TE, Weeber EJ, Banko J, Dickey CA. Phosphorylation dynamics regulate Hsp27-mediated rescue of neuronal plasticity deficits in tau transgenic mice. J Neurosci. 2010; 30:15374–15382. [PubMed: 21084594]
14. Abisambra JF, Jinwal UK, Suntharalingam A, Arulselvam K, Brady S, Cockman M, Jin Y, Zhang B, Dickey CA. DnaJA1 antagonizes constitutive Hsp70-mediated stabilization of tau. J Mol Biol. 2012; 421:653–661. [PubMed: 22343013]
15. Dickey CA, Kamal A, Lundgren K, Klosak N, Bailey RM, Dunmore J, Ash P, Shoraka S, Zlatkovic J, Eckman CB, Patterson C, Dickson DW, Nahman NS Jr, Hutton M, Burrows F, Petrucelli L. The high-affinity HSP90-CHIP complex recognizes and selectively degrades phosphorylated tau client proteins. J Clin Invest. 2007; 117:648–658. [PubMed: 17304350]
16. Jinwal UK, Akoury E, Abisambra JF, O'Leary JC 3rd, Thompson AD, Blair LJ, Jin Y, Bacon J, Nordhues BA, Cockman M, Zhang J, Li P, Zhang B, Borysov S, Uversky VN, Biernat J, Mandelkow E, Gestwicki JE, Zweckstetter M, Dickey CA. Imbalance of Hsp70 family variants fosters tau accumulation. FASEB J. 2013; 27:1450–1459. [PubMed: 23271055]
17. Moreno JA, Radford H, Peretti D, Steinert JR, Verity N, Martin MG, Halliday M, Morgan J, Dinsdale D, Ortori CA, Barrett DA, Tsaytler P, Bertolotti A, Willis AE, Bushell M, Mallucci GR. Sustained translational repression by eIF2alpha-P mediates prion neurodegeneration. Nature. 2012; 485:507–511. [PubMed: 22622579]
18. Papasozomenos SC, Binder LI. Phosphorylation determines two distinct species of Tau in the central nervous system. Cell Motil Cytoskeleton. 1987; 8:210–226. [PubMed: 2446784]
19. Nelson PT, Saper CB. Ultrastructure of neurofibrillary tangles in the cerebral cortex of sheep. Neurobiol Aging. 1995; 16:315–323. [PubMed: 7566341]
20. Ness GC, Sample CE, Smith M, Pendleton LC, Eichler DC. Characteristics of rat liver microsomal 3-hydroxy-3-methylglutaryl-coenzyme A reductase. Biochem J. 1986; 233:167–172. [PubMed: 3082322]

21. Lopez D, Abisambra Socarras JF, Bedi M, Ness GC. Activation of the hepatic LDL receptor promoter by thyroid hormone. Biochim Biophys Acta. 2007; 1771:1216–1225. [PubMed: 17572141]
22. Abisambra JF, Fiorelli T, Padmanabhan J, Neame P, Wefes I, Potter H. LDLR expression and localization are altered in mouse and human cell culture models of Alzheimer's disease. PLoS One. 2010; 5:e8556. [PubMed: 20049331]
23. Jinwal UK, Abisambra JF, Zhang J, Dharia S, O'Leary JC, Patel T, Braswell K, Jani T, Gestwicki JE, Dickey CA. Cdc37/Hsp90 protein complex disruption triggers an autophagic clearance cascade for TDP-43 protein. J Biol Chem. 2012; 287:24814–24820. [PubMed: 22674575]
24. Abisambra J, Jinwal UK, Miyata Y, Rogers J, Blair L, Li X, Seguin SP, Wang L, Jin Y, Bacon J, Brady S, Cockman M, Guidi C, Zhang J, Koren J, Young ZT, Atkins CA, Zhang B, Lawson LY, Weeber EJ, Brodsky JL, Gestwicki JE, Dickey CA. Allosteric heat shock protein 70 inhibitors rapidly rescue synaptic plasticity deficits by reducing aberrant tau. Biol Psychiatry. 2013; 74:367–374. [PubMed: 23607970]
25. Jones JR, Lebar MD, Jinwal UK, Abisambra JF, Koren J 3rd, Blair L, O'Leary JC, Davey Z, Trotter J, Johnson AG, Weeber E, Eckman CB, Baker BJ, Dickey CA. The diarylhep-tanoid (+)-aR,11S-myricanol and two flavones from bayberry (Myrica cerifera) destabilize the microtubule-associated protein tau. J Nat Prod. 2011; 74:38–44. [PubMed: 21141876]
26. Jinwal UK, Koren J 3rd, Borysov SI, Schmid AB, Abisambra JF, Blair LJ, Johnson AG, Jones JR, Shults CL, O'Leary JC 3rd, Jin Y, Buchner J, Cox MB, Dickey CA. The Hsp90 cochaperone, FKBP51, increases Tau stability and polymerizes microtubules. J Neurosci. 2010; 30:591–599. [PubMed: 20071522]
27. Bolte S, Cordelieres FP. A guided tour into subcellular colocalization analysis in light microscopy. J Microsc. 2006; 224:213–232. [PubMed: 17210054]
28. Zhai J, Strom AL, Kilty R, Venkatakrishnan P, White J, Everson WV, Smart EJ, Zhu H. Proteomic characterization of lipid raft proteins in amyotrophic lateral sclerosis mouse spinal cord. FEBS J. 2009; 276:3308–3323. [PubMed: 19438725]
29. Dhar SK, Zhang J, Gal J, Xu Y, Miao L, Lynn BC, Zhu H, Kasarskis EJ, St Clair DK. FUsed in sarcoma is a novel regulator of manganese superoxide dismutase gene transcription. Antioxid Redox Signal. 2014; 20:1550–1566. [PubMed: 23834335]
30. Griffith LM, Pollard TD. The interaction of actin filaments with microtubules and microtubule-associated proteins. J Biol Chem. 1982; 257:9143–9151. [PubMed: 6124545]
31. Li X, Kumar Y, Zempel H, Mandelkow EM, Biernat J, Mandelkow E. Novel diffusion barrier for axonal retention of Tau in neurons and its failure in neurodegeneration. EMBO J. 2011; 30:4825–4837. [PubMed: 22009197]
32. Fulga TA, Elson-Schwab I, Khurana V, Steinhilb ML, Spires TL, Hyman BT, Feany MB. Abnormal bundling and accumulation of F-actin mediates tau-induced neuronal degeneration *in vivo*. Nat Cell Biol. 2007; 9:139–148. [PubMed: 17187063]
33. Braak H, Braak E. Neuropathological stageing of Alzheimer-related changes. Acta Neuropathol. 1991; 82:239–259. [PubMed: 1759558]
34. Braak H, Braak E. Demonstration of amyloid deposits and neurofibrillary changes in whole brain sections. Brain Pathol. 1991; 1:213–216. [PubMed: 1669710]
35. Augustinack J, Schneider A, Mandelkow E-M, Hyman B. Specific tau phosphorylation sites correlate with severity of neuronal cytopathology in Alzheimer's disease. Acta Neuropathol. 2002; 103:26–35. [PubMed: 11837744]
36. Palade GE, Siekevitz P. Liver microsomes; an integrated morphological and biochemical study. J Biophys Biochem Cytol. 1956; 2:171–200. [PubMed: 13319380]
37. Abisambra JF, Scheff S. Brain injury in the context of tauopathies. J Alzheimers Dis. 2014; 40:495–518. [PubMed: 24496078]
38. Benyair R, Ron E, Lederkremer GZ. Protein quality control, retention, and degradation at the endoplasmic reticulum. Int Rev Cell Mol Biol. 2011; 292:197–280. [PubMed: 22078962]
39. McPherson PS, Garcia EP, Slepnev VI, David C, Zhang X, Grabs D, Sossin WS, Bauerfeind R, Nemoto Y, De Camilli P. A presynaptic inositol-5-phosphatase. Nature. 1996; 379:353–357. [PubMed: 8552192]

40. Horowitz PM, Patterson KR, Guillozet-Bongaarts AL, Reynolds MR, Carroll CA, Weintraub ST, Bennett DA, Cryns VL, Berry RW, Binder LI. Early N-terminal changes and caspase-6 cleavage of tau in Alzheimer's disease. J Neurosci. 2004; 24:7895–7902. [PubMed: 15356202]
41. Rissman RA, Poon WW, Blurton-Jones M, Oddo S, Torp R, Vitek MP, LaFerla FM, Rohn TT, Cotman CW. Caspase-cleavage of tau is an early event in Alzheimer disease tangle pathology. J Clin Invest. 2004; 114:121–130. [PubMed: 15232619]
42. Gamblin TC, Chen F, Zambrano A, Abraha A, Lagalwar S, Guillozet AL, Lu M, Fu Y, Garcia-Sierra F, LaPointe N, Miller R, Berry RW, Binder LI, Cryns VL. Caspase cleavage of tau: Linking amyloid and neurofibrillary tangles in Alzheimer's disease. Proc Natl Acad Sci U S A. 2003; 100:10032–10037. [PubMed: 12888622]
43. Rohn TT, Rissman RA, Davis MC, Kim YE, Cotman CW, Head E. Caspase-9 activation and caspase cleavage of tau in the Alzheimer's disease brain. Neurobiol Dis. 2002; 11:341–354. [PubMed: 12505426]
44. Papasozomenos SC. Tau protein immunoreactivity in dementia of the Alzheimer type. I. Morphology, evolution, distribution, and pathogenetic implications. Lab Invest. 1989; 60:123–137. [PubMed: 2492060]
45. Ding Q, Markesbery WR, Chen Q, Li F, Keller JN. Ribosome dysfunction is an early event in Alzheimer's disease. J Neurosci. 2005; 25:9171–9175. [PubMed: 16207876]
46. Pestova TV, Lomakin IB, Lee JH, Choi SK, Dever TE, Hellen CU. The joining of ribosomal subunits in eukaryotes requires eIF5B. Nature. 2000; 403:332–335. [PubMed: 10659855]
47. Strittmatter WJ, Saunders AM, Goedert M, Weisgraber KH, Dong LM, Jakes R, Huang DY, Pericak-Vance M, Schmechel D, Roses AD. Isoform-specific interactions of apolipoprotein E with microtubule-associated protein tau: Implications for Alzheimer disease. Proc Natl Acad Sci U S A. 1994; 91:11183–11186. [PubMed: 7972031]
48. Carlier MF, Simon C, Cassoly R, Pradel LA. Interaction between microtubule-associated protein tau and spectrin. Biochimie. 1984; 66:305–311. [PubMed: 6743699]
49. Higuchi M, Iwata N, Matsuba Y, Takano J, Suemoto T, Maeda J, Ji B, Ono M, Staufenbiel M, Suhara T, Saido TC. Mechanistic involvement of the calpain-calpastatin system in Alzheimer neuropathology. FASEB J. 2012; 26:1204–1217. [PubMed: 22173972]
50. Ringger NC, O'Steen BE, Brabham JG, Silver X, Pineda J, Wang KKW, Hayes RL, Papa L. A novel marker for traumatic brain injury: CSF alphaII-spectrin breakdown product levels. J Neurotrauma. 2004; 21:1443–1456. [PubMed: 15672634]
51. Gauthier-Kemper A, Weissmann C, Golovyashkina N, Sebo-Lemke Z, Drewes G, Gerke V, Heinisch JJ, Brandt R. The frontotemporal dementia mutation R406W blocks tau's interaction with the membrane in an annexin A2-dependent manner. J Cell Biol. 2011; 192:647–661. [PubMed: 21339331]
52. Crary JF, Trojanowski JQ, Schneider JA, Abisambra JF, Abner EL, Alafuzoff I, Arnold SE, Attems J, Beach TG, Bigio EH, Cairns NJ, Dickson DW, Gearing M, Grinberg LT, Hof PR, Hyman BT, Jellinger K, Jicha GA, Kovacs GG, Knopman DS, Kofler J, Kukull WA, Mackenzie IR, Masliah E, McKee A, Montine TJ, Murray ME, Neltner JH, Santa-Maria I, Seeley WW, Serrano-Pozo A, Shelanski ML, Stein T, Takao M, Thal DR, Toledo JB, Troncoso JC, Vonsattel JP, White CL 3rd, Wisniewski T, Woltjer RL, Yamada M, Nelson PT. Primary age-related tauopathy (PART): A common pathology associated with human aging. Acta Neuropathol. 2014; 128:755–766. [PubMed: 25348064]
53. Kim DJ, Martinez-Lemus LA, Davis GE. EB1, p150Glued, and Clasp1 control endothelial tubulogenesis through microtubule assembly, acetylation, and apical polarization. Blood. 2013; 121:3521–3530. [PubMed: 23444400]
54. DuBoff B, Gotz J, Feany MB. Tau promotes neurodegeneration via DRP1 mislocalization *in vivo*. Neuron. 2012; 75:618–632. [PubMed: 22920254]
55. Flanagan LA, Cunningham CC, Chen J, Prestwich GD, Kosik KS, Janmey PA. The structure of divalent cation-induced aggregates of PIP2 and their alteration by gelsolin and tau. Biophys J. 1997; 73:1440–1447. [PubMed: 9284311]

56. Ferhat L, Chevassus au Louis N, Jorquera I, Niquet J, Khrestchatisky M, Ben-Ari Y, Represa A. Transient increase of tenascin-C in immature hippocampus: Astroglial and neuronal expression. J Neurocytol. 1996; 25:53–66. [PubMed: 8852938]
57. Gold MS, Kobeissy FH, Wang KK, Merlo LJ, Bruijnzeel AW, Krasnova IN, Cadet JL. Methamphetamine-and trauma-induced brain injuries: Comparative cellular and molecular neurobiological substrates. Biol Psychiatry. 2009; 66:118–127. [PubMed: 19345341]
58. Song J, Goetz BD, Kirvell SL, Butt AM, Duncan ID. Selective myelin defects in the anterior medullary velum of the taiep mutant rat. Glia. 2001; 33:1–11. [PubMed: 11169787]
59. Avsar T, Korkmaz D, Tutuncu M, Demirci NO, Saip S, Kamasak M, Siva A, Turanli ET. Protein biomarkers for multiple sclerosis: Semi-quantitative analysis of cerebrospinal fluid candidate protein biomarkers in different forms of multiple sclerosis. Mult Scler. 2012; 18:1081–1091. [PubMed: 22252467]
60. Weinger JG, Davies P, Acker CM, Brosnan CF, Tsiperson V, Bayewitz A, Shafit-Zagardo B. Mice devoid of Tau have increased susceptibility to neuronal damage in myelin oligodendrocyte glycoprotein-induced experimental autoimmune encephalomyelitis. J Neuropathol Exp Neurol. 2012; 71:422–433. [PubMed: 22487860]
61. Garver TD, Oyler GA, Harris KA, Polavarapu R, Damuni Z, Lehman RA, Billingsley ML. Tau phosphorylation in brain slices: Pharmacological evidence for convergent effects of protein phosphatases on tau and mitogen-activated protein kinase. Mol Pharmacol. 1995; 47:745–756. [PubMed: 7723735]
62. Jicha GA, Lane E, Vincent I, Otvos L Jr, Hoffmann R, Davies P. A conformation- and phosphorylation-dependent antibody recognizing the paired helical filaments of Alzheimer's disease. J Neurochem. 1997; 69:2087–2095. [PubMed: 9349554]
63. Goedert M, Jakes R, Qi Z, Wang JH, Cohen P. Protein phosphatase 2A is the major enzyme in brain that dephosphorylates tau protein phosphorylated by proline-directed protein kinases or cyclic AMP-dependent protein kinase. J Neurochem. 1995; 65:2804–2807. [PubMed: 7595582]
64. Kimura T, Ono T, Takamatsu J, Yamamoto H, Ikegami K, Kondo A, Hasegawa M, Ihara Y, Miyamoto E, Miyakawa T. Sequential changes of tau-site-specific phosphorylation during development of paired helical filaments. Dementia. 1996; 7:177–181. [PubMed: 8835879]
65. Goedert M, Wischik CM, Crowther RA, Walker JE, Klug A. Cloning and sequencing of the cDNA encoding a core protein of the paired helical filament of Alzheimer disease: Identification as the microtubule-associated protein tau. Proc Natl Acad Sci U S A. 1988; 85:4051–4055. [PubMed: 3131773]
66. Hoffmann R, Lee VM, Leight S, Varga I, Otvos L Jr. Unique Alzheimer's disease paired helical filament specific epitopes involve double phosphorylation at specific sites. Biochemistry. 1997; 36:8114–8124. [PubMed: 9201960]
67. Hashiguchi M, Sobue K, Paudel HK. 14-3-3zeta is an effector of tau protein phosphorylation. J Biol Chem. 2000; 275:25247–25254. [PubMed: 10840038]
68. Chun J, Kwon T, Lee EJ, Kim CH, Han YS, Hong SK, Hyun S, Kang SS. 14-3-3 Protein mediates phosphorylation of microtubule-associated protein tau by serum-and glucocorticoid-induced protein kinase 1. Mol Cells. 2004; 18:360–368. [PubMed: 15650334]
69. Sluchanko NN, Seit-Nebi AS, Gusev NB. Phosphorylation of more than one site is required for tight interaction of human tau protein with 14-3-3zeta. FEBS Lett. 2009; 583:2739–2742. [PubMed: 19647741]
70. Infante AA, Infante D, Chan MC, How PC, Kutschera W, Linhartova I, Mullner EW, Wiche G, Propst F. Ferritin associates with marginal band microtubules. Exp Cell Res. 2007; 313:1602–1614. [PubMed: 17391669]
71. Schmitt-Ulms G, Matenia D, Drewes G, Mandelkow EM. Interactions of MAP/microtubule affinity regulating kinases with the adaptor complex AP-2 of clathrin-coated vesicles. Cell Motil Cytoskeleton. 2009; 66:661–672. [PubMed: 19536824]
72. Talaei F, Van Praag VM, Shishavan MH, Landheer SW, Buikema H, Henning RH. Increased protein aggregation in Zucker diabetic fatty rat brain: Identification of key mechanistic targets and the therapeutic application of hydrogen sulfide. BMC Cell Biol. 2014; 15:1. [PubMed: 24393531]

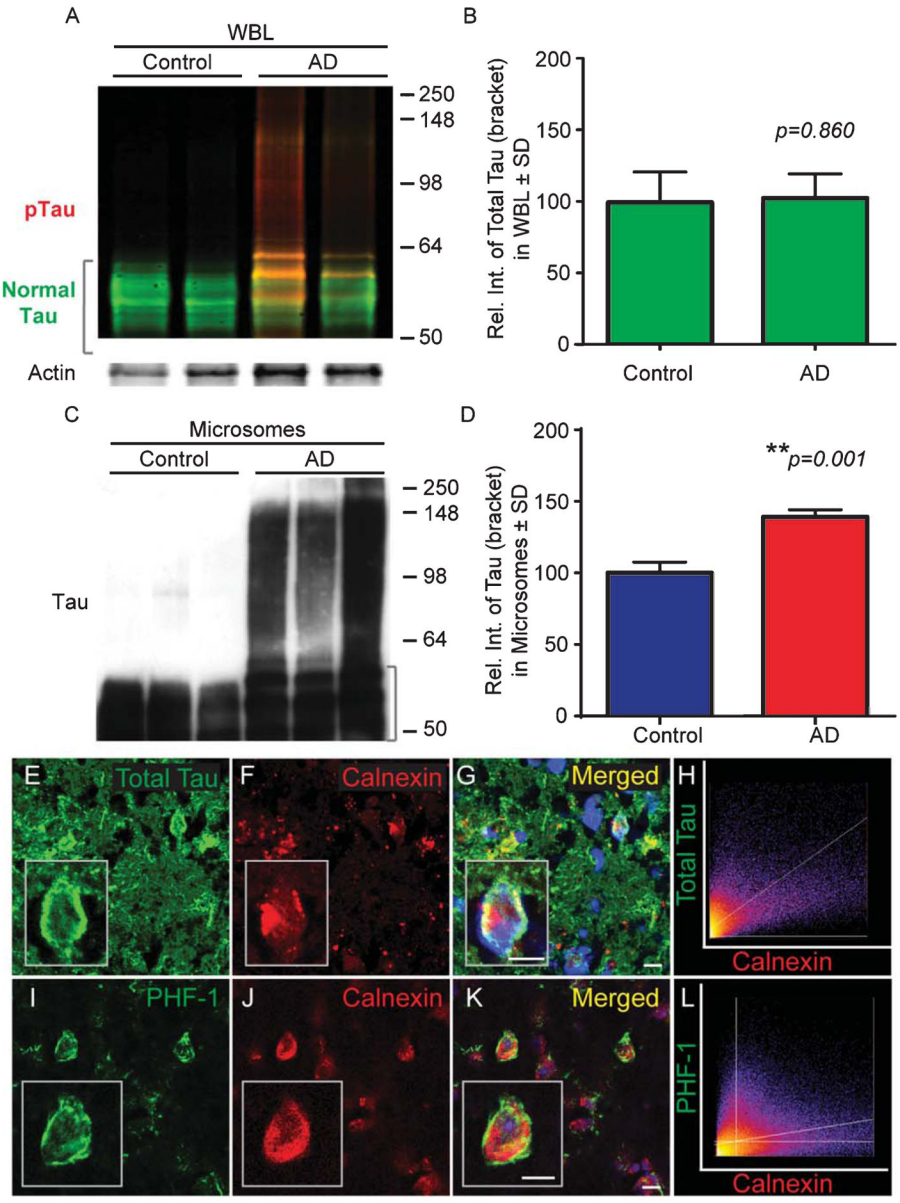

Fig. 1.

Tau is enriched in the endoplasmic reticulum of AD brains. A–D) Representative western blots and quantification analysis (of protein between 48–60kDa) for total tau in whole brain lysate (WBL) (A) or microsomes (C) in human non-demented control and AD brains. Hyperphosphorylated tau (pTau) was detected in the AD samples only (red bands in A). Actin was used as loading control for whole brain lysate. Ponceau S stain before incubation with antibody served as a loading control in the microsome blots. B) Total tau levels are not significantly different in the whole cell lysates of AD and control. D) Tau levels were increased in AD microsomes by 39%. E–L) Representative co-immunofluorescent images of human AD brain showing that both total tau and PHF1-positive signal partially co-localize with calnexin. Sections were stained with antibodies against total tau (green; E and G), PHF1 (green; I and K), and calnexin (red; F, G, J, and K). Cell nuclei were revealed with

DAPI staining (blue). H, L) Co-localization analysis with Manders (avg. 0.79 for total tau and 0.85 for PHF1) and Costes' coefficients reveals that tau partially co-localizes with calnexin. Scale bar = 10 μm.

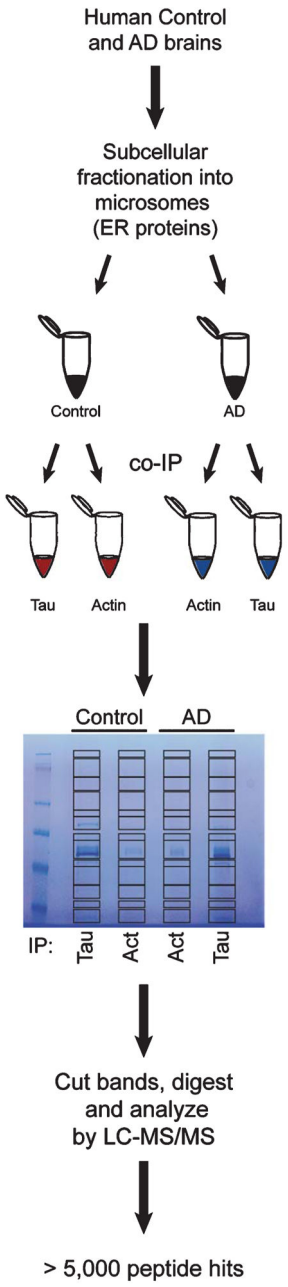

Fig. 2.

Experimental procedure for microsome co-IP-LC-MS/MS. First, microsomes were isolated from AD and non-AD control brains. Then, tau or actin were co-immunoprecipitated from the microsomal protein fractions. Samples were separated by SDS-PAGE, bands were revealed and consequently cut form the gel by Coomassie staining. Sample proteins were trypsinized and subjected to LC-MS/MS.

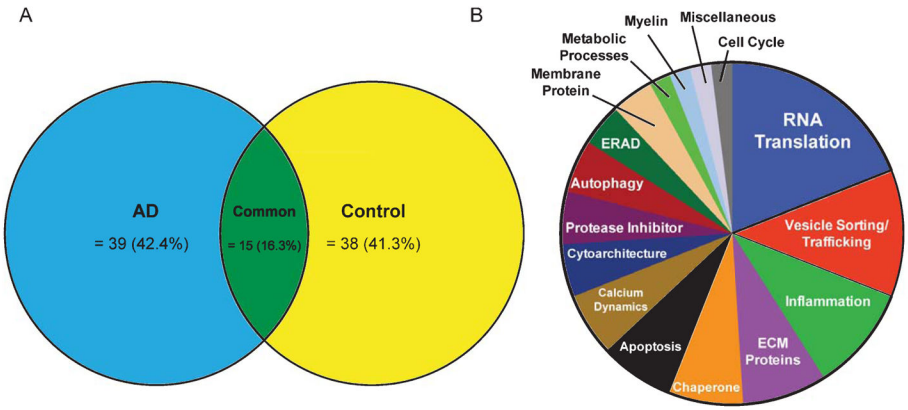

Fig. 3.

Comparison of tau-associated ER proteins in AD and non-AD brains. A) Venn diagram depicting the distribution of tau-associated ER proteins based on tissue of origin. Ninety-two tau-associated ER proteins were identified in AD and non-AD brains. Of these, 39 we only found in AD, 38 were only found in control, and 15 were common between both conditions. B) Pie chart showing the relative abundance of all tau-associated ER proteins identified by function. The identified proteins were grouped into functional categories.

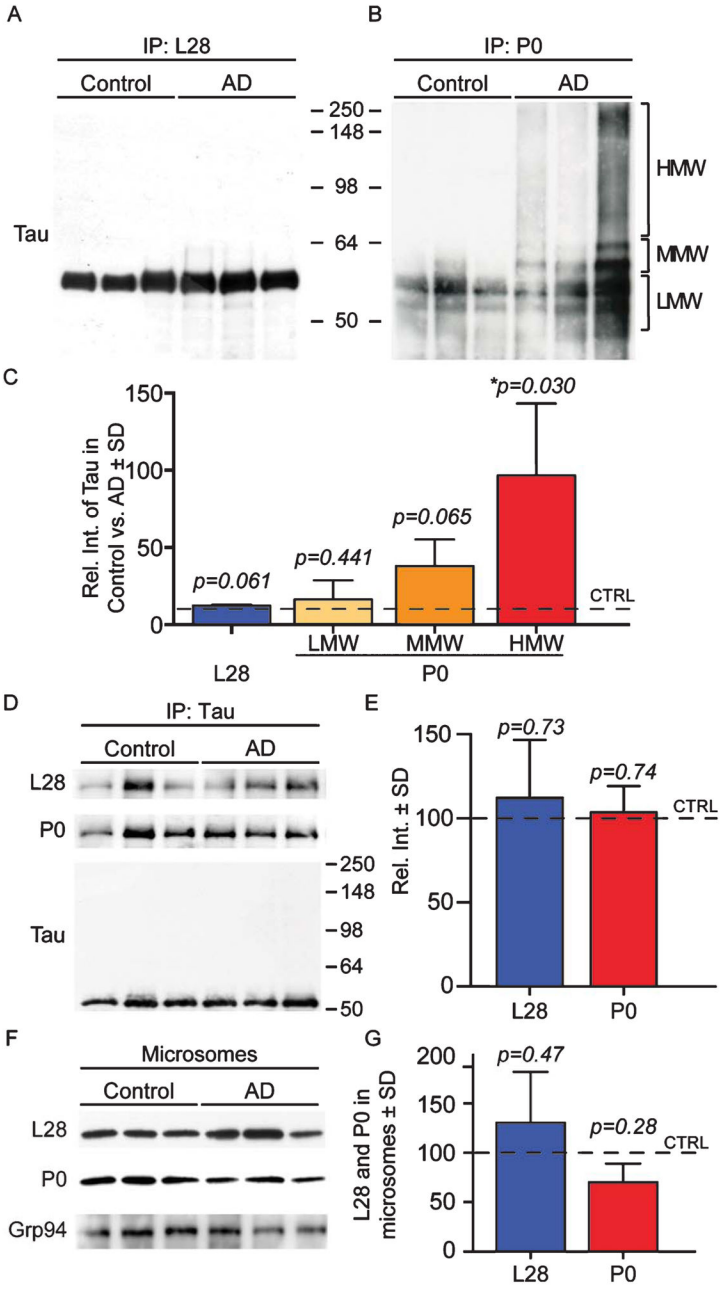

Fig. 4.

Tau associates differentially with L28 and P0 in both AD and control brains. A, B) Representative co-IP-western blots, in which the ribosomal proteins L28 (A) and P0 (B) were co-IP from human control and AD brains. Total tau association with P0 and L28 was determined with western blot with an antibody that recognizes the first 150 aa of tau. C) AD and control samples showed that similar levels of tau co-immunoprecipitated with L28. Tau co-immunoprecipitated more robustly with P0 in the high molecular weight range (HMW) when compared to the medium and low molecular weight bands (MMW and LMW). HMW = 65–250 kDa; MMW = 60–64 kDa; LMW = 50–60 kDa. D) Representative co-IP-western

blot with a tau antibody that recognizes aa 210–241 (Tau5) showed similar co-immunoprecipitation between tau and L28 or P0. E) Quantification of panel D shows that the association of P0 and L28 with Tau 5 is not significantly different. F, G) Representative western blot shows that the levels of L28 and P0 in human control and AD brain microsomes are not statistically significantly different. Grp94 was used as a loading control for microsomes.

Table 1

Tau-associated ER proteins in AD brain only

Accession	Description	Previously described as a tau-associated protein?	Score
Q06033	Inter-alpha-trypsin inhibitor heavy chain H3 OS = Homo sapiens GN = ITIH3 PE = 1 SV = 2 - [ITIH3_HUMAN]	No	203.13
Q9UN36	Protein NDRG2 OS = Homo sapiens GN = NDRG2 PE = 1 SV = 2 - [NDRG2_HUMAN]	No	79.01
Q8IXJ6	NAD-dependent deacetylase sirtuin-2 OS = Homo sapiens GN = SIRT2 PE = 1 SV = 2 - [SIRT2_HUMAN]	Indirect and correlative link with microtubule dynamics [53]	60.57
P27105	Erythrocyte band 7 integral membrane protein OS = Homo sapiens GN = STOM PE = 1 SV = 3 - [STOM_HUMAN]	No	55.41
P08237	6-phosphofructokinase, muscle type OS = Homo sapiens GN = PFKM PE = 1 SV = 2 - [K6PF_HUMAN]	No	54.69
P09525	Annexin A4 OS = Homo sapiens GN = ANXA4 PE = 1 SV = 4 - [ANXA4_HUMAN]	Interacting partner of tau to regulate membrane binding [51]	53.95
P06396	Gelsolin OS = Homo sapiens GN = GSN PE = 1 SV = 1 - [GELS_HUMAN]	No direct interaction; overexpression of gelsolin ameliorates neurodegeneration in tau transgenic mice [54]. Gelsolin and tau bind to PIP2 and have opposing effects on its aggregation [55].	50.52
P19823	Inter-alpha-trypsin inhibitor heavy chain H2 OS = Homo sapiens GN = ITIH2 PE = 1 SV = 2 - [ITIH2_HUMAN]	No	49.60
Q12931	Heat shock protein 75 kDa, mitochondrial OS = Homo sapiens GN = TRAP1 PE = 1 SV = 3 - [TRAP1_HUMAN]	No	45.81
O43813	LanC-like protein 1 OS = Homo sapiens GN = LANCL1 PE = 1 SV = 1 - [LANC1_HUMAN]	No	42.94
P24821	Tenascin OS = Homo sapiens GN = TNC PE = 1 SV = 3 - [TENA_HUMAN]	mRNA for tenascin and tau expressed in the same cells (immature neurons) [56].	42.44
Q13813	Spectrin alpha chain, brain OS = Homo sapiens GN = SPTAN1 PE = 1 SV = 3 - [SPTA2_HUMAN]	Tau interacts with spectrin [48]. Elevated levels in CSF of AD [49] and TBI [50]. Tau and spectrin are subject to cleavage in ischemia [57].	40.35
P23515	Oligodendrocyte-myelin glycoprotein OS = Homo sapiens GN = OMG PE = 1 SV = 2 - [OMGP_HUMAN]	Levels are inversely correlated in *taiep* oligodendrocytes [58]; both increased in CSF of multiple sclerosis clinical subtypes [59]; MOG-induced encephalomyelitis is ameliorated when tau is present [60].	38.81
P05388	60 S acidic ribosomal protein P0 OS = Homo sapiens GN = RPLP0 PE = 1 SV = 1 - [RLA0_HUMAN]	No	37.93
Q8NHW5	60 S acidic ribosomal protein P0-like OS = Homo sapiens GN = RPLP0P6 PE = 5 SV = 1 - [RLA0L_HUMAN]	No	37.93
P01024	Complement C3 OS = Homo sapiens GN = C3 PE = 1 SV = 2 - [CO3_HUMAN]	No	34.67
O75363	Breast carcinoma-amplified sequence 1 OS = Homo sapiens GN = BCAS1 PE = 1 SV = 2 - [BCAS1_HUMAN]	No	34.07
Q13085	Acetyl-CoA carboxylase 1 OS = Homo sapiens GN = ACACA PE = 1 SV = 2 - [ACACA_HUMAN]	No	33.82
P01834	Ig kappa chain C region OS = Homo sapiens GN = IGKC PE = 1 SV = 1 - [IGKC_HUMAN]	No	32.32

Accession	Description	Previously described as a tau-associated protein?	Score
P18583	Protein SON OS = Homo sapiens GN = SON PE = 1 SV = 4 - [SON_HUMAN]	No	31.63
Q9Y696	Chloride intracellular channel protein 4 OS = Homo sapiens GN = CLIC4 PE = 1 SV = 4 - [CLIC4_HUMAN]	No	31.05
Q99683	Mitogen-activated protein kinase kinase kinase 5 OS = Homo sapiens GN = MAP3K5 PE = 1 SV = 1 - [M3K5_HUMAN]	MAPK phosphorylates tau [61] at several sites associated with disease [62–66].	30.63
O75445	Usherin OS = Homo sapiens GN = USH2A PE = 1 SV = 3 - [USH2A_HUMAN]	No	29.78
Q6ZS92	Putative uncharacterized protein FLJ45721 OS = Homo sapiens PE = 5 SV = 2 - [YD022_HUMAN]	No	29.45
P02787	Serotransferrin OS = Homo sapiens GN = TF PE = 1 SV = 3 - [TRFE_HUMAN]	No	29.43
Q9C0B2	Uncharacterized protein KIAA1751 OS = Homo sapiens GN = KIAA1751 PE = 2 SV = 2 - [K1751_HUMAN]	No	29.30
Q16181	Septin-7 OS = Homo sapiens GN = SEPT7 PE = 1 SV = 2 - [SEPT7_HUMAN]	No	28.94
Q8N3Z3	GTP-binding protein 8 OS = Homo sapiens GN = GTPBP8 PE = 2 SV = 1 - [GTPB8_HUMAN]	No	28.86
Q6P5Z2	Serine/threonine-protein kinase N3 OS = Homo sapiens GN = PKN3 PE = 1 SV = 1 - [PKN3_HUMAN]	No	28.65
P37108	Signal recognition particle 14 kDa protein OS = Homo sapiens GN = SRP14 PE = 1 SV = 2 - [SRP14_HUMAN]	No	28.30
Q9NX45	Spermatogenesis- and oogenesis-specific basic helix-loop-helix-containing protein 2 OS = Homo sapiens GN = SOHLH2 PE = 2 SV = 2 - [SOLH2_HUMAN]	No	28.10
P52746	Zinc finger protein 142 OS = Homo sapiens GN = ZNF142 PE = 1 SV = 4 - [ZN142_HUMAN]	No	27.65
P09238	Stromelysin-2 OS = Homo sapiens GN = MMP10 PE = 1 SV = 1 - [MMP10_HUMAN]	No	26.30
Q14624	Inter-alpha-trypsin inhibitor heavy chain H4 OS = Homo sapiens GN = ITIH4 PE = 1 SV = 4 - [ITIH4_HUMAN]	No	26.05
P08195	4F2 cell-surface antigen heavy chain OS = Homo sapiens GN = SLC3A2 PE = 1 SV = 3 - [4F2_HUMAN]	No	25.65
Q9BXR6	Complement factor H-related protein 5 OS = Homo sapiens GN = CFHR5 PE = 1 SV = 1 - [FHR5_HUMAN]	No	25.64
P48643	T-complex protein 1 subunit epsilon OS = Homo sapiens GN = CCT5 PE = 1 SV = 1 - [TCPE_HUMAN]	No	24.40
O43896	Kinesin-like protein KIF1 C OS = Homo sapiens GN = KIF1 C PE = 1 SV = 3 - [KIF1C_HUMAN]	No	24.16
Q8WWZ7	ATP-binding cassette sub-family A member 5 OS = Homo sapiens GN = ABCA5 PE = 2 SV = 2 - [ABCA5_HUMAN]	No	24.10

Table 2

Tau-associated ER proteins in non-demented brain only

Accession	Description	Previously described as a tau-associated protein?	Score
Q04917	14-3-3 protein eta OS = Homo sapiens GN = YWHAH PE = 1 SV = 4 - [1433F_HUMAN]	Yes; particularly studied in relation with zeta subunit of 14-3-3 [67–69]	130.11
Q9Y2J2	Band 4.1-like protein 3 OS = Homo sapiens GN = EPB41L3 PE = 1 SV = 2 - [E41L3_HUMAN]	No	95.21
P31944	Caspase-14 OS = Homo sapiens GN = CASP14 PE = 1 SV = 2 - [CASPE_HUMAN]	No	84.42
Q5D862	Filaggrin-2 OS = Homo sapiens GN = FLG2 PE = 1 SV = 1 - [FILA2_HUMAN]	No	75.88
P06702	Protein S100-A9 OS = Homo sapiens GN = S100A9 PE = 1 SV = 1 - [S10A9_HUMAN]	No	75.56
P05109	Protein S100-A8 OS = Homo sapiens GN = S100A8 PE = 1 SV = 1 - [S10A8_HUMAN]	No	73.36
P09543	2′,3′-cyclic-nucleotide 3′-phosphodiesterase OS = Homo sapiens GN = CNP PE = 1 SV = 2 - [CN37_HUMAN]	No	61.21
O43426	Synaptojanin-1 OS = Homo sapiens GN = SYNJ1 PE = 1 SV = 2 - [SYNJ1_HUMAN]	No	61.16
P61421	V-type proton ATPase subunit d 1 OS = Homo sapiens GN = ATP6V0D1 PE = 1 SV = 1 - [VA0D1_HUMAN]	No	54.66
P31947	14-3-3 protein sigma OS = Homo sapiens GN = SFN PE = 1 SV = 1 - [1433S_HUMAN]	Yes; particularly studied in relation with zeta subunit of 14-3-3 [67–69]	41.58
P02794	Ferritin heavy chain OS = Homo sapiens GN = FTH1 PE = 1 SV = 2 - [FRIH_HUMAN]	Yes. [70]	40.73
Q8N8Y2	V-type proton ATPase subunit d 2 OS = Homo sapiens GN = ATP6V0D2 PE = 2 SV = 1 - [VA0D2_HUMAN]	No	40.48
P60201	Myelin proteolipid protein OS = Homo sapiens GN = PLP1 PE = 1 SV = 2 - [MYPR_HUMAN]	Levels are inversely correlated in *taiep* oligodendrocytes [58]	36.83
O43150	Arf-GAP with SH3 domain, ANK repeat and PH domain-containing protein 2 OS = Homo sapiens GN = ASAP2 PE = 1 SV = 3 - [ASAP2_HUMAN]	No	36.65
Q96A05	V-type proton ATPase subunit E 2 OS = Homo sapiens GN = ATP6V1E2 PE = 1 SV = 1 - [VATE2_HUMAN]	No	35.24
O94973	AP-2 complex subunit alpha-2 OS = Homo sapiens GN = AP2A2 PE = 1 SV = 2 - [AP2A2_HUMAN]	Tau associates with MARK via AP-2 [71]	35.06
Q9NZT1	Calmodulin-like protein 5 OS = Homo sapiens GN = CALML5 PE = 1 SV = 2 - [CALL5_HUMAN]	No	32.84
P17600	Synapsin-1 OS = Homo sapiens GN = SYN1 PE = 1 SV = 3 - [SYN1_HUMAN]	No	32.11
Q12888	Tumor suppressor p53-binding protein 1 OS = Homo sapiens GN = TP53BP1 PE = 1 SV = 2 - [TP53B_HUMAN]	No	30.20
Q6ZP68	Putative uncharacterized protein C13orf35 OS = Homo sapiens GN = C13orf35 PE = 2 SV = 1 - [CM035_HUMAN]	No	30.01
P20930	Filaggrin OS = Homo sapiens GN = FLG PE = 1 SV = 3 - [FILA_HUMAN]	No	29.89
O14594	Neurocan core protein OS = Homo sapiens GN = NCAN PE = 2 SV = 3 - [NCAN_HUMAN]	No	29.82
Q6PJG9	Leucine-rich repeat and fibronectin type-III domain-containing protein 4 OS = Homo sapiens GN = LRFN4 PE = 1 SV = 1 - [LRFN4_HUMAN]	No	28.84
P36957	Dihydrolipoyllysine-residue succinyltransferase component of 2-oxoglutarate dehydrogenase complex, mitochondrial OS = Homo sapiens GN = DLST PE = 1 SV = 3 - [ODO2_HUMAN]	No	28.56
P10915	Hyaluronan and proteoglycan link protein 1 OS = Homo sapiens GN = HAPLN1 PE = 2 SV = 2 - [HPLN1_HUMAN]	No	28.49

Accession	Description	Previously described as a tau-associated protein?	Score
Q92598	Heat shock protein 105 kDa OS = Homo sapiens GN = HSPH1 PE = 1 SV = 1 - [HS105_HUMAN]	No	28.36
Q16658	Fascin OS = Homo sapiens GN = FSCN1 PE = 1 SV = 3 - [FSCN1_HUMAN]	No	28.28
P51674	Neuronal membrane glycoprotein M6-a OS = Homo sapiens GN = GPM6A PE = 1 SV = 2 - [GPM6A_HUMAN]	No	27.75
Q9HCE3	Zinc finger protein 532 OS = Homo sapiens GN = ZNF532 PE = 1 SV = 2 - [ZN532_HUMAN]	No	27.03
P55774	C-C motif chemokine 18 OS = Homo sapiens GN = CCL18 PE = 1 SV = 1 - [CCL18_HUMAN]	No	26.36
Q15334	Lethal(2) giant larvae protein homolog 1 OS = Homo sapiens GN = LLGL1 PE = 1 SV = 3 - [L2GL1_HUMAN]	No	25.52
Q96BH1	E3 ubiquitin-protein ligase RNF25 OS = Homo sapiens GN = RNF25 PE = 1 SV = 1 - [RNF25_HUMAN]	No	25.18
Q9Y2K2	IK3 OS = Homo sapiens GN = SIK3 PE = 1 SV = 3 - [SIK3_HUMAN]	No	23.83
Q6SJ93	Protein FAM111B OS = Homo sapiens GN = FAM111B PE = 2 SV = 1 - [F111B_HUMAN]	No	23.50
O43264	Centromere/kinetochore protein zw10 homolog OS = Homo sapiens GN = ZW10 PE = 1 SV = 3 - [ZW10_HUMAN]	No	23.43
Q9H254	Spectrin beta chain, brain 3 OS = Homo sapiens GN = SPTBN4 PE = 1 SV = 2 - [SPTN4_HUMAN]	No	21.74
Q6N021	Probable methylcytosine dioxygenase TET2 OS = Homo sapiens GN = TET2 PE = 1 SV = 3 - [TET2_HUMAN]	No	20.86
Q9NU22	Midasin OS = Homo sapiens GN = MDN1 PE = 1 SV = 2 - [MDN1_HUMAN]	No	26.11

Table 3

Tau-associated ER proteins common in AD and control brains

Accession	Description	Previously described as a tau-associated protein?	Score
P10636	Microtubule-associated protein tau OS = Homo sapiens GN = MAPT PE = 1 SV = 4 - [TAU_HUMAN]	Yes	721.33
P02751	Fibronectin OS = Homo sapiens GN = FN1 PE = 1 SV = 4 - [FINC_HUMAN]	Fibronectin and tau inclusions are present in Zucker diabetic fatty rat brain [72]	180.85
P68104	Elongation factor 1-alpha 1 OS = Homo sapiens GN = EEF1A1 PE = 1 SV = 1 - [EF1A1_HUMAN]	No	149.33
Q5VTE0	Putative elongation factor 1-alpha-like 3 OS = Homo sapiens GN = EEF1AL3 PE = 5 SV = 1 - [EF1A3_HUMAN]	No	149.33
Q05639	Elongation factor 1-alpha 2 OS = Homo sapiens GN = EEF1A2 PE = 1 SV = 1 - [EF1A2_HUMAN]	No	123.84
P00450	Ceruloplasmin OS = Homo sapiens GN = CP PE = 1 SV = 1 - [CERU_HUMAN]	No	108.22
Q9UK22	F-box only protein 2 OS = Homo sapiens GN = FBXO2 PE = 1 SV = 2 - [FBX2_HUMAN]	No	51.26
P00738	Haptoglobin OS = Homo sapiens GN = HP PE = 1 SV = 1 - [HPT_HUMAN]	No	47.95
P20742	Pregnancy zone protein OS = Homo sapiens GN = PZP PE = 1 SV = 4 - [PZP_HUMAN]	No	41.12
P01023	Alpha-2-macroglobulin OS = Homo sapiens GN = A2M PE = 1 SV = 3 - [A2MG_HUMAN]	No	41.12
Q92985	Interferon regulatory factor 7 OS = Homo sapiens GN = IRF7 PE = 1 SV = 2 - [IRF7_HUMAN]	No	33.87
P31946	14-3-3 protein beta/alpha OS = Homo sapiens GN = YWHAB PE = 1 SV = 3 - [1433B_HUMAN]	No	32.98
P46779	60 S ribosomal protein L28 OS = Homo sapiens GN = RPL28 PE = 1 SV = 3 - [RL28_HUMAN]	No	27.67
P02649	Apolipoprotein E OS = Homo sapiens GN = APOE PE = 1 SV = 1 - [APOE_HUMAN]	Yes [47]	24.52
Q6ZQQ6	WD repeat-containing protein 87 OS = Homo sapiens GN = WDR87 PE = 2 SV = 3 - [WDR87_HUMAN]	No	24.26

Brief Communications

Pathological Tau Promotes Neuronal Damage by Impairing Ribosomal Function and Decreasing Protein Synthesis

Shelby Meier,[1] Michelle Bell,[1] Danielle N. Lyons,[1] Jennifer Rodriguez-Rivera,[1] Alexandria Ingram,[1] Sarah N. Fontaine,[1] Elizabeth Mechas,[1] Jing Chen,[2] Benjamin Wolozin,[3] Harry LeVine III,[1,2] Haining Zhu,[2] and Jose F. Abisambra[1,4]

[1]Sanders Brown Center on Aging, [2]Departments of Molecular and Cellular Biochemistry, and [3]Pharmacology, Boston University School of Medicine, Boston, Massachusetts 02118, and [4]Department of Physiology, College of Medicine, University of Kentucky, Lexington, Kentucky 40536-0230

One of the most common symptoms of Alzheimer's disease (AD) and related tauopathies is memory loss. The exact mechanisms leading to memory loss in tauopathies are not yet known; however, decreased translation due to ribosomal dysfunction has been implicated as a part of this process. Here we use a proteomics approach that incorporates subcellular fractionation and coimmunoprecipitation of tau from human AD and non-demented control brains to identify novel interactions between tau and the endoplasmic reticulum (ER). We show that ribosomes associate more closely with tau in AD than with tau in control brains, and that this abnormal association leads to a decrease in RNA translation. The aberrant tau–ribosome association also impaired synthesis of the synaptic protein PSD-95, suggesting that this phenomenon contributes to synaptic dysfunction. These findings provide novel information about tau-protein interactions in human brains, and they describe, for the first time, a dysfunctional consequence of tau–ribosome associations that directly alters protein synthesis.

Key words: **Alzheimer; ribosome; RNA; tau; tauopathies; translation**

Significance Statement

Despite the identification of abnormal tau–ribosomal interactions in tauopathies >25 years ago, the consequences of this association remained elusive until now. Here, we show that pathological tau associates closely with ribosomes in AD brains, and that this interaction impairs protein synthesis. The overall result is a stark reduction of nascent proteins, including those that participate in synaptic plasticity, which is crucial for learning and memory. These data mechanistically link a common pathologic sign, such as the appearance of pathological tau inside brain cells, with cognitive impairments evident in virtually all tauopathies.

Introduction

Aberrant accumulation of tau is associated with the etiology of >18 known neurodegenerative diseases collectively termed tauopathies. Alzheimer's disease (AD), the most common tauopathy, affects >36 million people world-wide (Alzheimer's Association, 2014). A common and early symptom in tauopathic patients is progressive memory loss. There is no cure for tauopathies, and current therapeutics stave off symptoms only temporarily. This is partly due to limited understanding of the molecular mechanisms linking tau and disease onset.

Synaptic function depends on constant protein synthesis; therefore, neurons are especially vulnerable to chronic attenuation of RNA translation (Moreno et al., 2012). Although, transient suppression of translation is an adaptive cellular response to endoplasmic reticulum (ER) stress (Harding et al., 1999), chronic inhibition of RNA translation contributes to

Received Aug. 11, 2015; revised Dec. 2, 2015; accepted Dec. 12, 2015.

Author contributions: S.M., S.N.F., B.W., and J.F.A. designed research; S.M., M.B., D.N.L., J.R.-R., A.I., E.M., J.C., H.L., H.Z., and J.F.A. performed research; S.M., D.L., J.R.-R., H.Z., and J.F.A. analyzed data; S.M., S.N.F., B.W., and J.F.A. wrote the paper.

The University of Kentucky Alzheimer's Disease Center (UK-ADC) and its Neuropathology Core is supported by NIH/NIA P30 AG028383; the University of Kentucky Proteomics Core is partially supported by grants from the NIH/NIGMS (P20GM103486) and the NIH/NCI (P30CA177558); this work was also supported in part by NIH R01NS077284 (H.Z.); the LC-MS/MS instrument was acquired with a High-End Instrumentation Grant S10RR029127 (H.Z.) from the National Institutes of Health; NIH/NINDS P30NS051220 supported the maintenance of the microscopy core used for imaging; J.F.A., D.L., and S.M. were supported by NIH/NINDS 1R01 NS091329-01, Alzheimer's Association NIRG-14-322441, NIH/NCATS 5UL1TR000117-04, NIH/NIGMS 5P30GM110787, GlaxoSmithKline, Department of Defense AZ140097, UK-ADC Pilot Award 8.1 supported by NIH/NIA P30 AG028383, the University of Kentucky Epilepsy Center and NIH/NIMHD L32 MD009205-01. We thank Dr Pedro Vera and the Lexington, VA Medical Center for support, Dr Peter Davies for his generous contribution of the PHF1 antibody used for immunofluorescent staining, Dr Chad Dickey for developing and sharing the iHEK cell lines and the tau plasmids, Ela Patel and Sonya Anderson with their assistance accessing the human brain tissue, Dr Fred Schmitt for insightful discussions and crucial intellectual contributions to this study, and the generous contribution of oligomers and T22 antibodies from Dr Rakez Kayed and Urmi Sengupta.

The authors declare no competing financial interests.

Correspondence should be addressed to Dr Jose F. Abisambra, Sanders-Brown Center on Aging and Department of Physiology, College of Medicine, University of Kentucky, 800 South Limestone Street, Lexington, KY 40536-0230. E-mail: joe.abisambra@uky.edu.

DOI:10.1523/JNEUROSCI.3029-15.2016

 0270-6474/16/361001-07$15.00/0

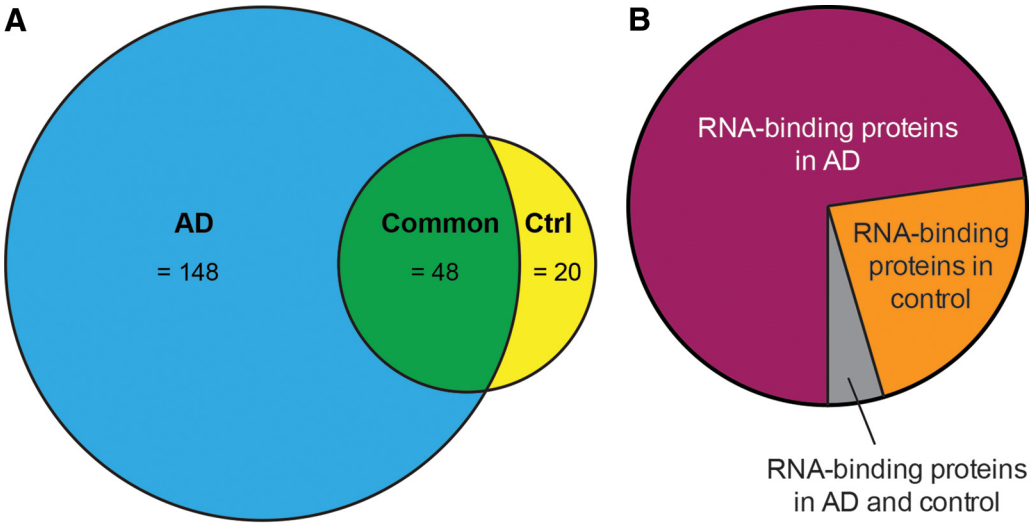

C

Tau-associated RNA-binding proteins		
Unique to AD samples	Unique to Control samples	Common in AD and Ctrl
60S ribosomal protein L23	60S ribosomal protein L19	60S ribosomal protein L18
60S ribosomal protein L24	60S ribosomal protein L14	
40S ribosomal protein S23	60S acidic ribosomal protein P2	60S ribosomal protein L15
60S acidic ribosomal protein P0	60S acidic ribosomal protein P1	
60S acidic ribosomal protein P0-like	40S ribosomal protein S17	60S ribosomal protein L29
60S ribosomal protein L35	40S ribosomal protein SA	
60S ribosomal protein L10	60S ribosomal protein L26-like	60S ribosomal protein L17
40S ribosomal protein S3a	40S ribosomal protein S25	
40S ribosomal protein S13	40S ribosomal protein S7	60S ribosomal protein L26
60S ribosomal protein L13a	Eukaryotic translation initiation factor 4H	
Putative 60S ribosomal protein L13a-like	Eukaryotic translation initiation factor 5A-1	60S ribosomal protein L23a
60S ribosomal protein L21	Elongation factor 2	
WD repeat-containing protein 33	Elongation factor Tu	Phenylalanyl-tRNA synthetase alpha chain
Kinesin heavy chain isofom 5C	Phenylalanyl-tRNA synthetase beta chain	

Figure 1. Tau associates with ER proteins differentially in AD versus control brains. ***A***, Venn diagram showing the number of tau-associated ER proteins unique to AD brains (blue), unique to control brains (yellow), and common to both (green). A major group of proteins that was identified corresponded to RNA-binding proteins. ***B***, Pie chart showing relative abundance of tau-associated, RNA-binding proteins identified in human AD and control brains by LC-MS/MS. ***C***, List of proteins identified in ***B***.

the pathogenesis of multiple neurodegenerative disorders, including tauopathies (Vanderweyde et al., 2012; Abisambra et al., 2013b; Ash et al., 2014). Pronounced ribosomal deficiencies appear in regions where tau pathology is evident (Ding et al., 2005), yet the link between tau and ribosomal function has not been established.

Protein synthesis drives memory formation (Duvarci et al., 2008). The fact that progressive memory loss is common to virtually all tauopathies suggests that ribosomal dysfunction could be an underlying mechanism leading to clinical symptoms. Indeed, tau binds to ribosomes in the brain, and this interaction is enhanced in tauopathic brains (Papasozomenos and Binder, 1987; Piao et al., 2002).

Here we show that ribosomes associate with pathologic and nonpathological tau. Consequently, ribosomal function becomes impaired and global protein synthesis is reduced including the synaptic protein PSD-95. These data suggest that tau-mediated ribosomal dysfunction is a common pathogenic process that affects synapses leading to cognitive impairment.

Materials and Methods

Human brain samples. Human samples were obtained from the University of Kentucky (UK) Alzheimer's Disease Center. Sample collection and experimental procedures involving human tissue were in compliance with the UK Institutional Review board. Samples from Brodmann areas 21/22 were used. AD tissues were scored as Braak V (female, 93-year-old), VI (male, 88-year-old), and VI (female, 80-year-old); samples from non-demented controls were Braak I (male, 79-year-old), II (female, 94-year-old), and II (female, 88-year-old). The average postmortem interval was 3 h.

Microsomes, coimmunoprecipitation, and liquid-chromatography tandem mass spectrometry. Microsomes were isolated as previously described (Lopez et al., 2007) and modified for the brain (Abisambra et al., 2010). Coimmunoprecipitation (co-IP) was performed as previously described (Jinwal et al., 2012) using anti-Tau46 (Cell Signaling Technology) and anti-actin (Sigma-Aldrich). Protein complexes were identified using liquid-chromatography tandem mass spectrometry (LC-MS/MS) and UNIPROT as previously described (Meier et al., 2015).

In vitro *translation assay.* 1-Step IVT Kit (Thermo) was used with minor modifications: a black bottom 96-well plate was loaded with *in*

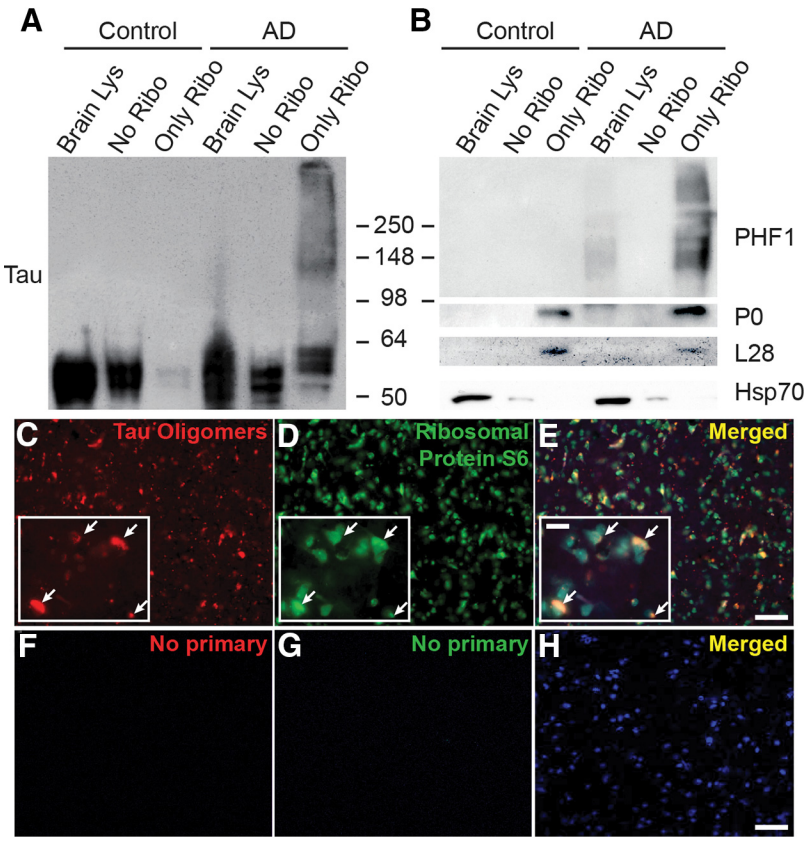

Figure 2. Pathological tau associates closely with ribosomes in AD brains. Representative immunoblots showing total tau (***A***) and PHF1-positive smear (***B***) enriched in AD brain ribosomal fraction. P0 and L28 (ribosomal proteins) and Hsp70 (cytosolic) confirm subcellular fractionation. ***C–E***, Representative IF of AD brains showing overlap of oligomeric tau and rpS6 in human AD brain. Co-IF labeling of tau oligomers with T22 (red; ***C***), rpS6 (green; ***D***), and neurons (Neurotrace; blue). ***E***, Merged inset image shows red and green overlap (arrowheads). ***F–H***, Representative images of AD brains in which primary antibody incubation was omitted.

vitro translation (IVT)-kit components and 10 ng of recombinant proteins. GFP (ex-482 nm/em-512 nm) was measured every 15 min in a BioTek Synergy HT at 30°C for 6 h. Each sample was run in triplicate and analyzed using GraphPad Prism (Student's *t* test).

Cell culture, primary neurons, and immunoblotting. Cell maintenance, harvesting, and tau expression were performed as previously described (Abisambra et al., 2012, 2013b). P0–P1 primary neurons were obtained as previously described (Abisambra et al., 2013a). Samples were processed for immunoblotting as described earlier using BCA (Pierce) to estimate protein concentration, tris-glycine gels (Invitrogen), and PVDF membranes (Jones et al., 2011). Primary antibodies: anti-tau h-150 (1:1000; Santa Cruz Biotechnology), actin (1:1000, Sigma-Aldrich), RPL28 and RPP0 (1:1000, GeneTex), PHF1 (1:500), Hsp70 (1:1000, ENZO), PSD-95 (1:1000, Cell Signaling Technology), and puromycin (1:1000, EMD Millipore). Bands were detected using (Pierce ECL). Image analysis was performed using ImageJ. Bands of the protein of interest were normalized to a loading control. Statistical analysis was performed using Student's *t* test in GraphPad Prism.

Surface sensing of translation. Surface sensing of translation (SUnSET) was performed as previously described (Schmidt et al., 2009) with minor modifications: cells were incubated with 10 μg/ml of puromycin in cell culture media for 1 h before harvest. Proteins were analyzed using immunoblots.

Immunofluorescence. Immunofluorescence (IF) was performed as previously described (Abisambra et al., 2013b). Primary antibodies: T22 (1:100) and RPS6 (1:250; Santa Cruz Biotechnology). Tissues were also stained with Sudan black and Neurotrace (1:200). Slides with AD and control sections were stained omitting primary antibodies to establish nonspecific background signal.

Microscopy. A Nikon Eclipse Ti laser-scanning confocal microscope was used to capture images. Fields analyzed using 40× and 100× objectives included areas of tau staining with morphologic distribution in agreement with Neurotrace labeling. All acquisition intensities, field sizes, and settings were kept consistent across all images. Images were prepared using the NIS Elements 4.20 (Nikon) and Photoshop Cs6 (Adobe) software and were based upon cells that most closely represented the group.

Quantitative real-time PCR. Total RNA was extracted from rTg4510 tau transgenic and littermate control primary neuronal cultures using EZNA total RNA Kit II according to manufacture instructions (Omega Bio-tek, catalog #R6934-01). RNA was quantified using a BioTek spectrophotometer and cDNA was produced using SuperScript IV (Invitrogen). Quantitative real-time PCR was performed using TaqMan Gene Expression probes for PSD-95 and GAPDH using a ViiA 7 Real Time PCR System (Applied Biosystems). PSD-95 expression was evaluated by normalizing to GAPDH as an internal control. The real-time values for each sample were average and evaluated using the comparative CT method.

Results

We recently determined ER-bound proteins associate with tau (Abisambra et al., 2013b; Meier et al., 2015). To identify tau-associated ER proteins in AD, microsomes were isolated from non-demented control and AD brain tissues. Full-length tau (or actin as control) was co-IP from microsomes, and tau-associated peptides were identified using LC-MS/MS. Of the 216 identified proteins, 68.5% were unique in AD, 22.2% were unique in control, and 9.3% were common between both groups (Fig. 1*A*). Proteins were grouped into functional categories based on UNIPROT. A striking difference was that tau associated with more RNA-binding proteins in AD than in control (Fig. 1*B*,*C*).

To further characterize the tau–ribosome association, we compared tau levels in AD and control subcellular fractions (Fig. 2*A*). Although tau levels were similar between the fractions lacking ribosomes, tau was significantly increased in the AD ribosomal fraction (Fig. 2*A*). We also detected a PHF1-positive smear in the AD ribosomes (Fig. 2*B*). PHF1 recognizes pS396/S404, which is associated with late stage tangles in AD (Greenberg et al., 1992).

Recent studies show that oligomeric tau is highly toxic (Lasagna-Reeves et al., 2011), and it exhibits a prion-like behavior by propagating and seeding (Guo and Lee, 2011). We speculated that if aberrant tau–ribosome complexes were pathogenic, then tau oligomers would associate with ribosomes. To test this, we co-IF labeled tau oligomers and a ribosomal protein, rpS6, in AD and control brain sections (Fig. 2*C–H*). Confocal imaging revealed that tau oligomers and rpS6 signals overlapped (Fig. 2*C–E*), suggesting that oligomeric tau associates closely with ribosomes in AD.

The consequences of the tau–ribosome association are unknown. We hypothesized that the aberrant interaction between pathological tau species and ribosomes impairs translation. To test this, we measured the impact of tau on ribosomal function in

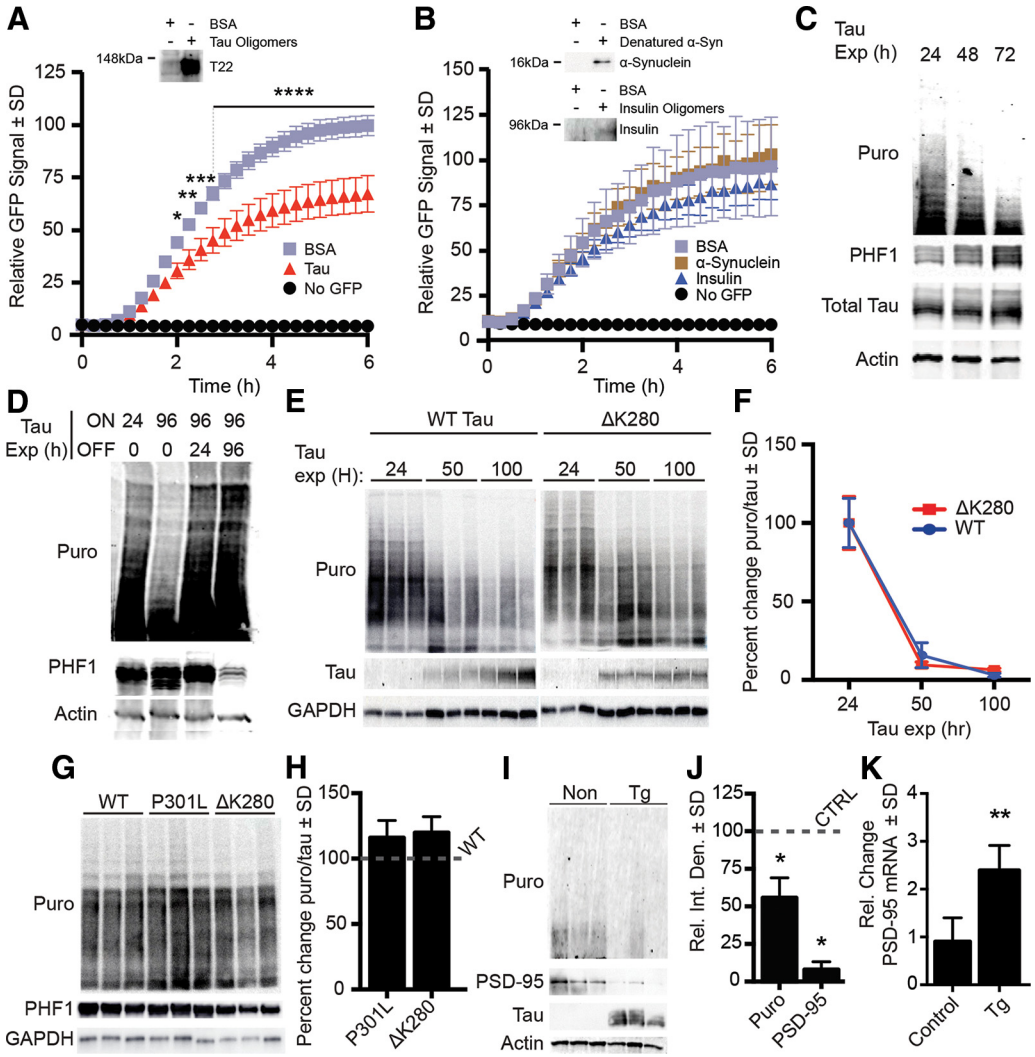

Figure 3. Pathological tau species decrease translation. ***A***, IVT graph showing 32% reduction of translational output (after 6 h) in wells with tau oligomers compared with BSA control. ***B***, Oligomeric α-synuclein and insulin did not affect translation. Immunoblots confirm the presence of oligomers in the translation assay; α-synuclein samples were denatured to yield monomers because high molecular weight oligomeric conformers are not detectable with anti-α-synuclein antibodies. ***C***, Total and PHF1 tau are inversely proportional to the rate of protein synthesis. iHEK-Tau cells were stimulated with tetracycline to express tau for 4 d. Nascent proteins were tagged with puromycin. ***D***, Cessation of tau expression rescues protein synthesis. Tau expression was induced with tetracycline for 24 or 96 h (lanes 1 and 2). At 96 h, puromycin levels decreased, whereas PHF1 increased. After continuous tau expression for 96 h (lanes 3 and 4), cells were washed and incubated with media lacking tetracycline, thereby halting tau expression for 24 or 96 h (lanes 3 and 4, respectively). ***E***, Representative immunoblots showing the effect of wild-type (WT) and ΔK280 tau on protein synthesis. Changes in tau levels inversely correlated with puromycin. ***F***, Quantification of ***E*** showing no significant difference in levels of protein synthesis between wild-type and ΔK280 mutant tau-expressing cells. ***G***, SUnSET comparing the effect of P301L, ΔK280 tau, and WT in transiently transfected HEK293 cells. ***H***, Quantification of ***G*** showing no significant difference between translation levels. ***I***, Blot showing that overall translation (Puro) and PSD-95 are decreased in rTg4510 primary neurons. ***J***, Quantification of ***I***. Puromycin and PSD-95 were significantly decreased in rTg4510 neurons by 43 and 92%, respectively (*$p < 0.05$). ***K***, Quantification of PSD-95 mRNA expression from rTg4510 neurons as measured by RT-PCR (**$p = 0.0013$).

three model systems. First, we tested the effect of tau oligomers on translation using a cell-free assay. We added recombinant tau oligomers or bovine serum albumin (BSA) as control with *in vitro* translation assay components and a GFP plasmid reporter. The rate of translation, measured by GFP, was significantly decreased in the presence of tau oligomers (Fig. 3*A*). To determine whether this effect was specific to tau oligomers, we tested the impact of oligomeric α-synuclein and insulin on translation (Fig. 3*B*). We found no significant change in GFP, suggesting that this effect is specific to tau.

We next measured the effect of pathological tau on the rate of translation in eukaryotic cells using SUnSET (Schmidt et al., 2009): a puromycin-based pulse assay. Puromycin, which is incorporated into recently translated proteins, was added to medium 1 h before harvesting cells. Nascent proteins, which appear as a smear, can then be quantified via immunoblots with anti-puromycin antibodies.

We used iHEK-Tau cells, an inducible HEK line that overexpresses wild-type human 4R0N tau upon addition of tetracycline (Abisambra et al., 2013b). Use of tetracycline allowed control over the start and overall duration of tau expression. We first performed a time course experiment in which tetracycline was added to iHEK-Tau cells over 72 h. We found that increased PHF1 and total tau levels correlated with decreased puromycin signal (Fig. 3*C*). We then performed a rescue experiment in which tau was expressed for 96 h and then tau expression was turned off for 24 or 96 h (Fig. 3*D*). We found that puromycin levels were rescued back to normal control once PHF1 levels were reduced.

Because mutations on tau are associated with risk for many tauopathies, we sought to determine whether mutant tau variants

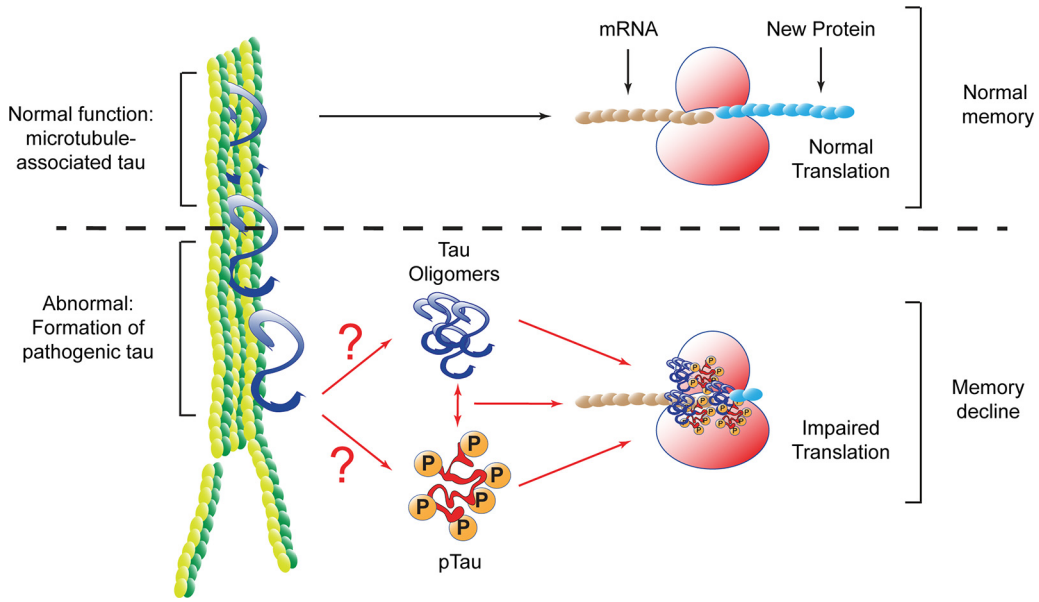

Figure 4. Schematic representation showing the consequences of pathological tau association with ribosomes. Under normal conditions, tau promotes tubulin polymerization and stabilizes microtubules. *De novo* protein synthesis, and in particular nascent neurotransmitter production is necessary for normal learning and memory. Our data suggest that in tauopathic brains, tau adopts aberrant conformations that associate with ribosomes. This interaction reduces nascent protein synthesis. Abrogation of new proteins impairs memory. This mechanism links the most common symptom of tauopathies.

inhibited protein synthesis. To this end, we performed SUnSET in iHEK cells that overexpress the disease-associated ΔK280 tau (Rosso et al., 2003). We found that expression of WT or ΔK280 tau decreased protein synthesis (Fig. 3*E*), and that this reduction was not significantly different between the two cell lines (Fig. 3*F*). We then compared translation levels between mutant forms of tau by transiently transfecting HEK293 cells with WT, ΔK280, or P301L tau plasmids. We found no significant difference in protein synthesis levels between WT, ΔK280, or P301L-expressing cells (Fig. 3*G*,*H*). These data suggest that tau expression and accumulation of hyperphosphorylated tau impairs protein synthesis.

To determine the impact of pathological tau species in a more neurologically relevant model, we measured changes in the rate of translation in primary neurons derived from rTg4510 tau transgenic and control mice using SUnSET. The rTg4510 model overexpresses human P301L mutant tau (Santacruz et al., 2005). At 14 DIV, puromycin was added to the medium and primary neurons were harvested. Puromycin-tagged proteins were decreased by 43% in rTg4510 neurons ($^*p = 0.011$) compared with control (Fig. 3*I*,*J*). We then investigated whether a more direct correlate of synaptic integrity could be affected by pathological tau in this model. To this end, we measured the levels of the PSD-95 and found that it was reduced by 92% in rTg4510 neurons ($^*p = 0.049$; Fig. 3*I*,*J*). We hypothesized that tau-mediated disruption of RNA translation would result in increased mRNA levels. We performed RT-PCR and found that PSD-95 cDNA was increased by twofold in rTg4510 primary neurons compared with controls (Fig. 3*K*). These data suggest that P301L tau impairs RNA translation, and that this pathological mechanism directly affects translation without impairing gene expression.

Discussion

This study couples cellular and biochemical approaches with proteomics to expand the understanding of the ER-specific tau interactome. The unbiased proteomics approach (Fig. 1) identified 216 tau-associated ER proteins; many of which were unreported. The largest change corresponded to an increase in the association of ribosomal proteins with tau in AD. Using three *in vitro* models, we show that protein synthesis was significantly decreased as a consequence of the aberrant tau–ribosome association. Although it has been previously reported that tau interacted with ribosomes (Papasozomenos and Binder, 1987; Nelson et al., 1993), the functional consequences of this interaction was unknown until now. We have identified a dysfunctional consequence of tau–ribosome association that impairs protein synthesis, providing the first steps to understanding the mechanism delineating cognitive decline symptoms in tauopathic patients (Fig. 4).

LC-MS/MS results suggest that many other ER proteins (216 total) associate with tau. The use of mass spectrometry for identification of protein-protein interactions is limited and only provides a "first pass" suggestion. For example, whether these interactions are direct, indirect, or false-positives need to be investigated further. As shown in Figure 2, we validated the interaction between tau and ribosomes, and the validation of other interactions is currently underway. When comparing the RNA-binding proteins that associate with tau, we did not find elongation or initiation factors associating with tau in AD samples (Fig. 1*C*). These data suggest that the association of pathological tau with ribosomes abrogates the recruitment of translation factors to the tau–ribosome complex, and this could lead to reduced translation.

To avoid false-positive results from the LC-MS/MS, we implemented rigorous exclusion criteria (Meier et al., 2015), which omitted well known tau-associated proteins, but increased confidence in these interactions. Our co-IP focused on identifying mature, and not nascent, tau. We used a tau antibody (Tau46) that recognizes the carboxy-terminal tau sequence (404–441). As such this approach obviates caspase-cleaved tau, which is cleaved at D421 and is implicated in the formation of neurofibrillary tangles in AD (Rissman et al., 2004). Future efforts to identify cleaved tau-associated ER proteins might determine novel pathologic mechanisms. Nonetheless, our current list does provide fur-

ther information about the diverse interactions of tau and other ER proteins.

Although tau mutations are not typically associated with risk for AD, there are 48 tau mutations that are associated with onset of other tauopathies (for review, see Zhang et al., 2015). The defining pathologic hallmark of tangles in AD is hyperphosphorylated tau (Grundke-Iqbal et al., 1986). Interestingly, we found that protein synthesis was impaired equally by WT and two disease-associated mutant tau variants: P301L and ΔK280. P301L tau is most commonly associated with frontotemporal dementia and Parkinsonism linked to chromosome 17 (FTDP-17; Clark et al., 1998). Expression of this form of tau in the rTg4510 transgenic mice leads to earlier onset and robust neurofibrillary tangle formation (Santacruz et al., 2005). The ΔK280 tau mutant is also associated with FTDP-17 (Rosso et al., 2003), as well as AD (Momeni et al., 2009). The presence of this mutation decreases tau's ability to bind to microtubules (Rizzu et al., 1999), and leads to increased levels of tau aggregation (Barghorn et al., 2000). Our findings indicate that tau-mediated impairment of protein synthesis could be a common mechanism of neuronal dysfunction between tauopathies (Fig. 4).

Our data support the hypothesis that pathological tau specifically reduces ribosomal function, which could lead to memory alterations in tauopathies. We also found that PSD-95, a synaptic protein that participates in learning and memory (Migaud et al., 1998), was decreased in rTg4510 neurons (Fig. 3*I*,*J*). Cognitive impairment seen tauopathy models could be attributed not only to reduced protein synthesis, but also to targeted decrease of synaptic proteins.

Interestingly, oligomers of other proteins (α-synuclein and insulin) did not alter ribosomal function (Fig. 3*B*). This finding suggests that there is a mechanism of ribosomal downregulation that specifically implicates tau, but not all other oligomeric and pathologically altered proteins. However, it is possible that proteins involved in the pathogenic mechanisms of other neurodegenerative disorders such as Aβ, poly-glutamines, and TDP-43 could also inhibit *de novo* protein synthesis. Experiments to test the effects of these oligomers are currently underway.

Characterization of this ribosome-directed molecular mechanism of tauopathies could provide novel therapeutic opportunities. For instance, therapeutic strategies aiming to uncouple pathological tau from the ribosome might restore RNA translation and prove effective to treat AD and other tauopathies. To do this, specific ribosomal proteins that associate with tau need to be identified as well as the discreet regions where tau binds to these proteins. This would guide the proof-of-concept use of peptides resembling these amino acid stretches to outcompete tau from associating with the ribosome and thereby restore protein synthesis.

This work suggests a direct effect of tau on translation by its association with ribosomes; however, there is also an indirect relationship between tau and translation. One of these is the chronic activation of the protein kinase RNA-like endoplasmic reticulum kinase (PERK). Accumulation of tau impairs ER-associated degradation, which then activates the unfolded protein response and subsequently the PERK pathway (Abisambra et al., 2013b). The prolonged activation of the PERK pathway leads to a reduction in RNA translation through phosphorylation of the initiation factor eIF2α (Marciniak et al., 2006). This alteration could be a cumulative result of tau's direct and indirect effects on translation. Our study provides further evidence that tau's involvement in disease is multi-faceted, that pathological tau heavily affects translation of vital proteins, and that the tau–ribosome complex could serve as a key therapeutic target for tauopathies.

References

Abisambra JF, Fiorelli T, Padmanabhan J, Neame P, Wefes I, Potter H (2010) LDLR expression and localization are altered in mouse and human cell culture models of Alzheimer's disease. PloS One 5:e8556. CrossRef Medline

Abisambra JF, Jinwal UK, Suntharalingam A, Arulselvam K, Brady S, Cockman M, Jin Y, Zhang B, Dickey CA (2012) DnaJA1 antagonizes constitutive Hsp70-mediated stabilization of tau. J Mol Biol 421:653–661. CrossRef Medline

Abisambra J, Jinwal UK, Miyata Y, Rogers J, Blair L, Li X, Seguin SP, Wang L, Jin Y, Bacon J, Brady S, Cockman M, Guidi C, Zhang J, Koren J, Young ZT, Atkins CA, Zhang B, Lawson LY, Weeber EJ, et al. (2013a) Allosteric heat shock protein 70 inhibitors rapidly rescue synaptic plasticity deficits by reducing aberrant tau. Biol Psychiatry 74:367–374. CrossRef Medline

Abisambra JF, Jinwal UK, Blair LJ, O'Leary JC 3rd, Li Q, Brady S, Wang L, Guidi CE, Zhang B, Nordhues BA, Cockman M, Suntharalingham A, Li P, Jin Y, Atkins CA, Dickey CA (2013b) Tau accumulation activates the unfolded protein response by impairing endoplasmic reticulum-associated degradation. J Neurosci 33:9498–9507. CrossRef Medline

Alzheimer's Association (2014) 2014 Alzheimer's disease facts and figures. Alzheimers Dement 10:e47–e92. CrossRef Medline

Ash PE, Vanderweyde TE, Youmans KL, Apicco DJ, Wolozin B (2014) Pathological stress granules in Alzheimer's disease. Brain Res 1584:52–58. CrossRef Medline

Barghorn S, Zheng-Fischhöfer Q, Ackmann M, Biernat J, von Bergen M, Mandelkow EM, Mandelkow E (2000) Structure, microtubule interactions, and paired helical filament aggregation by tau mutants of frontotemporal dementias. Biochemistry 39:11714–11721. CrossRef Medline

Clark LN, Poorkaj P, Wszolek Z, Geschwind DH, Nasreddine ZS, Miller B, Li D, Payami H, Awert F, Markopoulou K, Andreadis A, D'Souza I, Lee VM, Reed L, Trojanowski JQ, Zhukareva V, Bird T, Schellenberg G, Wilhelmsen KC (1998) Pathogenic implications of mutations in the tau gene in pallido-ponto-nigral degeneration and related neurodegenerative disorders linked to chromosome 17. Proc Natl Acad Sci U S A 95:13103–13107. CrossRef Medline

Ding Q, Markesbery WR, Chen Q, Li F, Keller JN (2005) Ribosome dysfunction is an early event in Alzheimer's disease. J Neurosci 25:9171–9175. CrossRef Medline

Duvarci S, Nader K, LeDoux JE (2008) *De novo* mRNA synthesis is required for both consolidation and reconsolidation of fear memories in the amygdala. Learn Mem 15:747–755. CrossRef Medline

Greenberg SG, Davies P, Schein JD, Binder LI (1992) Hydrofluoric acid-treated tau PHF proteins display the same biochemical properties as normal tau. J Biol Chem 267:564–569. Medline

Grundke-Iqbal I, Iqbal K, Tung YC, Quinlan M, Wisniewski HM, Binder LI (1986) Abnormal phosphorylation of the microtubule-associated protein tau (tau) in Alzheimer cytoskeletal pathology. Proc Natl Acad Sci U S A 83:4913–4917. CrossRef Medline

Guo JL, Lee VM (2011) Seeding of normal tau by pathological tau conformers drives pathogenesis of Alzheimer-like tangles. J Biol Chem 286:15317–15331. CrossRef Medline

Harding HP, Zhang Y, Ron D (1999) Protein translation and folding are coupled by an endoplasmic-reticulum-resident kinase. Nature 397:271–274. CrossRef Medline

Jinwal UK, Abisambra JF, Zhang J, Dharia S, O'Leary JC, Patel T, Braswell K, Jani T, Gestwicki JE, Dickey CA (2012) Cdc37/Hsp90 protein complex disruption triggers an autophagic clearance cascade for TDP-43 protein. J Biol Chem 287:24814–24820. CrossRef Medline

Jones JR, Lebar MD, Jinwal UK, Abisambra JF, Koren J 3rd, Blair L, O'Leary JC, Davey Z, Trotter J, Johnson AG, Weeber E, Eckman CB, Baker BJ, Dickey CA (2011) The diarylheptanoid (+)-aR,11S-myricanol and two flavones from bayberry (*Myrica cerifera*) destabilize the microtubule-associated protein tau. J Nat Prod 74:38–44. CrossRef Medline

Lasagna-Reeves CA, Castillo-Carranza DL, Sengupta U, Clos AL, Jackson GR, Kayed R (2011) Tau oligomers impair memory and induce synaptic and mitochondrial dysfunction in wild-type mice. Mol Neurodegener 6:39. CrossRef Medline

Lopez D, Abisambra Socarrás JF, Bedi M, Ness GC (2007) Activation of the hepatic LDL receptor promoter by thyroid hormone. Biochim Biophys Acta 1771:1216–1225. CrossRef Medline

Marciniak SJ, Garcia-Bonilla L, Hu J, Harding HP, Ron D (2006) Activation-dependent substrate recruitment by the eukaryotic translation initiation factor 2 kinase PERK. J Cell Biol 172:201–209. CrossRef Medline

Meier S, Bell M, Lyons DN, Ingram A, Chen J, Gensel JC, Zhu H, Nelson PT, Abisambra JF (2015) Identification of novel tau interactions with endoplasmic reticulum proteins in Alzheimer's brain. J Alzheimers Dis 48: 687–702. CrossRef Medline

Migaud M, Charlesworth P, Dempster M, Webster LC, Watabe AM, Makhinson M, He Y, Ramsay MF, Morris RG, Morrison JH, O'Dell TJ, Grant SG (1998) Enhanced long-term potentiation and impaired learning in mice with mutant postsynaptic density-95 protein. Nature 396:433–439. CrossRef Medline

Momeni P, Pittman A, Lashley T, Vandrovcova J, Malzer E, Luk C, Hulette C, Lees A, Revesz T, Hardy J, de Silva R (2009) Clinical and pathological features of an Alzheimer's disease patient with the MAPT delta K280 mutation. Neurobiol Aging 30:388–393. CrossRef Medline

Moreno JA, Radford H, Peretti D, Steinert JR, Verity N, Martin MG, Halliday M, Morgan J, Dinsdale D, Ortori CA, Barrett DA, Tsaytler P, Bertolotti A, Willis AE, Bushell M, Mallucci GR (2012) Sustained translational repression by eIF2alpha-P mediates prion neurodegeneration. Nature 485: 507–511. CrossRef Medline

Nelson PT, Marton L, Saper CB (1993) Alz-50 immunohistochemistry in the normal sheep striatum: a light and electron microscope study. Brain Res 600:285–297. CrossRef Medline

Papasozomenos SC, Binder LI (1987) Phosphorylation determines two distinct species of tau in the central nervous system. Cell Motil Cytoskeleton 8:210–226. CrossRef Medline

Piao YS, Hayashi S, Wakabayashi K, Kakita A, Aida I, Yamada M, Takahashi H (2002) Cerebellar cortical tau pathology in progressive supranuclear palsy and corticobasal degeneration. Acta Neuropathol 103:469–474. CrossRef Medline

Rissman RA, Poon WW, Blurton-Jones M, Oddo S, Torp R, Vitek MP, LaFerla FM, Rohn TT, Cotman CW (2004) Caspase-cleavage of tau is an early event in Alzheimer disease tangle pathology. J Clin Invest 114: 121–130. CrossRef Medline

Rizzu P, Van Swieten JC, Joosse M, Hasegawa M, Stevens M, Tibben A, Niermeijer MF, Hillebrand M, Ravid R, Oostra BA, Goedert M, van Duijn CM, Heutink P (1999) High prevalence of mutations in the microtubule-associated protein tau in a population study of frontotemporal dementia in The Netherlands. Am J Hum Genet 64:414–421. CrossRef Medline

Rosso SM, Donker Kaat L, Baks T, Joosse M, de Koning I, Pijnenburg Y, de Jong D, Dooijes D, Kamphorst W, Ravid R, Niermeijer MF, Verheij F, Kremer HP, Scheltens P, van Duijn CM, Heutink P, van Swieten JC (2003) Frontotemporal dementia in The Netherlands: patient characteristics and prevalence estimates from a population-based study. Brain 126: 2016–2022. CrossRef Medline

Santacruz K, Lewis J, Spires T, Paulson J, Kotilinek L, Ingelsson M, Guimaraes A, DeTure M, Ramsden M, McGowan E, Forster C, Yue M, Orne J, Janus C, Mariash A, Kuskowski M, Hyman B, Hutton M, Ashe KH (2005) Tau suppression in a neurodegenerative mouse model improves memory function. Science 309:476–481. CrossRef Medline

Schmidt EK, Clavarino G, Ceppi M, Pierre P (2009) SUnSET, a nonradioactive method to monitor protein synthesis. Nat Methods 6:275–277. CrossRef Medline

Vanderweyde T, Yu H, Varnum M, Liu-Yesucevitz L, Citro A, Ikezu T, Duff K, Wolozin B (2012) Contrasting pathology of the stress granule proteins TIA-1 and G3BP in tauopathies. J Neurosci 32:8270–8283. CrossRef Medline

Zhang CC, Xing A, Tan MS, Tan L, Yu JT (2015) The role of MAPT in neurodegenerative diseases: genetics, mechanisms and therapy. Mol Neurobiol. Advance online publication. Retrieved Sep. 12, 2015. CrossRef Medline

Send Orders for Reprints to reprints@benthamscience.ae

146 *Current Alzheimer Research*, 2016, *13*, 146-159

FINAL

PERK-Opathies: An Endoplasmic Reticulum Stress Mechanism Underlying Neurodegeneration

Michelle C. Bell, Shelby E. Meier, Alexandria L. Ingram and Jose F. Abisambra*

Sanders-Brown Center on Aging and Department of Physiology, College of Medicine, University of Kentucky, 800 S Limestone Street, Lexington, KY 40536-0230, USA

Jose F. Abisambra

Abstract: The unfolded protein response (UPR) plays a vital role in maintaining cell homeostasis as a consequence of endoplasmic reticulum (ER) stress. However, prolonged UPR activity leads to cell death. This time-dependent dual functionality of the UPR represents the adaptive and cytotoxic pathways that result from ER stress. Chronic UPR activation in systemic and neurodegenerative diseases has been identified as an early sign of cellular dyshomeostasis.

The Protein Kinase R-like ER Kinase (PERK) pathway is one of three major branches in the UPR, and it is the only one to modulate protein synthesis as an adaptive response. The specific identification of prolonged PERK activity has been correlated with the progression of disorders such as diabetes, Alzheimer's disease, and cancer, suggesting that PERK plays a role in the pathology of these disorders. For the first time, the term "PERK-opathies" is used to group these diseases in which PERK mediates detriment to the cell culminating in chronic disorders. This article reviews the literature documenting links between systemic disorders with the UPR, but with a specific emphasis on the PERK pathway. Then, articles reporting links between the UPR, and more specifically PERK, and neurodegenerative disorders are presented. Finally, a therapeutic perspective is discussed, where PERK interventions could be potential remedies for cellular dysfunction in chronic neurodegenerative disorders.

Keywords: eIF2α, EIF2AK3, endoplasmic reticulum, neurodegeneration, PERK, tau, unfolded protein response.

INTRODUCTION

The endoplasmic reticulum (ER) provides an optimal environment to host fundamental biological processes such as protein folding, calcium storage, and lipid metabolism, making it an indispensable organelle for cell survival [1-3]. As such, evolutionarily conserved mechanisms regulate ER dynamics to ensure maintenance of these functions. Over a third of nascent proteins are folded in the ER lumen, where molecular chaperones triage misfolded proteins for refolding or degradation [4]. If they cannot be refolded, chaperone substrates (or clients) are targeted for degradation either by a proteasome-dependent pathway called ER-associated degradation (ERAD) or autophagy [5]. Effective chaperone function and clearance of clients out of the ER prevents secretion of unfolded or misfolded proteins. Unfolded and misfolded proteins have exposed hydrophobic signatures, and if they are released into the cytoplasm, the exposed unfolded sequence would trigger a heat shock protein response [5].

In neurological tissues, the aggregation of unfolded or misfolded proteins appears as the hallmark of several proteinopathies such as tauopathies (*e.g.* Alzheimer's disease, fronto-temporal dementia, and progressive supranuclear palsy), synucleinopathies (*e.g.* Lewy body disease and Parkinson's disease), aggregation of TDP-43 (amyotrophic lateral sclerosis, frontotemporal dementia, and hippocampal sclerosis), and diseases of poly-glutamine aggregation (*e.g.* Huntington's disease and ataxias), among many others.

Increasing evidence suggests that several neurodegenerative disorders are rooted in aberrant ER function. For instance, amyloid precursor protein (APP) is processed by secretases on the ER membrane. Under pathogenic conditions, APP processing yields the amyloid beta (Aβ) peptide that is responsible for neurotoxicity and amyloid plaque formation [5]. In AD, cleavage of APP favors production of Aβ, which is released from the ER membrane and initiates neurotoxic cascades. On the other hand, soluble and pathogenic tau, the aggregation of which leads to formation of tangles in AD and nineteen other tauopathies, impairs ER-associated degradation (ERAD) leading to chronic activation of the UPR [6]. In Parkinson's and Lewy Body Disease, α-synuclein is internalized in the ER, where it impairs protein transport between the ER and the Golgi network [7]. The mechanisms with which the ER combats proteinopathic insults are grouped into the unfolded protein response (UPR).

ER STRESS AND THE UNFOLDED PROTEIN RESPONSE

ER stress results from abnormalities that overwhelm normal ER performance. ER stress can be elicited by viral infection [5], blockage of ER protein clearance pathways such as ERAD [8], calcium disruptors, hypoglycemia, expos-

*Address correspondence to this author at the Sanders-Brown Center on Aging and Department of Physiology, College of Medicine, University of Kentucky, 800 S Limestone Street, Lexington, KY 40536-0230, USA; Tel: (859) 218-3852; Fax: (859) 323-0894; E-mail: joe.abisambra@uky.edu

1567-2050/16 $58.00+.00

ing cells to compounds such as tunicamycin, thapsigargin, and dithiothreitol, and hypoxia [9]. In response to ER stress, the cell activates the UPR [2]. The overall goal of this response is to restore ER function by decreasing input of nascent proteins and increasing output of folded proteins. In consequence, the UPR regulates size, shape, and abundance of luminal and transmembrane proteins [10], all of which contribute to the reestablishment of homeostasis.

Activation of the UPR begins by the dissociation of glucose-regulating proteins (GRPs) from three types of ER transmembrane anchors, namely IRE1 (Inositol-Requiring Protein 1 or Serine/Threonine-Protein Kinase/Endoribonuclease), ATF6 (Activating Transcription Factor α or Cyclic AMP-Dependent Transcription Factor), or PERK. GRPs are ER chaperones that facilitate refolding of nascent proteins [4]. Once detached from the membrane, GRPs associate with nascent proteins to facilitate their folding and secretion from the ER. Therefore, GRPs are ER-resident chaperones, and their dysfunction alone can lead to conditions such as juvenile onset glaucoma and blindness [6]. The most abundant GRPs are Grp78 (binding immunoglobulin protein or BiP) and Grp94 [11]. Meanwhile, each anchor, IRE1, ATF6, and PERK is free to initiate its own signaling pathways (Fig. **1**).

Under homeostatic conditions, IRE1 is constitutively attached to Grp78 under homeostatic conditions. Once detached, IRE1 dimerizes and autophosphorylates, which in turn activates RNase domains. Phosphorylated and active IRE1 targets and cleaves X box-binding protein 1 (XBP1), which is a transcriptional activator of UPR target genes such as ERAD proteins and ER chaperones [12, 13] (Fig. **1**). Other downstream transcription factors that are activated by XBP1 facilitate production of phospholipids that allow the ER membranes to expand under stress [12, 13]. If ER stress is maintained, sustained IRE1 function mediates activation of signaling cascades involved in cell death. Specifically, this apoptotic cascade activates the apoptosis signal-regulated kinase 1 (ASK1) and c-Jun N-terminal kinase (JNK) [14, 15] (Fig. **1**).

The ATF6 pathway also begins by its dissociation from Grp78, which provides S1 and S2 proteases to release ATF6 from the membrane. ATF6 translocates to the nucleus, where it promotes expression of Grp78, XBP1, C-EBP-Homologous Protein / Growth Arrest DNA Damage-Inducible transcript 3 (CHOP/GADD153), and Grp94. These effectors participate in protein folding, protein secretion, and ERAD [9, 16-19]. Together, this response facilitates protein output from the ER thereby offering relief and restoration of other functions.

PERK

The third branch of the UPR is initiated by PERK. The immediate objective of this cascade is to reduce translation of RNA in order to limit the input of nascent proteins in the ER. PERK has two regions: a luminal region that changes conformation when in contact with unfolded proteins and a cytoplasmic region containing a kinase domain that is necessary for activation [9]. Upon dissociation from Grp78, PERK dimerizes and autophosphorylates in a manner that is similar to the activation of IRE1. In turn, phosphorylation of PERK activates the kinase domain, which then targets substrates to activate the cascade. The best characterized PERK target is the eukaryotic initiation factor 2α (eIF2α) [5]. Phosphorylation of eIF2α prevents it from forming a complex with GTP, a step that is necessary for reloading eIF2 to initiate translation of mRNA. Therefore, p-eIF2α reduces protein synthesis [2, 20, 21]. Nonetheless, proteins that participate in UPR such as ERAD components, ER chaperones, UPR transcription factors, and mediators of the three branches of the UPR elude this mechanism (reviewed in [22]). The mRNA for these proteins contains pseudo-open or upstream open reading frames (uORFs) that avoid the p-eIF2α-mediated attenuation of translation. As a result of increased and selective expression of uORF-containing transcripts, the UPR pathways become robust permitting a return to homeostasis or activation of apoptosis [21].

Activating Transcription Factor-4 (ATF4) is another downstream effector of the PERK cascade. ATF4 is selectively enriched during ER stress by eluding PERK-mediated suppression of translation [20, 21, 23]. ATF4 plays a critical role in both relieving the ER for cell adaptation and activating apoptosis. As in the case of IRE1 and ASK1, the mechanisms responsible to this dual ATF4 function are crucial to understand the role of the UPR in cell survival versus death decisions. A key factor regulating the switch from activating pro-survival to favoring cell death pathways is the extent of time in which the UPR is active [24, 25].

In the case of acute PERK activity, ATF4 stimulates expression of proteins involved in cell recovery and adaptation such as ER chaperones. However, when PERK activity is chronic, sustained ATF4 levels upregulate pro-apoptotic proteins such as CHOP and growth arrest and DNA damage-inducible 34 (GADD34) [1, 2, 26]. Therefore, increased ATF4 decreases cell survival suggesting that prolonged translation of ATF4 is a primary signal for apoptosis under ER stress [3, 20]. ATF4 facilitates expression of CHOP, which in turn promotes apoptosis by enhancing expression of DR5 and *tribbles*-related protein 3. In parallel, ATF4 also participates in the inhibition of peroxisome proliferator-activated receptor γ, which triggers pro-apoptotic signals [4, 26-28].

Besides CHOP, ATF4 also induces the phosphatase activity of GADD34, which targets p-eIF2α. Initial expression of GADD34 negatively feeds back on the PERK pathway by dephosphorylating eIF2α to restore protein synthesis to its normal rate [29, 30]. However, extended GADD34 activity is associated with apoptosis via phosphorylation of (cellular tumor antigen p53) TP53 [31] (Fig. **1**).

Nrf2 (nuclear factor erythroid 2-related factor 2) is another direct substrate of PERK [32]. This second PERK substrate is a transcriptional activator that promotes expression of proteins involved in adaptation to oxidative stress [33]. Nrf2 exists ubiquitously in the cytoplasm attached to Keap1 (Kelch-like ECH-associated protein 1). Upon activation of the UPR, PERK-directed phosphorylation of Nrf2 dissociates the Keap1/Nrf2 complex. Consequently, Nrf2 is translocated to the nucleus where it activates transcription of proteins with antioxidant activity.

In addition to these direct interactions between PERK and eIF2α or PERK and Nrf2, the PERK pathway plays a central role in regulating the entire UPR. Expression of dominant-negative PERK facilitates activation of ATF6 and its downstream effector XBP1 [28]. The inability of cells to activate the PERK pathway under conditions of ER stress (*e.g.* exposure to tunicamycin) results in attenuated phosphorylation of eIF2α and delayed suppression of translation. In response, the ATF6 pathway is further enhanced compared to control cells [28]. These data suggest that UPR activity is exquisitely tuned in three different yet integrated branches. In addition, PERK facilitates ATF6 function by enhancing transport of ATF6 from the ER and Golgi [34]. These studies suggest that PERK is a central integrator of the UPR, and specific modulation of PERK activity could lead to overall UPR-directed cell survival/death pathways.

SYSTEMIC IMPLICATIONS

Diabetes Mellitus

Diabetes mellitus is caused by impaired insulin signals and decreased insulin secretion [35]. In both Type I and Type II diabetes, apoptosis of β-cells is the primary mechanism of cell death [35]. According to the American Diabetes Association, diabetes mellitus symptomatology includes frequent urination, feeling excessively thirsty or hungry, extreme fatigue, blurry vision, cuts and bruises that heal slowly, and tingling or numbness in the hands or feet. In the United States, 29.1 million people have diabetes, with approximately 27.8% of those people being undiagnosed. According to the Centers for Disease Control and Prevention's 2014 "National Diabetes Statistics Report: Estimates of Diabetes and Its Burden in the United States", 1.7 million Americans aged 20 or older were diagnosed with the disease in 2012.

PERK-mediated cell death, is implicated in the pathogenic process leading to diabetes mellitus [35]. Secretory cells, such as islet β-cells that are integral for insulin production, produce high levels of PERK [35, 36]. Demand for insulin requires these β-cells to produce upwards of one million molecules per minute, meaning the ER must modify and package the proteins for proper use [37]. PERK signaling is important for the normal function and survival of secretory cells [36]. The pancreatic β-cells are particularly susceptible to ER stress and therefore depend on PERK for proper function [35]; however, PERK might be responsible for this susceptibility. Just like in other cells, PERK can be protective and harmful in the pancreas. Under normal cellular conditions, the survival properties of PERK dominate; but under extreme stress, such as what is associated with diabetes, induction of cell death pathways becomes more prevalent [36].

PERK abnormalities are directly associated with diabetes. In Scandinavians, the PERK gene maps to a locus that is implicated in the development of Type I diabetes [36]. Under more severe conditions, a mutation in the PERK gene, *EIF2AK3*, causes Wolcott-Rallison Syndrome (WRS), a rare form of monogenic diabetes that manifests as infantile-onset, insulin requiring diabetes [38]. WRS is characterized by early destruction of pancreatic beta cells [36]. This disease is very rare, with under 60 cases noted as of 2010 [39, 40], although it may be underdiagnosed due to death occurring before patients exhibit the typical signs and symptoms [41]. Alongside neonatal diabetes, the main features of this WRS include multiple epiphyseal dysplasia (impaired ability of bones to elongate and grow normally) and hepatic dysfunction [39, 41, 42]. More recent studies have reported 39 distinct mutations in the PERK gene in WRS patients, which result in early termination of the protein or missense mutations in the kinase domains [41]. As of yet, there is no link between any specific mutation and WRS symptoms or onset.

As a key mediator of the UPR, PERK activity is necessary to protect cells from the apoptotic signals inherent in prolonged UPR activation. Studies using *in vitro* and *in vivo* models show that PERK-deficient pancreatic β-cells are more sensitive to apoptosis induced by the ER. In addition, PERK-deficient mice develop neonatal hyperglycemia caused by islet proliferation defects and increased apoptosis [43]. In fact, embryonic development of β-cells requires eIF2α phosphorylation, and peIF2α maintains full function of differentiated β-cells [43]. Although there are other enzymes that can also phosphorylate eIF2α, these data suggest that the PERK pathway is a primary mediator of β-cell development.

PERK knockout mice are born with seemingly normal islets of Langerhans, but there is progressive destruction of β-cells over the first few weeks of their lives [36]. This is likely the result of inability to cope with the high demand for insulin. These data suggest that PERK cycling is critical for adaptation to ER function under extreme conditions of protein secretion. PERK knockdown in cells shows similar results, where reduced PERK activity keeps eIF2α in a dephosphorylated state, which also inhibits the GTP cycling and obstructs translation [21]. As a result, cells become sensitive to ER dysfunction and accumulation of misfolded proteins in the ER [44]. PERK loci variants are associated with the risk of prediabetes, such as the minor C allele of rs867529 (a PERK SNP), which has been linked with a 1.3-fold increased risk [38].

Obesity, a leading cause of Type II Diabetes Mellitus, is associated with initiation of cellular stress signaling and inflammatory pathways, including ER stress [45]. Deprivation of nutrients and glucose or increased synthesis of secretory proteins is a major change in response to obesity; compounded over time, these factors induce ER stress [45]. UPR proteins such as Grp78 are also increased in obese mice, indicating that the ER is undergoing stress and the UPR is active during obesity [45]. In addition, PERK, peIF2α, and JNK are increased in liver extracts of obese mice when compared to lean control mice [45]. These data suggest that obesity is directly linked to chronic induction of ER stress and the UPR (Fig. **1B**). These data also suggest that the duration of the UPR could be suspended by removing the need for increased metabolic demands and protein synthesis.

A widely used model for diabetes, the Akita mouse, has a spontaneous mutation that causes early-onset non-obese diabetes [46]. In the Akita mouse, the ER of secretory β-cells distends and contains increased levels of BiP indicating that the ER has become stressed [23, 36]. In addition, progressive hyperglycemia is accompanied by CHOP induction, which

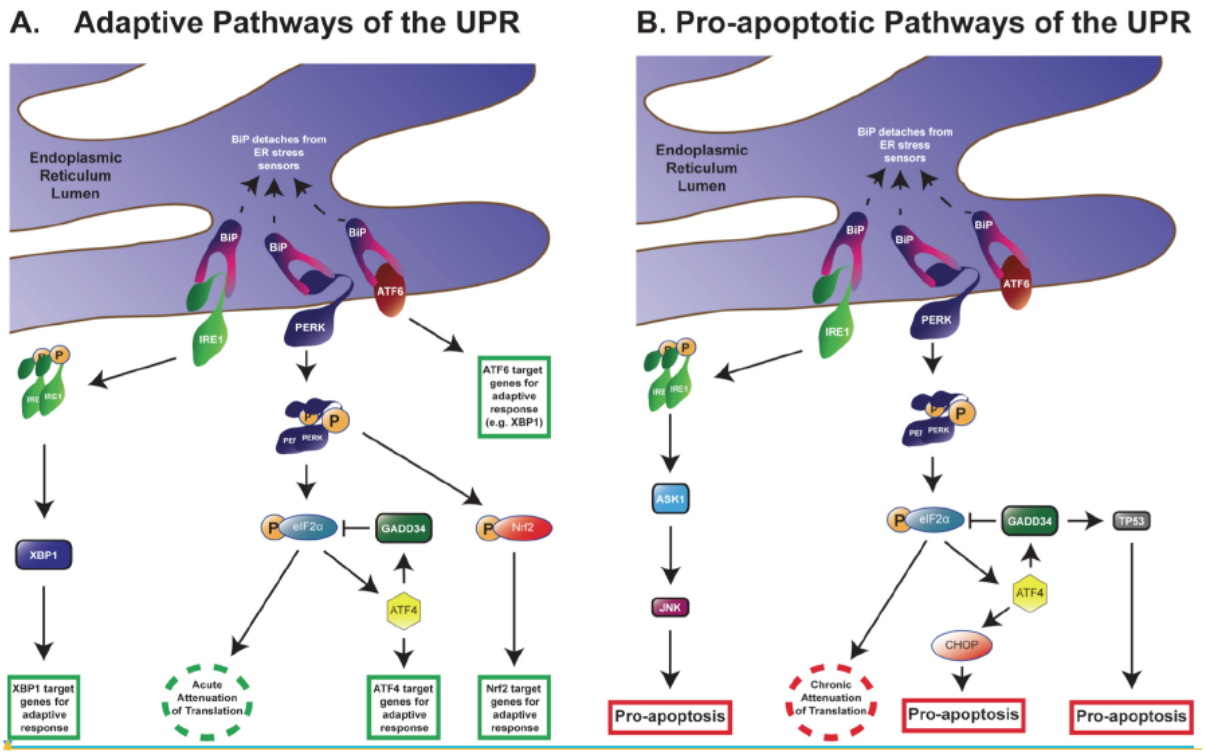

Fig. (1). Adaptive and pro-apoptotic pathways of the UPR. Under homeostatic conditions, IRE1, PERK, and ATF6 are anchored to the ER membrane by association with BiP. Upon activation of the UPR, BiP releases the effectors of the three branches of the UPR. (**A**) In the pro-survival, adaptive response, IRE1 dimerizes and autophosphorylates. Phosphorylated IRE1 activates XBP1, which in turn is translocated into the nucleus to upregulate the transcription of other adaptive UPR genes. Meanwhile, PERK dimerizes, autophosphorylates, and targets eiF2α and Nrf2. Once phosphorylated, eIF2α cannot contribute to activation of eIF2 thereby halting the initiation of translation. This provides relief to the ER by reducing input. Nonetheless, uORF-containing transcripts, such as ATF4, elude the attenuation of translation and become enriched. ATF4 can transactivate other adaptive UPR genes as well as trigger GADD34 activity. In turn, GADD34 dephosphorylates eIF2α, which restarts initiation of translation. Once phosphorylated, Nrf2 also serves as a transactivator for pro-survival genes. ATF6, the third branch of the UPR, translocates into the nucleus to enhance transcription of UPR genes such as XBP1. (**B**) Chronic activation of the UPR leads to pro-apoptotic signals. IRE1 induces apoptosis by activating ASK1 and consequently JNK. In the PERK pathway, sustained attenuation of translation by p-eIF2α suppresses protein synthesis. Neurons are particularly susceptible to the impact of prolonged reduction of nascent proteins. In the pro-apoptotic phase of ATF4, CHOP induces cell death cascades; long-term activation of the ATF4-GADD34 pathway leads to activation of the pro-apoptotic protein TP53. Abbreviations: UPR: unfolded protein response; IRE1: inositol-requiring enzyme 1; PERK: protein kinase R-like ER kinase; ATF6: cyclic AMP-dependent transcription factor-6; XBP1: X box-binding protein 1; eIF2α: eukaryotic initiation factor 2α; Nrf2: nuclear factor erythroid 2-related factor 2; ATF4: cyclic AMP-dependent transcription factor-4; uORF: upstream open reading frame; GADD34: growth arrest DNA damage-inducible GADD34; ASK1: apoptosis signal-regulated kinase 1; JNK: c-Jun N-terminal kinase; CHOP: C-EBP-homologous protein; TP53: cellular tumor antigen p53.

occurs downstream of PERK and leads to apoptosis [23, 35]. Conversely, CHOP knockout mice have a delayed onset of islet cell destruction and hyperglycemia as well as reduced cell death by any kind of ER stress [23]. These studies highlight the important role of CHOP as a downstream effector of the PERK pathway and mediator of cell death.

Tumor Growth and Cancer

ER stress also plays a role in various cancers and tumor growth. Cancer cells become highly dependent on glycolysis due to increased metabolic demands for growth and propagation [47]. Increased demand of the glycolytic pathway causes glucose deprivation inducing ER stress [47]. In response, the UPR pathway is an effective early sensor of cellular stress associated with tumorigenesis [48]. Further research into the UPR's relationship with cancer and tumor growth could provide useful information for early detection. In addition, targeting the UPR with pro-apoptotic compounds (*e.g.* PERK enhancers) could serve as therapeutic strategies.

PERK activity regulates tumor growth in several tissues. Tumors from MMTV-Neu transgenic mice were transduced with a retrovirus that excised PERK [48]. When transplanted into mammary fat pads of SCID mice, the PERK-deficient tumors had a reduced volume compared to PERK-positive cells [48]. This function extrapolates to other cell types throughout the body, where partial blocking of the UPR via PERK/ATF4 knockdown reduces the production of angiogenic mediators [20]. Knockdown of PERK also leads to reduced cell migration, which in turn reduces metastasis [49]. Further, PERK-deficient tumor cells have markedly less volume compared to PERK-positive cells [48]. Therefore, PERK knockdown leads to attenuation of tumor cell

growth. Tests *in vivo* show that PERK silencing slows tumor growth and decreases the blood vessel density in tumors.

Due to their increased growth rate, cancer cells require aberrantly amplified ER activity in order to handle the ER membrane swelling demands in protein folding [47]. This increase in ER activity and cellular demand causes tumor cells to outgrow their blood supply. As a result, solid tumors, and in particular malignant tumors, present a toxic tumor microenvironment, which is characterized by sustained hypoxic conditions [4]. In response, the cell undergoes ER stress and activates the UPR. Various types of cancers have increased levels of BiP that correlates with tumor growth and proliferation [47]. In fact, the level of BiP expression directly correlates with stage of malignancy [4]. Therefore, hypoxia-mediated activation of the UPR, and its angiogenic properties become beneficial for tumor cells [4, 50]. Indeed, specific PERK activation helps upregulate angiogenic genes [50].

Another complex mechanism within the UPR-PERK pathway is one that impacts autophagy-related proteins. Hypoxia-mediated activation of PERK/ATF4 induces Lysosomal-Associated Membrane Protein 3 (LAMP3), which is necessary for autophagy [49, 51]. The activation kinetics of LAMP3 closely resembles those of the PERK pathway. ATF4 knockdown using siRNA or disrupting the phosphorylation of eIF2α, prevents LAMP3 induction even under hypoxic conditions [51]. For a therapeutic perspective in other stages of cancer progression, the LAMP3 homologs, LAMP1 and LAMP2, are associated with metastasis in breast cancer [49]. While the mechanism by which LAMP3 associates with cancer progression is not yet clear, LAMP expression associates with metastasis in the cervix and it is implicated in breast cancer [49]. Therefore, as an upstream facilitator of LAMP expression, PERK could serve as a therapeutic target or downstream sensor.

NEUROLOGICAL IMPLICATIONS

Many neurodegenerative diseases show upregulation of the UPR including amyotrophic lateral sclerosis (ALS), Huntington's disease (HD), Parkinson's disease (PD), Alzheimer's disease (AD), Progressive Supranuclear Palsy (PSP), and Frontotemporal Dementia (FTD). The mechanisms linking these diseases and the UPR are not yet clear; however, an underlying molecular phenomenon of these disorders is the aberrant accrual of unfolded / misfolded proteins such as poly-glutamine, Aβ, tau, synuclein, and TDP-43, among others.

In the context of neurotoxicity, PERK has received special attention. This is in part due to the genetic risk for onset of some tauopathies inherent to SNPs on the gene coding for PERK [52-55], identification of increased pPERK in various neurodegenerative disorders [56-60], and a link between chronic PERK activation and decreased synthesis of synaptic proteins [61]. Neurons require constant protein production for synaptic function, which makes them particularly vulnerable to chronic attenuation of protein translation. Therefore, the PERK pathway hampers neuronal function well before it initiates pro-apoptotic cascades. As a result, PERK is a potent mediator of neuronal dysfunction, which underscores the interest of PERK in the field of neurodegeneration research.

Abrogating the extended activity of other branches of the UPR, that is IRE1 and ATF6, could offer benefits to long-term cell function and survival and ameliorate the long-term consequences of synaptic dysfunction. However, the neuronal dependence on nascent protein production makes the PERK pathway critical for synaptic function. The requirement for nascent protein synthesis extends to proper cellular function and it quickly and potently impacts overall brain function [62].

Amyotrophic Lateral Sclerosis (ALS)

ALS is a motor neuron disease showing neurodegeneration in the spinal ventral horn, most of the nuclei in the brainstem, and cerebral cortex. An estimated 5,000 people are diagnosed with ALS every year [63] and more than 12,000 people meet the standard surveillance definition of ALS [64]. ALS is fatal, and it leads to loss of motor function due to muscle atrophy with death typically occurring less than four years after diagnosis. [2, 65-68]. Phenotypic variation in the onset of this disease contributes to the difficulty in understanding ALS to the fullest extent. Spinal onset, seen in the majority of ALS cases, begins around 60 years of age. Initially, a painless weakness in one limb leads to a clinical examination that reveals further muscle atrophy, hyperreflexia, fasciculation, and hypertonia [69, 70]. The early symptoms are observed at an inconsistent rate, but show contiguous spread in the majority of patients [71]. Bulbar onset is seen in around 20% of all ALS cases [69, 72]. Common symptoms include dysarthria, dysphagia, tongue fasciculation, and jaw jerkiness [69, 72]. Bulbar onset has a worse prognosis than spinal onset, with life expectancy after diagnosis only being 2 years. Respiratory onset is the least common form in ALS, seen in only 3-5% of patients. These patients show orthopnea or dyspnea, with mild or absent spinal or bulbar onset symptoms. This pattern of onset is seen predominantly in males. The short-term life expectancy after diagnosis is 1.4 years with no long-term survival (>10 years) [72, 73]. The majority of cases are sporadic (~90%), but a few cases (~10%) are known to show genetic patterns of inheritance [2]. More than half of familial cases of ALS can be attributed to mutations in SOD1 (superoxide dismutase 1), TARDBP (the gene encoding the protein TDP-43), *C9orf72*, and the FUS gene [71].

Expression of mutant forms of TDP-43 and SOD1 are associated with PERK activation. TDP-43 is a DNA binding protein found predominantly in the nucleus. However, even under normal circumstances, part of TDP-43 is cytoplasmic, and aberrant localization and sorting of TDP-43 contributes to disease progression [74-76]. Interestingly, TDP-43 can also be a part of co-morbidities in disease when brains are confounded by pathological tau [77]. Previous studies have shown that stress granule formation correlates with expression of ALS-associated mutations [78]. Stress granules are intracellular aggregates composed of mRNAs, ribosomal subunits, and various proteins. Phosphorylation of eIF2α and consequent attenuation of protein translation increases the risk for the formation of stress granules [79]. Recent studies have shown that overall cellular stress can induce stress granule formation [80-82] and PERK-mediated phosphorylation of eIF2α initiates stress granule formation of TDP-43 [83, 84].

Accumulation of mutant SOD1 in the ER, which is implicated in some cases of ALS, induces ER stress through association with BiP. BiP is believed to chaperone the transport of SOD1 into the ER, with the protein-binding domain (residues 392-509) playing a critical role in the binding of SOD1 and BiP [68]. SOD1 is a protein that binds to copper or zinc ions to form cytoplasmic and mitochondrial isozymes that eliminate free superoxide radicals. In SOD1G93A transgenic mouse model of ALS, PERK is activated. The consequent phosphorylation of eIF2α leads to increased expression of ATF4. ATF4 activation as a result of the PERK pathway was evidenced in disease-affected areas such as the spinal cords. However, ATF4 was not activated in unaffected areas such as cerebellum, suggesting that PERK activation is selectively activated in discreet regions [68]. Mutant SOD1 also increases mitochondrial and oxidative stress, which in turn induces PERK-mediated phosphorylation of eIF2α [66].

Huntington's Disease (HD)

Huntington's disease is an autosomal dominant, neurodegenerative disease caused by a cytosine-adenine-guanine (CAG) repeat expansion within the huntingtin gene. This mutant gene leads to a pathogenic form of the huntingtin protein [85]. Mutant huntingtin aggregates and damages the striatum and cerebral cortex via mechanisms that are not yet clear. These pathological pathways lead to cognitive decline and motor impairment [86-88]. Generally, the life expectancy of HD is approximately 10-30 years after onset of symptoms but this prognosis can vary greatly depending on the number of repeats on the gene [5]. Along with HD, there is an array of Huntington's disease-like (HDL) syndromes. HDL-1 is an autosomal dominant prion disease caused by additional octapeptide repeats in the prion protein gene. [89, 90]. Clinical symptoms such as ataxia are similar to those seen in HD; however, spongiosis is not prevalent [91, 92]. HDL-2 is autosomal dominant as well, but is caused by expansions of a CTG-CAG triplet repeat in the junctophilin-3 (JPH3) gene on chromosome 16q24.3 [93]. This form of HDL manifests very similarly to HD. HDL-3 an autosomal recessive disease that has only been seen in two Saudi Arabian families. It has an early age of onset (3-4 years) and very little is known about this disease [94]. HDL-4, also known as spinocerebellar ataxia type 17 (SCA17), is an autosomal disease caused by triplet repeat expansions in the TATA box-binding protein (TBP) gene located on chromosome 6q27. This is the most commonly inherited type of HDL with the most common clinically observed feature being cerebral ataxia [95]. Even though it is classified as an HDL syndrome, very few cases show a high level of similarity to symptoms seen in HD.

Aggregation of mutant huntingtin induces ER stress and activates the UPR. The UPR-PERK pathway has not been extensively studied in HD. However, levels of p-eIF2α are increased in cells expressing mutant huntingtin and addition of salubrinal showed decreased aggregates and increased cell viability [96]. This further suggests that sustained chronic eIF2α inhibition beyond that of the PERK pathway might show reversal of the PERK-mediated neurotoxic effects. In addition, p-eIF2α levels in wild type NIH 3T3 striatal cells are much lower than other cells types. However, p-eIF2α levels are increased upon transfection of mutant huntingtin into HEK 293T cells, suggesting that huntingtin overexpression induces the PERK pathway. Conversely, reduction of p-eIF2α levels by inhibition of the PERK pathway reverses toxicity of the mutant huntingtin protein [97]. In addition, functional assays in these studies showed that low levels of p-eIF2α were necessary for optimal striatal neuron function [98]. A later study by Li *et al.*, showed that Grp78 is upregulated in cells expressing mutant huntingtin protein. The same study also showed that Grp78 reduces aggregation of mutant huntingtin protein [99]. Grp78 activation and dislodging form PERK suggests that the other UPR pathways are also activated, and in these cases, UPR activation is chronic. Still, very few results have been published about the PERK pathway specifically. More studies must be done to conclusively determine the role of PERK in HD and weigh the therapeutic potential of PERK.

Parkinson's Disease (PD)

Parkinson's disease is a neurodegenerative disease that is clinically diagnosed based on common symptoms: rest tremor, rigidity, bradykinesia, and postural instability. Confirmation of clinical diagnosis is done by post-mortem analysis. An estimated 1.5 million people in the US suffer from Parkinson's. The classic hallmark of the disease is the presence of Lewy bodies, which typically include large accumulations of α-synuclein in neurons [100-103]. Norepinephrine deficiency is another contributing factor to the progression of the disease, which accounts for much of the impairment seen in the autonomic system of PD patients. Reduction in norepinephrine levels happens before reduction in dopamine levels [104]; however, it is unclear which neurotransmitter is the first or the major problem seen in the disease. The death of dopaminergic neurons in the substantia nigra is the most prominent and well-established sign of the disease and has provided a therapeutic target. Initially, dopamine deficiency leads to decline of motor skills that are accompanied by behavioral changes and dementia seen in late stages of the disease. The cause of death of dopaminergic neurons is largely unknown [56, 58]. The most common pharmacological treatment for PD is administration of Levadopa, which is converted to dopamine by L-dopa decarboxylase. While treatment with Levodopa has increased the standard of living for many patients with PD, there is substantial resistance to using the drug on the basis of dopamine dysregulation and its dire effects on reward stimulation and schizophrenic symptomatology. A compelling argument stems from the critical connectivity of the basal ganglia with other structures in the brain [105-109].

The most established location for a connection between the molecular basis of PD and chronic activation of the UPR was identified in dopaminergic neurons of Parkinson's brain. Indeed, the levels of pPERK and p-eIF2α are significantly increased in dopaminergic neurons compared to age-matched control brains [56, 58]. However, there is no colocalization of α-synuclein and pPERK or of α-synuclein and p-eIF2α, suggesting that synuclein does not play a role in activating the UPR or its participation is indirect. A recent study by Le Masson *et al.* found that α-synuclein is localized in mitochondrial-associated ER membranes (MAM). Different mutations of α-synuclein determine the level of association seen with MAM and contribute to the overall level of mitochon-

drial dysfunction [110]. While not directly identifying the UPR or the PERK pathway, this discovery provides support to the idea α-synuclein association with the ER is detrimental in PD and confirms that the UPR is a potentially promising therapeutic target.

Alzheimer's Disease

Alzheimer's disease (AD) is a progressive neurodegenerative disorder that is pathologically characterized by the appearance of amyloid plaques and tau tangles [111]. With current demographics showing 5.2 million Americans suffering from the disease, it is the most common cause of dementia in the US. Initial symptoms include difficulty with acquisition and recall of recent episodic memory. Progressive symptomatology expands to problems with overall cognitive function such as the inability to recognize places or family members. Late-stage AD patients show total loss of voluntary and involuntary muscle control [111].

The two major pathological hallmarks of Alzheimer's disease are amyloid plaques and neurofibrillary tangles, which are composed of amyloid beta (Aβ) peptides and aberrantly folded microtubule-associated protein tau, respectively. Both Aβ and tau, and their diverse pathological conformations, interfere with cellular homeostasis. AD brains show signs of chronic UPR activation as evidenced by increased levels of Grp78, pPERK, pIRE1α, peIF2α, and ATF4 [57, 59, 112, 113]. As previously described, increased expression and availability of membrane-detached Grp78 suggests activation of the three branches of the UPR (Fig. **1**). These studies corroborate activation of the IRE1 branch, but no other downstream effectors of this pathway are documented. Similarly, data suggesting activation of the ATF6 pathway is scant. Meanwhile, increased levels of pPERK, peIF2α, and ATF4 indicate that there is activation of the PERK pathway. Sustained ATF4 activity directly leads to activation of pro-apoptotic cascades [20]. Therefore, chronic activation of the PERK-ATF4 pathway could be a major mechanism mediating apoptotic cell death in AD. Nonetheless, the extent of UPR activation in AD has not been fully characterized. More information will help dissect the full regulation of the UPR and identify potential therapeutic targets to balance pro-survival vs. pro-apoptotic pathways.

The timing during which the UPR is initially activated in correlation with disease is a matter of debate, but at least in AD brains, pPERK levels accrue in hippocampal neurons that experience pre-tangle pathology [57]. Hoozemans *et al.*, determined that pPERK directly co-localized with AT8-positive tau species and not with neurofibrillary tangles. In addition, pPERK levels positively correlate with the extent of tau pathology as marked by their Braak score [114]. Of importance is the identification of pPERK in hippocampal neurons where tau pathology begins in AD brains [114, 115]. These data argue for a temporal response to pathological tau aggregation where early pathological steps in the disease process activate the UPR. However, more recent data do not extricate early pathological tau species as indirect mediators of ER stress. Indeed, soluble tau is responsible for impairing ERAD, which in turn increases ER burden and activates the UPR [6].

Interestingly, UPR activation is associated with another pathological sign that is common in AD brains: granulovacuolar degenerating bodies (GVDs). These are deposits of autophagic vacuoles that seem to originate from smooth ER; their membranes contain lipid raft proteins like flotillin-1, and they encapsulate ubiquitinated proteins that are destined for autophagic destruction [116-118]. GVDs are not unique to AD pathology; they have been identified in brains suffering from Down's syndrome, progressive supranuclear palsy (PSP), parkinsonism dementia complex of Guam, Pick's disease, pallido-ponto-nigral degeneration, Parkinson's disease, dementia with Lewy bodies, ALS, and elderly controls [119-121]. The common pathological hallmark associated with GVDs in these disorders is the colocalization with hyperphosphorylated tau. In turn, GVDs also show intense pPERK immunoreactivity in AD. Therefore, tau-mediated clogging of the autophagic pathway could result in another indirect mechanism by which tau induces ER stress in pre-tangle stages of disease. In addition, these findings support the idea that the UPR is active in other tauopathies. Depending on its conformation, tau clearance is directed in part by chaperone-co-chaperone interactions [122], which can direct tau for proteasomal or autophagic clearance [123].

The mechanism by which tau induces ER stress was recently established [6]. We previously showed increased levels of active PERK in the brains of rTg4510 mice, a tau transgenic mouse model that overexpresses FTD-related P301L mutant tau and show extensive neurofibrillary tangle pathology and cognitive deficits [124]. Hoozemans *et al.* shows co-localization of diffuse phosphorylated tau (AT8-positive) with phosphorylated PERK but neurofibrillary tangles show little to no PERK reactivity, suggesting that the mechanism of tau-mediated PERK activation is indirect. Indeed, we identified that pathological soluble tau species, some of the earliest and most neurotoxic tau species, are responsible for preventing egress of proteasome-bound ER substrates. As a result, ERAD is impaired, leading to an increased volume of nascent proteins in the ER lumen. In response, the UPR is activated.

More recent data suggest that there is a reverse link by which PERK increases the abundance of pathological tau species. In fact, three PERK-mediated pathways could lead to aberrant tau species (Fig. **2**). First, pPERK activates GSK3β, a tau kinase that is implicated in tauopathy [125]. Second, PERK activates caspases that cleave tau [126]; the accumulation of caspase-cleaved tau (cTau) is an early indicator of pre-tangle pathology in AD and other tauopathies [122, 127, 128]. Mechanistically, cTau sensitizes neurons to ER stress-induced cell death, and it stimulates mitochondrial dysfunction [129, 130]. Moreover, preventing caspase cleavage of tau reduces tau filament formation [131]. Third, it was recently established that PERK itself could phosphorylate tau on residues that are associated with late stage pathology [132]. These data support the idea that PERK-mediated caspase activation could play a role in potentiating pathological tau species. This places PERK as a node in a bidirectional cycle of cell death whereby pathological tau species activate PERK and sustained PERK activity mediates cell death downstream while propagating the appearance of pathological tau species. In turn, increased pathological tau can cause neurotoxicity through many other pathways.

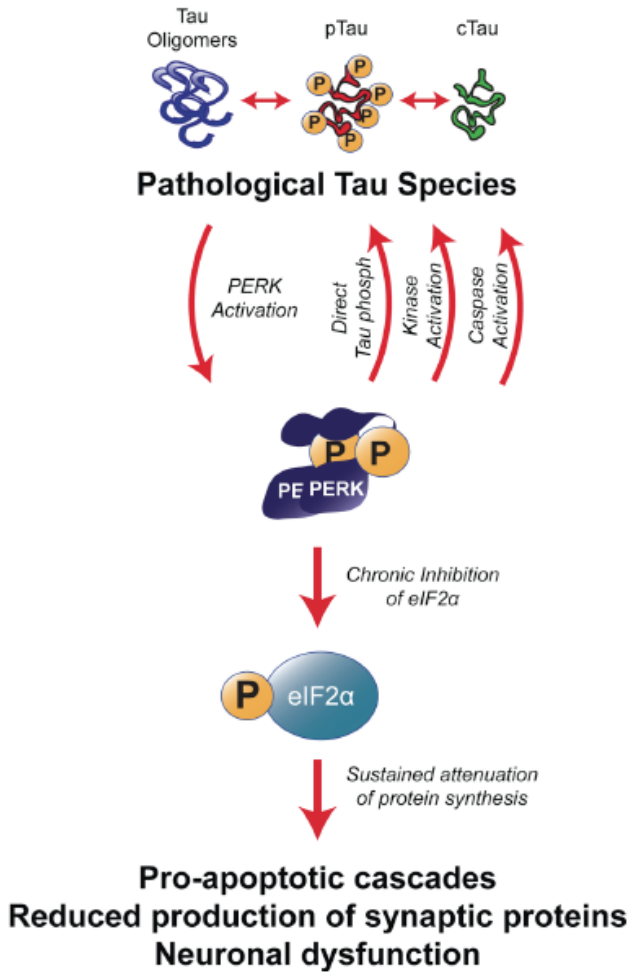

Fig. (2). PERK is a bimodal mediator of tau toxicity. Pathological tau species chronically activate PERK leading to long-term reduction of protein synthesis via p-eIF2α. Chronic reduction of synaptic proteins causes neuronal dysfunction, which contributes to symptomatology in neurodegenerative disorders. Sustained levels of pPERK activate pro-apoptotic cascades downstream. Other downstream targets of the PERK pathway are identified to act on tau pathologically, such as GSK3β, caspase-3, and phosphorylate tau directly. Abbreviations: pTau: hyperphosphorylated tau; cTau: caspase-cleaved tau; PERK: protein kinase R-like ER kinase; eIF2α: eukaryotic initiation factor 2α; GSK3β: glycogen synthase kinase β.

UPR activation becomes evident in cells overexpressing APP, cells treated with Aβ oligomers, and iPSCs (induced-pluripotent stem cells) from familial and sporadic AD patients; albeit, the degree of UPR activation is discrepant in iPSCs [133-136]. The relationship between ER stress and Aβ appears to stem from retention and processing of APP in the ER. For instance, there is indication that APP-mediated activation of the UPR leads to enriched subcellular localization and abnormal processing of APP on the ER [137], which would cause strain on the ER membrane. Another potential mechanism could be mediated by APP processing into Aβ oligomers that would interfere with ER function; indeed, mechanisms of APP and Aβ-mediated ER dysfunction have been associated to impaired vesicle transport originating from the ER [138].

Another product of APP processing that is uniquely linked to the UPR is the APP-intracellular domain (AICD), a transcription factor that results from APP cleavage. AICD stimulates transcription of CHOP, which suggests a normal role of APP in mediating the UPR; an imbalance in this regulation (i.e. overproduction of APP) would induce further production of CHOP [136, 139, 140]. This could be one of the many mechanisms underlying neurotoxicity in AD, the consequences of which would be increased cell death.

While other ER stress markers are markedly changed by amyloid beta and APP, there is no current evidence linking amyloid beta or APP to PERK dysfunction. While human AD brains present increased levels of several UPR makers including pPERK, the Tg2576 mouse model of amyloidosis (a model overexpressing the Swedish mutation-containing APP gene), does not show pPERK reactivity [135]. Meanwhile, rTg4510 mice show robust tau-mediated accumulation of pPERK and BiP [6]. Consistent with the finding that pPERK is abundant in tangle bearing neurons of FTD, PSP, and AD brains, it is likely that tau more directly links UPR activation than Aβ [60].

Progressive Supranuclear Palsy

Progressive supranuclear palsy is a neurodegenerative disease with a wide variety of clinical symptoms and seven different documented phenotypes [141]. The most common symptoms seen in early stages of all types of PSP are bradykinesia, increased falls, postural instability, tremors, cognitive changes, and supranuclear palsy of the vertical gaze [141, 142]. This disease is especially hard to diagnose, as early clinical symptoms overlap heavily with PD and other dementias [143, 144]. Approximately five per 100,000 people are affected by PSP with the average age of onset being 63 [145]. PSP is classified as a tauopathy due to the prevalence of tau aggregates in multiple brain regions including the basal ganglia, diencephalon, brainstem and cerebellum [146]. The hallmark characteristic that differentiates PSP from other tauopathies are the tufted astrocytes [147].

Activation of the PERK pathway has been seen in human tissue samples and amplified pPERK levels correlate with increasing levels of tau [60]. The most direct causal connection that links PERK with PSP onset is a genetic variation in *EIF2AK3*, the gene that codes for PERK. The largest genome-wide association study for PSP revealed a SNP in the *EIF2AK3* that is associated with risk for the disease (rs7571971) [55]. Interestingly, this same SNP is in linkage disequilibrium with a series of other SNPs that change specific residues on the coding region of PERK [52-54]. The genetic impact of this risk for PSP seems to increase PERK activity, further suggesting that PERK inhibition could be an attractive therapeutic strategy. Furthermore, considering that inheritance of this SNP increases the risk for a wide spectrum of PSP phenotypes, AD, and lower bone mineral density, current efforts should strive to investigate the efficacy of PERK-inhibiting compounds. A noteworthy observation from these studies is that novel therapeutic targets for these disorders could exist downstream in the PERK pathway. For instance, inhibition of ATF4 could be an attractive therapeutic strategy that would have less of an overall effect on the UPR.

Frontotemporal Dementia (FTD)

Frontotemporal dementia is a clinically and pathologically diverse neurodegenerative disease typically classified by tau aberrancy [148]. The term frontotemporal dementia is used to describe the clinical syndromes seen in the disease, while the term frontotemporal lobar degeneration (FTLD) is used to describe the neuropathology of the disease seen post mortem. In adults 45-65 years old, FTD is almost as prevalent as AD, occurring in about fifteen people per 100,000 [149]. The major syndromes associated with FTD include behavioral variant FTD (bvFTD), semantic dementia (SD), progressive non-fluent aphasia (PNFA), corticobasal syndrome (CBS), and progressive supranuclear palsy syndrome (PSPS). All of these diagnoses are based on behavioral changes including personality changes, change in language function, and motor changes. Post mortem diagnosis of FTLD based on pathological biomarkers of most FTD patients can be split into two categories: FTLD-TDP and FTLD-tau. The other cases that do not fall into either of those categories are then divided into the ubiquitin proteasome syndrome (FTLD-UPS), the fused in sarcoma protein (FTLD-FUS), ubiquitin only (FTLD-U), or lack inclusions completely (FTLD-ni) [148].

To date, there have been few studies exploring the link between PERK and FTLD. Correlation between increasing tau levels and increasing PERK levels is seen in FTLD-tau brains. Specifically, the region showing highest reactivity was the hippocampus. FTLD-TDP and FTLD-FUS brain tissue samples, however, show no increase in PERK activity [60]. Validation of the lack of PERK activation in FTLD-TDP was shown by Tong *et al*. Transgenic rats bred to express mutant human TDP-43 exclusively in the forebrain showed no activation of PERK (or any other UPR markers) [150]. The disparity in the results of these studies may be due to differences clinical symptoms of FTD and pathology seen in FTLD. This leaves a large niche to fill in regards to finding therapeutic treatments.

THERAPEUTICS

The data on PERK and its role in disease implicate its pathway as a therapeutic target for treatment of PERK-opathies. Further insight into the pathway itself and the molecular mechanisms through which it functions could yield significant insight into the understanding and treatment of many neuropathological and systemic diseases discussed in this review. Promising results in experimental phases of PERK inhibitors have fueled the development of PERK-targeting strategies [50, 151-153]. Despite the toxicity of on- and off-target effects, inhibitors such as GSK2606414 have shown exciting therapeutic (not just preventative) rescue of normal phenotypes.

Long-term PERK inhibition could have adverse consequences to ER homeostasis. To avoid this risk we propose to explore the therapeutic potential of inhibiting downstream effectors of the PERK pathway. For instance, inhibition of ATF4 could be an attractive therapeutic strategy that would have less of an overall effect on the UPR. Targeting downstream effectors of the PERK pathway could mitigate potential side effects caused by prolonged PERK activation or inhibition throughout the body. However, development of these tools is still in its infancy, and more needs to be learned from the intricate regulation of the UPR. It remains to be seen whether inhibiting the PERK pathway exerts feedback regulation of other pathways such as the UPR and beyond; it is also not clear whether this phenomenon would be beneficial. It would be exciting to find intermittent strategies that would ultimately activate and inhibit PERK to offer optimal outcomes: activate PERK to alleviate the ER, but inhibit PERK to prevent cell death in a timely manner.

PERK targeting is an attractive strategy for cancer therapeutics due to antiproliferative properties of long-term inhibition. The effects of PERK knockdown continue to provide key insights into the physiology of different cancers, which could see advancements in treatment through therapeutic modification or modulation of the PERK pathway. Inhibiting PERK in cancer cells may limit their ability to thrive under hypoxic and nutrient deprived conditions, which in turn leads to apoptosis of cancerous cells or tumor growth inhibition [50]. This has been shown using PERK inhibitors in various cancer models where PERK inhibition precludes tumor cell growth [49]. Whether these data will lead to curative effects in humans still remains to be seen.

The general therapeutic strategy presented here is to inhibit PERK to de-repress protein synthesis. While chronic PERK activity shows neurotoxicity, inhibition of the eIF2α phosphatase GADD34 with salubrinal effectively increases phosphorylation of eIF2α and abrogates translation [154]. However, GADD34 inhibition improves motoneuron function and increases lifespan in SOD1G93A transgenic mice [154]. As discussed earlier in this review, interruption of protein synthesis for an extended period of time underlines neurotoxicity. Nonetheless, chronic PERK activity with increased eIF2α inhibition/phosphorylation in this model shows improved outcomes. It is possible that reducing overall translation might effectively reduce synthesis of mutant SOD1 thereby abrogating other SOD1-mediated neurotoxic insults. While this would be effective in models where protein over-expression is the culprit of the disease phenotype, it bears limited appeal to therapeutics in diseases where accumulation of the pathogenic protein is indifferent to protein synthesis. However, salubrinal might have important ramifications for individuals with trisomy 21, where expression of three copies of APP is ascribed to onset of Alzheimer's-like pathology and cognitive decline [155].

CONCLUSIONS

The data reviewed suggest that PERK is a potent mediator of neuronal dysfunction that is linked to neurodegenerative disorders. Many of these disorders are tauopathies (AD, PSP, FTD, among others), which have no cure. Since tauopathies are the most devastating cognitive threat to the aging population, there is an urgent need to identify therapeutic targets like PERK. Notwithstanding, a vast amount of unresolved issues in the strategy, therapeutic window, and safety impede progress at this time.

Future studies aiming to identify the earliest time points in which the PERK pathway is active will help identify an early therapeutic window. Equally important is the identifi-

cation of neuronal dysfunction and cell death after PERK activation. With this information, it is possible to carefully trace the timeline during which PERK stops being beneficial and initiates deleterious cascades.

The compound GSK2606414 is a potent and selective PERK inhibitor [50]. It was recently used in a study to show alleviation of motor deficits in a rodent model of prion disease [151]. The compound successfully reduced the prion phenotype both in preventative and therapeutic interventions. However, treatment for more than three months caused the mice to lose 20% of their body weight and moderately increase their blood glucose levels. These data suggest that the compound has on-target effects on a pancreatic homolog of PERK, PKR. These interactions preclude current PERK inhibitors to be funneled through to clinical testing. These data also frame the proof-of-concept that inhibition of the PERK pathway is an attractive and novel therapeutic strategy, and they substantiate efforts to develop next generation PERK inhibitors that are more specific.

PERK's fundamental role in the cell suggests that inhibition of its pathway could lead to unexpected deleterious consequences. As described in the first part of this article, the UPR is a complex pathway with three branches that self regulate. Two potential outcomes of long-term PERK suppression on overall UPR function are that the UPR system could reset itself after chronic inhibition of PERK or that the UPR will not correct itself upon PERK inhibition and pro-apoptotic cascades will ensue. It is possible that cross talk between all UPR players could elicit a compensatory state where future ER stress activates a moderate UPR (without activation of the PERK pathway) without initiating pro-apoptotic cascades.

Another caveat to PERK-mediated treatments for neurodegenerative disorders is the varied etiology of these diseases. For instance, not all tauopathic brains show a similar amount of UPR activation status [156]. This is likely because of different stages of disease; however, it is also possible that based on the diverse molecular mechanisms through which the UPR can be induced, different identities and conformations of pathogenic proteins could activate/inhibit the UPR in different ways [157]. In the case of PERK, this is important because it could help identify diverse activity levels that favor one branch over another. In addition, modulating the UPR could help prevent pro-apoptotic cascades thereby promoting cell survival in neurodegenerative disorders.

Despite these concerns, it is clear that PERK activity is common to many systemic and neurodegenerative disorders. Recent genetic and biochemical data suggest that PERK plays a pathogenic role in some cases, while in others it potentiates disease progression. It is not clear yet what would be the long-term cost of inhibiting the UPR. Nonetheless, important and exciting studies to characterize and challenge the PERK pathway of the UPR are currently underway, and they could unlock not only clues into the mechanisms of disease onset and progression, but also effective therapeutic paradigms.

LIST OF ABBREVIATIONS

AD = Alzheimer's disease

ASK1 = apoptosis signal-regulated kinase 1

ATF4 = cyclic AMP-dependent transcription factor-4

ATF6 = cyclic AMP-dependent transcription factor-6

BiP = immunoglobulin heavy chain-binding protein

CHOP = C-EBP-Homologous Protein

cTau = caspase-cleaved tau

eIF2α = eukaryotic initiation factor 2α

ER = endoplasmic reticulum

FTD = fronto-temporal dementia

GADD153 = growth arrest DNA damage-inducible transcript 3

GADD34 = growth arrest dna damage-inducible GADD34

Grp = glucose-regulated protein

GSK3β = glycogen synthase kinase β.

HD = Huntington's disease

IRE1 = inositol-requiring enzyme 1

JNK = c-Jun N-terminal kinase

Nrf2 = nuclear factor erythroid 2-related factor 2

PD = Parkinson's disease

PERK = protein kinase R-like ER kinase

PSP = progressive supranuclear palsy

pTau = hyperphosphorylated tau

uORF = upstream open reading frames

UPR = unfolded protein response

XBP1 = X box-binding protein 1

CONFLICT OF INTEREST

The author(s) confirm that this article content has no conflict of interest.

ACKNOWLEDGEMENTS

We acknowledge funding support from the Alzheimer's Association NIRG-14-322441. MCB and SEM contributed equally to the work.

REFERENCES

[1] Schonthal AH. Endoplasmic reticulum stress: its role in disease and novel prospects for therapy. Scientifica 2012: 857516 (2012).

[2] Matus S, Valenzuela V, Medinas DB, Hetz C. ER Dysfunction and Protein Folding Stress in ALS. Intern J Cell Biol 2013: 674751 (2013).

[3] Han J, Back SH, Hur J, Lin YH, Gildersleeve R, Shan J*, et al.* ER-stress-induced transcriptional regulation increases protein synthesis leading to cell death. Nat Cell Biol 15(5): 481-90 (2013).

[4] Kaufman RJ. Orchestrating the unfolded protein response in health and disease. J Clin Invest 110(10): 1389-98 (2002).

[5] Shineman DW, Basi GS, Bizon JL, Colton CA, Greenberg BD, Hollister BA*, et al.* Accelerating drug discovery for Alzheimer's disease: best practices for preclinical animal studies. Alzheimers Res Ther 3(5): 28 (2011).

[6] Abisambra JF, Jinwal UK, Blair LJ, O'Leary JC, 3rd, Li Q, Brady S, *et al.* Tau Accumulation Activates the Unfolded Protein Response by Impairing Endoplasmic Reticulum-Associated Degradation. J Neurosci 33(22): 9498-507 (2013).

[7] Cooper AA, Gitler AD, Cashikar A, Haynes CM, Hill KJ, Bhullar B, *et al.* Alpha-synuclein blocks ER-Golgi traffic and Rab1 rescues neuron loss in Parkinson's models. Science 313(5785): 324-8 (2006).

[8] Duennwald ML, Lindquist S. Impaired ERAD and ER stress are early and specific events in polyglutamine toxicity. Genes Develop 22(23): 3308-19 (2008).

[9] Yoshida H. ER stress and diseases. FEBS J 274(3): 630-58 (2007).

[10] Wang WA, Groenendyk J, Michalak M. Endoplasmic reticulum stress associated responses in cancer. Biochim Biophys Acta 1843(10): 2143-9 (2014).

[11] Spindler SR, Crew MD, Mote PL, Grizzle JM, Walford RL. Dietary energy restriction in mice reduces hepatic expression of glucose-regulated protein 78 (BiP) and 94 mRNA. J Nutr 120(11): 1412-7 (1990).

[12] Ron D, Hubbard SR. How IRE1 reacts to ER stress. Cell 132(1): 24-6 (2008).

[13] Shaffer AL, Shapiro-Shelef M, Iwakoshi NN, Lee AH, Qian SB, Zhao H, *et al.* XBP1, downstream of Blimp-1, expands the secretory apparatus and other organelles, and increases protein synthesis in plasma cell differentiation. Immunity 21(1): 81-93 (2004).

[14] Nishitoh H, Matsuzawa A, Tobiume K, Saegusa K, Takeda K, Inoue K, *et al.* ASK1 is essential for endoplasmic reticulum stress-induced neuronal cell death triggered by expanded polyglutamine repeats. Genes Develop 16(11): 1345-55 (2002).

[15] Urano F, Wang X, Bertolotti A, Zhang Y, Chung P, Harding HP, *et al.* Coupling of stress in the ER to activation of JNK protein kinases by transmembrane protein kinase IRE1. Science 287(5453): 664-6 (2000).

[16] Healy SJ, Gorman AM, Mousavi-Shafaei P, Gupta S, Samali A. Targeting the endoplasmic reticulum-stress response as an anticancer strategy. Eur J Pharmacol 625(1-3): 234-46 (2009).

[17] Yamamoto K, Sato T, Matsui T, Sato M, Okada T, Yoshida H, *et al.* Transcriptional induction of mammalian ER quality control proteins is mediated by single or combined action of ATF6alpha and XBP1. Develop Cell 13(3): 365-76 (2007).

[18] Adachi Y, Yamamoto K, Okada T, Yoshida H, Harada A, Mori K. ATF6 is a transcription factor specializing in the regulation of quality control proteins in the endoplasmic reticulum. Cell Struct Funct 33(1): 75-89 (2008).

[19] Parmar VM, Schroder M. Sensing endoplasmic reticulum stress. Adv Exp Med Biol 738: 153-68 (2012).

[20] Wang Y, Alam GN, Ning Y, Visioli F, Dong Z, Nor JE, *et al.* The unfolded protein response induces the angiogenic switch in human tumor cells through the PERK/ATF4 pathway. Cancer Res 72(20): 5396-406 (2012).

[21] Harding HP, Novoa I, Zhang Y, Zeng H, Wek R, Schapira M, *et al.* Regulated translation initiation controls stress-induced gene expression in mammalian cells. Mol Cell 6(5): 1099-108 (2000).

[22] Wethmar K, Smink JJ, Leutz A. Upstream open reading frames: molecular switches in (patho)physiology. BioEssays 32(10): 885-93 (2010).

[23] Harding HP, Ron D. Endoplasmic reticulum stress and the development of diabetes: a review. Diabetes 51(3): S455-61 (2002).

[24] Lu PD, Jousse C, Marciniak SJ, Zhang Y, Novoa I, Scheuner D, *et al.* Cytoprotection by pre-emptive conditional phosphorylation of translation initiation factor 2. EMBO J 23(1): 169-79 (2004).

[25] Lin JH, Li H, Zhang Y, Ron D, Walter P. Divergent effects of PERK and IRE1 signaling on cell viability. PloS one 4(1): e4170 (2009).

[26] Walter P, Ron D. The unfolded protein response: from stress pathway to homeostatic regulation. Science 334(6059): 1081-6 (2011).

[27] Ohoka N, Yoshii S, Hattori T, Onozaki K, Hayashi H. TRB3, a novel ER stress-inducible gene, is induced via ATF4-CHOP pathway and is involved in cell death. EMBO J 24(6): 1243-55 (2005).

[28] Yamaguchi Y, Larkin D, Lara-Lemus R, Ramos-Castaneda J, Liu M, Arvan P. Endoplasmic reticulum (ER) chaperone regulation and survival of cells compensating for deficiency in the ER stress response kinase, PERK. J Biol Chem 283(25): 17020-9 (2008).

[29] Novoa I, Zeng H, Harding HP, Ron D. Feedback inhibition of the unfolded protein response by GADD34-mediated dephosphorylation of eIF2alpha. J Biol Chem 153(5): 1011-22 (2001).

[30] Kojima E, Takeuchi A, Haneda M, Yagi A, Hasegawa T, Yamaki K, *et al.* The function of GADD34 is a recovery from a shutoff of protein synthesis induced by ER stress: elucidation by GADD34-deficient mice. FASEB J 17(11): 1573-5 (2003).

[31] De Angelis PM, Svendsrud DH, Kravik KL, Stokke T. Cellular response to 5-fluorouracil (5-FU) in 5-FU-resistant colon cancer cell lines during treatment and recovery. Mol Can 5: 20 (2006).

[32] Cullinan SB, Zhang D, Hannink M, Arvisais E, Kaufman RJ, Diehl JA. Nrf2 is a direct PERK substrate and effector of PERK-dependent cell survival. Mol Cell Biol 23(20): 7198-209 (2003).

[33] Huang HC, Nguyen T, Pickett CB. Regulation of the antioxidant response element by protein kinase C-mediated phosphorylation of NF-E2-related factor 2. Proc Nat Acad Sci USA 97(23): 12475-80 (2000).

[34] Teske BF, Wek SA, Bunpo P, Cundiff JK, McClintick JN, Anthony TG, *et al.* The eIF2 kinase PERK and the integrated stress response facilitate activation of ATF6 during endoplasmic reticulum stress. Mol Biol Cell 22(22): 4390-405 (2011).

[35] Araki E, Oyadomari S, Mori M. Endoplasmic reticulum stress and diabetes mellitus. Intern Med 42(1): 7-14 (2003).

[36] Harding HP, Zeng H, Zhang Y, Jungries R, Chung P, Plesken H, *et al.* Diabetes mellitus and exocrine pancreatic dysfunction in perk-/- mice reveals a role for translational control in secretory cell survival. Mol Cell 7(6): 1153-63 (2001).

[37] Maly DJ, Papa FR. Druggable sensors of the unfolded protein response. Nat Chem Biol 10(11): 892-901 (2014).

[38] Feng N, Ma X, Wei X, Zhang J, Dong A, Jin M, *et al.* Common variants in PERK, JNK, BIP and XBP1 genes are associated with the risk of prediabetes or diabetes-related phenotypes in a Chinese population. Chin Med J 127(13): 2438-44 (2014).

[39] Ozbek MN, Senee V, Aydemir S, Kotan LD, Mungan NO, Yuksel B, *et al.* Wolcott-Rallison syndrome due to the same mutation (W522X) in EIF2AK3 in two unrelated families and review of the literature. Pediatr Diabetes 11(4): 279-85 (2010).

[40] Rubio-Cabezas O, Patch AM, Minton JA, Flanagan SE, Edghill EL, Hussain K, *et al.* Wolcott-Rallison syndrome is the most common genetic cause of permanent neonatal diabetes in consanguineous families. J Clin Endocrinol Metabol 94(11): 4162-70 (2009).

[41] Julier C, Nicolino M. Wolcott-Rallison syndrome. Orphanet J Rare Dis 5: 29 (2010).

[42] Wolcott CD, Rallison ML. Infancy-onset diabetes mellitus and multiple epiphyseal dysplasia. J Pediatr 80(2): 292-7 (1972).

[43] Back SH, Scheuner D, Han J, Song B, Ribick M, Wang J, *et al.* Translation attenuation through eIF2alpha phosphorylation prevents oxidative stress and maintains the differentiated state in beta cells. Cell Metabol 10(1): 13-26 (2009).

[44] Harding HP, Zhang Y, Ron D. Protein translation and folding are coupled by an endoplasmic-reticulum-resident kinase. Nature 397(6716): 271-4 (1999).

[45] Ozcan U, Cao Q, Yilmaz E, Lee AH, Iwakoshi NN, Ozdelen E, *et al.* Endoplasmic reticulum stress links obesity, insulin action, and type 2 diabetes. Science 306(5695): 457-61 (2004).

[46] Zito E, Chin KT, Blais J, Harding HP, Ron D. ERO1-beta, a pancreas-specific disulfide oxidase, promotes insulin biogenesis and glucose homeostasis. J Cell Biol 188(6): 821-32 (2010).

[47] Kosakowska-Cholody T, Lin J, Srideshikan SM, Scheffer L, Tarasova NI, Acharya JK. HKH40A downregulates GRP78/BiP expression in cancer cells. Cell Death Dis 5: e1240\ (2014).

[48] Bobrovnikova-Marjon E, Grigoriadou C, Pytel D, Zhang F, Ye J, Koumenis C, *et al.* PERK promotes cancer cell proliferation and tumor growth by limiting oxidative DNA damage. Oncogene 29(27): 3881-95 (2010).

[49] Nagelkerke A, Bussink J, Mujcic H, Wouters BG, Lehmann S, Sweep FC, *et al.* Hypoxia stimulates migration of breast cancer cells via the PERK/ATF4/LAMP3-arm of the unfolded protein response. Breast Can Res 15(1): R2 (2013).

[50] Axten JM, Medina JR, Feng Y, Shu A, Romeril SP, Grant SW, *et al.* Discovery of 7-methyl-5-(1-{[3-(trifluoromethyl)phenyl] acetyl}-2,3-dihydro-1H-indol-5-yl)-7H-p yrrolo[2,3-d]pyrimidin-4-

amine (GSK2606414), a potent and selective first-in-class inhibitor of protein kinase R (PKR)-like endoplasmic reticulum kinase (PERK). J Med Chem 55(16): 7193-207 (2012).

[51] Mujcic H, Rzymski T, Rouschop KM, Koritzinsky M, Milani M, Harris AL*, et al.* Hypoxic activation of the unfolded protein response (UPR) induces expression of the metastasis-associated gene LAMP3. Radiotherapy Oncol 92(3): 450-9 (2009).

[52] Ferrari R, Ryten M, Simone R, Trabzuni D, Nicolaou N, Hondhamuni G*, et al.* Assessment of common variability and expression quantitative trait loci for genome-wide associations for progressive supranuclear palsy. Neurobiol Aging 35(6): 1514 e1-12 (2014).

[53] Stutzbach LD, Xie SX, Naj AC, Albin R, Gilman S, Group PSPGS*, et al.* The unfolded protein response is activated in disease-affected brain regions in progressive supranuclear palsy and Alzheimer's disease. Acta Neuropathol Commun 1(1): 31 (2013).

[54] Liu J, Hoppman N, O'Connell JR, Wang H, Streeten EA, McLenithan JC*, et al.* A functional haplotype in EIF2AK3, an ER stress sensor, is associated with lower bone mineral density. JOF Bone Min Res 27(2): 331-41.(2012).

[55] Hoglinger GU, Melhem NM, Dickson DW, Sleiman PM, Wang LS, Klei L*, et al.* Identification of common variants influencing risk of the tauopathy progressive supranuclear palsy. Nat Genet 43(7): 699-705 (2011).

[56] Hoozemans JJ, van Haastert ES, Eikelenboom P, de Vos RA, Rozemuller JM, Scheper W. Activation of the unfolded protein response in Parkinson's disease. Biochem Biophys Res Commun 354(3): 707-11 (2007).

[57] Hoozemans JJ, van Haastert ES, Nijholt DA, Rozemuller AJ, Eikelenboom P, Scheper W. The unfolded protein response is activated in pretangle neurons in Alzheimer's disease hippocampus. Am J Pathol 174(4): 1241-51 (2009).

[58] Hoozemans JJ, van Haastert ES, Nijholt DA, Rozemuller AJ, Scheper W. Activation of the unfolded protein response is an early event in Alzheimer's and Parkinson's disease. Neuro-degenerative Dis 10(1-4): 212-5 (2012).

[59] Hoozemans JJ, Veerhuis R, Van Haastert ES, Rozemuller JM, Baas F, Eikelenboom P*, et al.* The unfolded protein response is activated in Alzheimer's disease. Acta Neuropathol 110(2): 165-72 (2005).

[60] Nijholt DA, van Haastert ES, Rozemuller AJ, Scheper W, Hoozemans JJ. The unfolded protein response is associated with early tau pathology in the hippocampus of tauopathies. J Pathol 226(5): 693-702 (2012).

[61] Moreno JA, Radford H, Peretti D, Steinert JR, Verity N, Martin MG*, et al.* Sustained translational repression by eIF2alpha-P mediates prion neurodegeneration. Nature 485(7399): 507-11 (2012).

[62] Duvarci S, Nader K, LeDoux JE. De novo mRNA synthesis is required for both consolidation and reconsolidation of fear memories in the amygdala. Learning Mem 15(10): 747-55 (2008).

[63] Hirtz D, Thurman DJ, Gwinn-Hardy K, Mohamed M, Chaudhuri AR, Zalutsky R. How common are the "common" neurologic disorders? Neurology 68(5): 326-37 (2007).

[64] Mehta P, Antao V, Kaye W, Sanchez M, Williamson D, Bryan L*, et al.* Prevalence of amyotrophic lateral sclerosis - United States, 2010-2011. Morb Mortal Weekly Rep Surveill Summ 63(7): 1-14 (2014).

[65] Walker AK, Soo KY, Sundaramoorthy V, Parakh S, Ma Y, Farg MA*, et al.* ALS-associated TDP-43 induces endoplasmic reticulum stress, which drives cytoplasmic TDP-43 accumulation and stress granule formation. PloS One 8(11): e81170 (2013).

[66] Ilieva EV, Ayala V, Jove M, Dalfo E, Cacabelos D, Povedano M*, et al.* Oxidative and endoplasmic reticulum stress interplay in sporadic amyotrophic lateral sclerosis. Brain 130(Pt 12): 3111-23 (2007).

[67] Grosskreutz J, Van Den Bosch L, Keller BU. Calcium dysregulation in amyotrophic lateral sclerosis. Cell Cal 47(2): 165-74 (2010).

[68] Kikuchi H, Almer G, Yamashita S, Guegan C, Nagai M, Xu Z*, et al.* Spinal cord endoplasmic reticulum stress associated with a microsomal accumulation of mutant superoxide dismutase-1 in an ALS model. Proc Nat Acad Sci USA 103(15): 6025-30 (2006).

[69] Amato AA, Russell JA. Neuromuscular disorders. New York: McGraw-Hill Medical (2008).

[70] Rowland LP, Shneider NA. Amyotrophic lateral sclerosis. New Eng J Med 344(22): 1688-700 (2001).

[71] Swinnen B, Robberecht W. The phenotypic variability of amyotrophic lateral sclerosis. Nat Rev Neurol 10(11): 661-70 (2014).

[72] Chio A, Calvo A, Moglia C, Mazzini L, Mora G, group Ps. Phenotypic heterogeneity of amyotrophic lateral sclerosis: a population based study. J Neurol Neurosurg Psychiatr 82(7): 740-6 (2011).

[73] Shoesmith CL, Findlater K, Rowe A, Strong MJ. Prognosis of amyotrophic lateral sclerosis with respiratory onset. J Neurol Neurosurg Psychiatry 78(6): 629-31 (2007).

[74] Buratti E, Dork T, Zuccato E, Pagani F, Romano M, Baralle FE. Nuclear factor TDP-43 and SR proteins promote *in vitro* and *in vivo* CFTR exon 9 skipping. EMBO J 20(7): 1774-84 (2001).

[75] Winton MJ, Igaz LM, Wong MM, Kwong LK, Trojanowski JQ, Lee VM. Disturbance of nuclear and cytoplasmic TAR DNA-binding protein (TDP-43) induces disease-like redistribution, sequestration, and aggregate formation. J Biol Chem 283(19): 13302-9 (2008).

[76] Wang IF, Reddy NM, Shen CK. Higher order arrangement of the eukaryotic nuclear bodies. Proc Nat Acad Sci USA 99(21): 13583-8 (2002).

[77] Jinwal UK, Abisambra JF, Zhang J, Dharia S, O'Leary JC, Patel T*, et al.* Cdc37/Hsp90 protein complex disruption triggers an autophagic clearance cascade for TDP-43 protein. J Biol Chem 287(29): 24814-20 (2012).

[78] Winton MJ, Van Deerlin VM, Kwong LK, Yuan W, Wood EM, Yu CE*, et al.* A90V TDP-43 variant results in the aberrant localization of TDP-43 *in vitro*. FEBB Lett 582(15): 2252-6 (2008).

[79] Dewey CM, Cenik B, Sephton CF, Johnson BA, Herz J, Yu G. TDP-43 aggregation in neurodegeneration: are stress granules the key? Brain Res 1462: 16-25 (2012).

[80] Liu-Yesucevitz L, Bilgutay A, Zhang YJ, Vanderweyde T, Citro A, Mehta T*, et al.* Tar DNA binding protein-43 (TDP-43) associates with stress granules: analysis of cultured cells and pathological brain tissue. PloS one 5(10): e13250 (2010).

[81] McDonald KK, Aulas A, Destroismaisons L, Pickles S, Beleac E, Camu W*, et al.* TAR DNA-binding protein 43 (TDP-43) regulates stress granule dynamics via differential regulation of G3BP and TIA-1. Hum Mol Genet 20(7): 1400-10 (2011).

[82] Dewey CM, Cenik B, Sephton CF, Dries DR, Mayer P, 3rd, Good SK*, et al.* TDP-43 is directed to stress granules by sorbitol, a novel physiological osmotic and oxidative stressor. Mol Cell Biol 31(5): 1098-108 (2011).

[83] Kedersha NL, Gupta M, Li W, Miller I, Anderson P. RNA-binding proteins TIA-1 and TIAR link the phosphorylation of eIF-2 alpha to the assembly of mammalian stress granules. J Cell Biol 147(7): 1431-42 (1999).

[84] Kedersha N, Anderson P. Regulation of translation by stress granules and processing bodies. Prog Mol Biol Transl Sci 90: 155-85 (2009).

[85] Group THsDCR. A novel gene containing a trinucleotide repeat that is expanded and unstable on Huntington's disease chromosomes. The Huntington's Disease Collaborative Research Group. Cell 72(6): 971-83 (1993).

[86] Reiner A, Albin RL, Anderson KD, D'Amato CJ, Penney JB, Young AB. Differential loss of striatal projection neurons in Huntington disease. Proc Natl Acad Sci USA 85(15): 5733-7 (1988).

[87] Subramaniam S, Sixt KM, Barrow R, Snyder SH. Rhes, a striatal specific protein, mediates mutant-huntingtin cytotoxicity. Science 324(5932): 1327-30 (2009).

[88] Roze E, Cahill E, Martin E, Bonnet C, Vanhoutte P, Betuing S*, et al.* Huntington's Disease and Striatal Signaling. Front Neuroanat 5: 55 (2011).

[89] Moore RC, Xiang F, Monaghan J, Han D, Zhang Z, Edstrom L*, et al.* Huntington disease phenocopy is a familial prion disease. Am J Hum Genet 69(6): 1385-8 (2001).

[90] Schneider SA, Bhatia KP. Huntington's disease look-alikes. Handbook Clin Neurol 100: 101-12 (2011).

[91] Xiang F, Almqvist EW, Huq M, Lundin A, Hayden MR, Edstrom L*, et al.* A Huntington disease-like neurodegenerative disorder maps to chromosome 20p. Am J Hum Genet 63(5): 1431-8 (1998).

[92] Laplanche JL, Hachimi KH, Durieux I, Thuillet P, Defebvre L, Delasnerie-Laupretre N*, et al.* Prominent psychiatric features and early onset in an inherited prion disease with a new insertional

mutation in the prion protein gene. Brain 122 (Pt 12): 2375-86 (1999).

[93] Holmes SE, O'Hearn E, Rosenblatt A, Callahan C, Hwang HS, Ingersoll-Ashworth RG*, et al.* A repeat expansion in the gene encoding junctophilin-3 is associated with Huntington disease-like 2. Nat Genet 29(4): 377-8 (2001).

[94] Kambouris M, Bohlega S, Al-Tahan A, Meyer BF. Localization of the gene for a novel autosomal recessive neurodegenerative Huntington-like disorder to 4p15.3. Am J Hum Genet 66(2): 445-52.(2000).

[95] Santos C, Wanderley H, Vedolin L, Pena SD, Jardim L, Sequeiros J. Huntington disease-like 2: the first patient with apparent European ancestry. Clin Gen 73(5): 480-5 (2008).

[96] Reijonen S, Putkonen N, Norremolle A, Lindholm D, Korhonen L. Inhibition of endoplasmic reticulum stress counteracts neuronal cell death and protein aggregation caused by N-terminal mutant huntingtin proteins. Exp Cell Res 314(5): 950-60 (2008).

[97] Wang H, Blais J, Ron D, Cardozo T. Structural determinants of PERK inhibitor potency and selectivity. Chem Biol Drug Des 76(6): 480-95.(2010).

[98] Leitman J, Barak B, Benyair R, Shenkman M, Ashery U, Hartl FU*, et al.* ER stress-induced eIF2-alpha phosphorylation underlies sensitivity of striatal neurons to pathogenic huntingtin. PloS one 9(3): e90803.(2014).

[99] Jiang Y, Lv H, Liao M, Xu X, Huang S, Tan H*, et al.* GRP78 counteracts cell death and protein aggregation caused by mutant huntingtin proteins. Neurosci Lett 516(2): 182-7 (2012).

[100] Spillantini MG, Schmidt ML, Lee VM, Trojanowski JQ, Jakes R, Goedert M. Alpha-synuclein in Lewy bodies. Nature 388(6645): 839-40 (1997).

[101] Abdullah R, Basak I, Patil KS, Alves G, Larsen JP, Moller SG. Parkinson's disease and age: The obvious but largely unexplored link. Exp Gerontol (2014).

[102] Singleton AB, Farrer M, Johnson J, Singleton A, Hague S, Kachergus J*, et al.* alpha-Synuclein locus triplication causes Parkinson's disease. Science 302(5646): 841 (2003).

[103] Chartier-Harlin MC, Kachergus J, Roumier C, Mouroux V, Douay X, Lincoln S*, et al.* Alpha-synuclein locus duplication as a cause of familial Parkinson's disease. Lancet 364(9440): 1167-9 (2004).

[104] Rommelfanger KS, Weinshenker D. Norepinephrine: The redheaded stepchild of Parkinson's disease. Biochem Pharmacol 74(2): 177-90 (2007).

[105] Denny-Brown D. Diseases of the basal ganglia. Their relation to disorders of movement. Lancet 2(7161): 1155-62 (1960).

[106] Mettler FA. Substantia nigra and Parkinsonism. Arch Neurol 11: 529-42 (1964).

[107] Seiden LS, Carlsson A. Brain and Heart Catecholamine Levels after L-Dopa administration in reserpine treated mice: correlations with a conditioned avoidance response. Psychopharmacologia 5: 178-81 (1964).

[108] Bertler A, Rosengren E. Possible role of brain dopamine. Pharmacol Rev 18(1): 769-73 (1966).

[109] Vogt M. Functional aspects of the role of catecholamines in the central nervous system. Br Med Bull 29(2): 168-72.(1973).

[110] Le Masson G, Przedborski S, Abbott LF. A computational model of motor neuron degeneration. Neuron 83(4): 975-88 (2014).

[111] Thies W, Bleiler L, Alzheimers A. 2013 Alzheimer's disease facts and figures. Alzheimer's Dement 9(2): 208-45 (2013).

[112] Hamos JE, Oblas B, Pulaski-Salo D, Welch WJ, Bole DG, Drachman DA. Expression of heat shock proteins in Alzheimer's disease. Neurology 41(3): 345-50 (1991).

[113] Kohler C, Dinekov M, Gotz J. Granulovacuolar degeneration and unfolded protein response in mouse models of tauopathy and Abeta amyloidosis. Neurobiol Dis 71: 169-79.(2014).

[114] Braak H, Braak E. Neuropathological stageing of Alzheimer-related changes. Acta Neuropathol 82(4): 239-59.(1991).

[115] Braak H, Braak E. Alzheimer's disease affects limbic nuclei of the thalamus. Acta Neuropathol 81(3): 261-8.(1991).

[116] Okamoto K, Hirai S, Iizuka T, Yanagisawa T, Watanabe M. Reexamination of granulovacuolar degeneration. Acta Neuropathol 82(5): 340-5 (1991).

[117] Funk KE, Mrak RE, Kuret J. Granulovacuolar degeneration (GVD) bodies of Alzheimer's disease (AD) resemble late-stage autophagic organelles. Neuropathol App Neurobiol 37(3): 295-306.(2011).

[118] Nishikawa T, Takahashi T, Nakamori M, Yamazaki Y, Kurashige T, Nagano Y*, et al.* Phosphatidylinositol-4,5-bisphosphate is enriched in granulovacuolar degeneration bodies and neurofibrillary tangles. Neuropathol App Neurobiol 40(4): 489-501 (2014).

[119] Lagalwar S, Berry RW, Binder LI. Relation of hippocampal phospho-SAPK/JNK granules in Alzheimer's disease and tauopathies to granulovacuolar degeneration bodies. Acta Neuropathol 113(1): 63-73.(2007).

[120] Schwab C, DeMaggio AJ, Ghoshal N, Binder LI, Kuret J, McGeer PL. Casein kinase 1 delta is associated with pathological accumulation of tau in several neurodegenerative diseases. Neurobiol Aging 21(4): 503-10 (2000).

[121] Yamazaki Y, Matsubara T, Takahashi T, Kurashige T, Dohi E, Hiji M*, et al.* Granulovacuolar degenerations appear in relation to hippocampal phosphorylated tau accumulation in various neurodegenerative disorders. PloSOne 6(11): e26996 (2011).

[122] Abisambra JF, Jinwal UK, Suntharalingam A, Arulselvam K, Brady S, Cockman M*, et al.* DnaJA1 antagonizes constitutive Hsp70-mediated stabilization of tau. J Mol Biol 421(4-5): 653-61 (2012).

[123] Dolan PJ, Johnson GV. A caspase cleaved form of tau is preferentially degraded through the autophagy pathway. J Biol Chem 285(29): 21978-87 (2010).

[124] Santacruz K, Lewis J, Spires T, Paulson J, Kotilinek L, Ingelsson M*, et al.* Tau suppression in a neurodegenerative mouse model improves memory function. Science 309(5733): 476-81 (2005).

[125] Hanger DP, Hughes K, Woodgett JR, Brion JP, Anderton BH. Glycogen synthase kinase-3 induces Alzheimer's disease-like phosphorylation of tau: generation of paired helical filament epitopes and neuronal localisation of the kinase. Neurosci Lett 147(1): 58-62 (1992).

[126] Jiang HY, Wek RC. Phosphorylation of the alpha-subunit of the eukaryotic initiation factor-2 (eIF2alpha) reduces protein synthesis and enhances apoptosis in response to proteasome inhibition. J Biol Chem 280(14): 14189-202 (2005).

[127] Newman J, Rissman RA, Sarsoza F, Kim RC, Dick M, Bennett DA*, et al.* Caspase-cleaved tau accumulation in neurodegenerative diseases associated with tau and alpha-synuclein pathology. Acta Neuropathol 110(2): 135-44 (2005).

[128] Rohn TT, Rissman RA, Davis MC, Kim YE, Cotman CW, Head E. Caspase-9 activation and caspase cleavage of tau in the Alzheimer's disease brain. Neurobiol J 11(2): 341-54.(2002).

[129] Matthews-Roberson TA, Quintanilla RA, Ding H, Johnson GV. Immortalized cortical neurons expressing caspase-cleaved tau are sensitized to endoplasmic reticulum stress induced cell death. Brain Res 1234: 206-12 (2008).

[130] Quintanilla RA, Matthews-Roberson TA, Dolan PJ, Johnson GV. Caspase-cleaved tau expression induces mitochondrial dysfunction in immortalized cortical neurons: implications for the pathogenesis of Alzheimer disease. J Biol Chem 284(28): 18754-66 (2009).

[131] Berry RW, Abraha A, Lagalwar S, LaPointe N, Gamblin TC, Cryns VL*, et al.* Inhibition of tau polymerization by its carboxy-terminal caspase cleavage fragment. Biochemistry 42(27): 8325-31 (2003).

[132] Cavallini A, Brewerton S, Bell A, Sargent S, Glover S, Hardy C*, et al.* An unbiased approach to identifying tau kinases that phosphorylate tau at sites associated with Alzheimer disease. J Biol Chem 288(32): 23331-47 (2013).

[133] Kondo T, Asai M, Tsukita K, Kutoku Y, Ohsawa Y, Sunada Y*, et al.* Modeling Alzheimer's disease with iPSCs reveals stress phenotypes associated with intracellular Abeta and differential drug responsiveness. Cell Stem Cell 12(4): 487-96 (2013).

[134] Yoon SO, Park DJ, Ryu JC, Ozer HG, Tep C, Shin YJ*, et al.* JNK3 perpetuates metabolic stress induced by Abeta peptides. Neuron 75(5): 824-37 (2012).

[135] Lee JH, Won SM, Suh J, Son SJ, Moon GJ, Park UJ*, et al.* Induction of the unfolded protein response and cell death pathway in Alzheimer's disease, but not in aged Tg2576 mice. Exp Mol Med 42(5): 386-94 (2010).

[136] Copanaki E, Schurmann T, Eckert A, Leuner K, Muller WE, Prehn JH*, et al.* The amyloid precursor protein potentiates CHOP induction and cell death in response to ER Ca2+ depletion. Biochim Biophys Acta 1773(2): 157-65 (2007).

[137] Tomimoto H, Akiguchi I, Wakita H, Nakamura S, Kimura J. Ultrastructural localization of amyloid protein precursor in the normal and postischemic gerbil brain. Brain Res 672(1-2): 187-95 (1995).

[138] Abisambra JF, Fiorelli T, Padmanabhan J, Neame P, Wefes I, Potter H. LDLR expression and localization are altered in mouse and human cell culture models of Alzheimer's disease. PloS one 5(1): e8556 (2010).

[139] Takahashi K, Niidome T, Akaike A, Kihara T, Sugimoto H. Amyloid precursor protein promotes endoplasmic reticulum stress-induced cell death via C/EBP homologous protein-mediated pathway. J Neurochem 109(5): 1324-37 (2009).

[140] Kogel D, Concannon CG, Muller T, Konig H, Bonner C, Poeschel S*, et al.* The APP intracellular domain (AICD) potentiates ER stress-induced apoptosis. Neurobiol Aging 33(9): 2200-9 (2012).

[141] Respondek G, Stamelou M, Kurz C, Ferguson LW, Rajput A, Chiu WZ*, et al.* The phenotypic spectrum of progressive supranuclear palsy: A retrospective multicenter study of 100 definite cases. Movement Disord 29(14): 1758-66 (2014).

[142] Respondek G, Roeber S, Kretzschmar H, Troakes C, Al-Sarraj S, Gelpi E*, et al*. Accuracy of the National Institute for Neurological Disorders and Stroke/Society for Progressive Supranuclear Palsy and neuroprotection and natural history in Parkinson plus syndromes criteria for the diagnosis of progressive supranuclear palsy. Movement Disord 28(4): 504-9 (2013).

[143] Boeve BF, Lang AE, Litvan I. Corticobasal degeneration and its relationship to progressive supranuclear palsy and frontotemporal dementia. Ann Neurol 54(5): S15-9 (2003).

[144] Liscic RM, Srulijes K, Groger A, Maetzler W, Berg D. Differentiation of progressive supranuclear palsy: clinical, imaging and laboratory tools. Acta Neurolog Scand 127(5): 362-70 (2013).

[145] Litvan I, Mangone CA, McKee A, Verny M, Parsa A, Jellinger K*, et al.* Natural history of progressive supranuclear palsy (Steele-Richardson-Olszewski syndrome) and clinical predictors of survival: a clinicopathological study. J Neurol Neurosurg Psychiatry 60(6): 615-20 (1996).

[146] Dickson DW, Ahmed Z, Algom AA, Tsuboi Y, Josephs KA. Neuropathology of variants of progressive supranuclear palsy. Curr Opin Neurol 23(4): 394-400 (2010).

[147] Nishimura M, Namba Y, Ikeda K, Oda M. Glial fibrillary tangles with straight tubules in the brains of patients with progressive supranuclear palsy. Neurosci Lett 143(1-2): 35-8 (1992).

[148] D'Alton S, Lewis J. Therapeutic and diagnostic challenges for frontotemporal dementia. Front Aging Neurosci 6: 204 (2014).

[149] Riedl L, Mackenzie IR, Forstl H, Kurz A, Diehl-Schmid J. Frontotemporal lobar degeneration: current perspectives. Neuropsychiatr Dis Treat 10: 297-310 (2014).

[150] Tong J, Huang C, Bi F, Wu Q, Huang B, Zhou H. XBP1 depletion precedes ubiquitin aggregation and Golgi fragmentation in TDP-43 transgenic rats. J Neurochem 123(3): 406-16 (2012).

[151] Moreno JA, Halliday M, Molloy C, Radford H, Verity N, Axten JM*, et al.* Oral treatment targeting the unfolded protein response prevents neurodegeneration and clinical disease in prion-infected mice. Sci Trans Med 5(206): 206ra138 (2013).

[152] Atkins C, Liu Q, Minthorn E, Zhang SY, Figueroa DJ, Moss K*, et al.* Characterization of a novel PERK kinase inhibitor with antitumor and antiangiogenic activity. Cancer Res 73(6): 1993-2002 (2013).

[153] Kim HJ, Raphael AR, LaDow ES, McGurk L, Weber RA, Trojanowski JQ*, et al.* Therapeutic modulation of eIF2alpha phosphorylation rescues TDP-43 toxicity in amyotrophic lateral sclerosis disease models. Nat Genet 46(2): 152-60 (2014).

[154] Saxena S, Cabuy E, Caroni P. A role for motoneuron subtype-selective ER stress in disease manifestations of FALS mice. Nat Neurosci 12(5): 627-36 (2009).

[155] Tanzi RE, McClatchey AI, Lamperti ED, Villa-Komaroff L, Gusella JF, Neve RL. Protease inhibitor domain encoded by an amyloid protein precursor mRNA associated with Alzheimer's disease. Nature 331(6156): 528-30 (1988).

[156] Unterberger U, Hoftberger R, Gelpi E, Flicker H, Budka H, Voigtlander T. Endoplasmic reticulum stress features are prominent in Alzheimer disease but not in prion diseases *in vivo*. J Neuropathol Exp Neurol 65(4): 348-57 (2006).

[157] Castillo-Carranza DL, Zhang Y, Guerrero-Munoz MJ, Kayed R, Rincon-Limas DE, Fernandez-Funez P. Differential activation of the ER stress factor XBP1 by oligomeric assemblies. Neurochem Res 37(8): 1707-17 (2012).

Received: ???????????????? **Revised:** ???????????????? **Accepted:** ????????????????

Neurobiology of Aging 56 (2017) 78–86

Contents lists available at ScienceDirect

Neurobiology of Aging

journal homepage: www.elsevier.com/locate/neuaging

Identification of changes in neuronal function as a consequence of aging and tauopathic neurodegeneration using a novel and sensitive magnetic resonance imaging approach

Sarah N. Fontaine [a,b], Alexandria Ingram [a], Ryan A. Cloyd [a], Shelby E. Meier [a,c], Emily Miller [a], Danielle Lyons [d], Grant K. Nation [a], Elizabeth Mechas [a], Blaine Weiss [a], Chiara Lanzillotta [e], Fabio Di Domenico [e], Frederick Schmitt [a], David K. Powell [f], Moriel Vandsburger [c,f], Jose F. Abisambra [a,b,c,d,*]

[a] Sanders-Brown Center on Aging, University of Kentucky, Lexington, KY, USA
[b] Epilepsy Center, University of Kentucky, Lexington, KY, USA
[c] Department of Physiology, College of Medicine, University of Kentucky, Lexington, KY, USA
[d] Spinal Cord Injury and Brain Injury Research Center, University of Kentucky, Lexington, KY, USA
[e] Department of Biochemical Sciences, Sapienza University of Rome, Rome, Italy
[f] Department of Biomedical Engineering, University of Kentucky, Lexington, KY, USA

ARTICLE INFO

Article history:
Received 3 November 2016
Received in revised form 9 March 2017
Accepted 9 April 2017
Available online 18 April 2017

Keywords:
MEMRI
Tau
Tangles
Manganese
rTg4510
Alzheimer

ABSTRACT

Tauopathies, the most common of which is Alzheimer's disease (AD), constitute the most crippling neurodegenerative threat to our aging population. Tauopathic patients have significant cognitive decline accompanied by irreversible and severe brain atrophy, and it is thought that neuronal dysfunction begins years before diagnosis. Our current understanding of tauopathies has yielded promising therapeutic interventions but have all failed in clinical trials. This is partly due to the inability to identify and intervene in an effective therapeutic window early in the disease process. A major challenge that contributes to the definition of an early therapeutic window is limited technologies. To address these challenges, we modified and adapted a manganese-enhanced magnetic resonance imaging (MEMRI) approach to provide sensitive and quantitative power to detect changes in broad neuronal function in aging mice. Considering that tau tangle burden correlates well with cognitive impairment in Alzheimer's patients, we performed our MEMRI approach in a time course of aging mice and an accelerated mouse model of tauopathy. We measured significant changes in broad neuronal function as a consequence of age, and in transgenic mice, before the deposition of *bona fide* tangles. This MEMRI approach represents the first diagnostic measure of neuronal dysfunction in mice. Successful translation of this technology in the clinic could serve as a sensitive diagnostic tool for the definition of effective therapeutic windows.

1. Introduction

Alzheimer's disease (AD) and related tauopathies are the most crippling cognitive threat to the aging population. There is no cure for tauopathies, and this is partly because of unclear understanding of tau pathogenesis. It is expected that in the United States we will spend approximately $1.2 trillion to maintain the constantly deteriorating quality of life of 16 million Americans with AD by 2050 (Alzheimer's, 2016). Despite promising results in in vivo models, therapeutic interventions fail to halt the disease process, and they only provide temporary benefits. A major challenge in the field is the lack of sensitive technologies to identify presymptomatic signs of disease. Consequently, neuronal damage in the patient population recruited for clinical trials might be too far advanced for therapeutics to be effective. Therefore, there is a critical need to identify an early therapeutic window in the prodromal stage of disease.

The current diagnostic imaging measure of pre-AD relies on amyloid plaque detection. Individuals are screened using anti-amyloid ligands (florbetapir) with positron emission tomography (PET) (Carome and Wolfe, 2011; Choi et al., 2009; Klunk et al., 2004; Mathis et al., 2004). In addition, development of effective and specific tau tangle ligands such as ^{18}F-T807 accelerated the possibility of measuring both pathological signs of AD and

* Corresponding author at: Sanders-Brown Center on Aging, University of Kentucky, 800S Limestone St, Lexington, KY 40536-0230, USA. Tel.: (859) 218-3852; fax: (859) 323-2866.
E-mail address: joe.abisambra@uky.edu (J.F. Abisambra).

0197-4580/$ – see front matter © 2017 Elsevier Inc. All rights reserved.
http://dx.doi.org/10.1016/j.neurobiolaging.2017.04.007

discriminating several diseases (Chien et al., 2014; Johnson et al., 2016; Marquie et al., 2015). There are several challenges for using PET technology to diagnose neurodegenerative processes. Accessibility to PET instruments is limited by location and cost, curtailing widespread availability of this technique. Moreover, the merging of PET molecular signatures to anatomical features requires the addition of structural imaging and in the case of computed tomography imaging, which leads to double exposure to radiation. The most pivotal obstacle with current imaging diagnostics is their focus on correlation between cognitive damage and mature pathology. Individuals in the prodromal stages of disease are only identified after PET-positive amyloid pathology appears. Moreover, [F18]-AV-1451 tracers detect PHF1-positive aggregates, which correspond to late-stage tangles enriched with pS396/S404 tau. Therefore, individuals who present pathological signs of disease and mild (mild cognitive impairment) to moderate symptomatology likely suffer simultaneous irreversible neurodegenerative processes making therapeutic interventions less efficacious (Dubois et al., 2016).

In contrast, access to MRI technology is widely available, and does not require the use of ionizing radiation. MRI can be combined with contrast enhancement agents to increase the sensitivity of this technique. Manganese-enhanced MRI (MEMRI) offers a powerful tool to repeatedly measure neuronal function in longitudinal in vivo studies. MEMRI is particularly well suited for brain imaging because manganese enters voltage-gated ion channels proportionally to calcium flux (Lin and Koretsky, 1997) and shortens the T1 relaxation time of neighboring water (Antkowiak et al., 2012; Bissig and Berkowitz, 2014; Drapeau and Nachshen, 1984; Koretsky and Silva, 2004; Vandsburger et al., 2012). Once in a neuron, manganese is trafficked through the cells and released in the postsynaptic density (Pautler et al., 1998), and this activity-dependent uptake and trafficking correlates with broad neuronal function (Pautler and Koretsky, 2002). In addition, manganese is taken up preferentially in the hippocampus (Shineman et al., 2011), a key brain region involved in learning and memory. Therefore, MEMRI is a powerful technique to quantify broad neuronal function in brain regions affected by age and neurodegenerative disease.

We tested the value of combined MEMRI and mapping of T1 relaxation times coupled with T2-mapping to determine changes in signatures over time and with disease in the rTg4510 transgenic mouse model of accelerated tauopathy (Santacruz et al., 2005). MEMRI recognized alterations in broad neuronal function during presymptomatic stages of pretangle pathology. Our results suggest that MEMRI is a sensitive, widely available, and noninvasive in vivo imaging technique for identification of early stages of neurodegeneration.

2. Materials and methods

2.1. Mice and ethics approval

All animal studies were approved by the University of Kentucky's Institutional Animal Care and Use Committee (IACUC) and abided by that committee's policies on animal care and use in accordance with the Guide for the Care and Use of Laboratory Animals, the Animal Welfare Regulations Title 9 Code of Federal Regulations Subchapter A, "Animal Welfare," Parts 1–3, and the Public Health Service Policy on Humane Care and Use of Laboratory Animals. This University of Kentucky program and the facilities for animal care and use are fully accredited by the Association for Assessment and Accreditation of Laboratory Animal Care International. The animals were kept in standard housing on a 14h light/10h dark cycle and received food and water ad libitum. The tau transgenic (rTg4510) and parental mice (rTta and TRE-4R0N-P301L MAPT, on an FVB background) were maintained and genotyped as described previously (Santacruz et al., 2005). All experiments were done in both male and female mice.

For MEMRI studies, at each age group (2, 3, and 10 months) a naïve group of mice were subjected to one MEMRI scan. As we observed, there were no differences in MEMRI between TRE-4R0N P301L MAPT (tau), rTta and wt littermates, and each experiment was performed with age- and sex-matched littermates of the non-rTg4510 genotype (ctrl).

2.2. Manganese-enhanced magnetic resonance imaging (MEMRI)

All MRI procedures were performed in accordance with the University of Kentucky Magnetic Resonance Imaging and Spectroscopy Core IACUC Protocol. Manganese, which is identical in charge and similar in ionic radius to calcium, enters voltage-gated calcium channels on neuronal membranes, follows calcium trafficking, and is released in the synaptic cleft and internalized by the postsynaptic neuron (Masumiya et al., 2003; Pautler et al., 1998). Manganese is also a potent MRI contrast agent that lengthens R1 (1/T1) relaxation rates as a function of concentration in tissue (Vandsburger et al., 2012). When MEMRI is combined with an imaging protocol to quantify tissue R1 relaxation rates, the acquired data reflects an in vivo measurement of underlying function of cells with voltage-gated calcium channels (Antkowiak et al., 2012). Manganese chloride (30 mM) prepared in saline was delivered to mice via intraperitoneal injection (66 mg/kg). All MR imaging was performed on a horizontal bore 7T Bruker ClinScan magnet (Bruker, Ettlingen, Germany) using a cylindrical volume coil for excitation and a cryocoil for detection. In preparation for imaging, animals are anesthetized using isoflurane (3%–5%) in oxygen at a rate of 0.5–1.0 L/min and maintained using 1%–3% isoflurane in oxygen. Body temperature was maintained using circulating water, and vital signs (core temperature and respirations) were monitored using a physiological monitoring system SA Instruments Inc (SAI, Stony Brook, NY, USA). Look-Locker imaging was performed following nonselective spin inversion in one slice of the brain containing large regions of hippocampus. Fifty images were acquired following inversion with image spacing of 100 ms (total sequence repetition time of 5s) to fully sample the T1 relaxation curve. Additional image parameters included TR/TE = 5500/1.9, Matrix = 128 × 128, number of averages = 3, field of view = 17 mm × 17 mm × 0.7 mm. T2-weighted images were acquired covering the entire brain (excluding the cerebellum and olfactory bulb) using a turbo-spin echo sequence with TR/TE = 3360/42, Slices = 21, Matrix = 448 × 336, number of averages = 2, field of view = 25 mm × 25 mm × 0.5 mm. The imaging procedures for scanning a mouse were completed in 45 minutes. Imaging was performed before the injection of $MnCl_2$ (baseline) and repeated at 6 hours after injection (Fig. 1). Image mapping and analysis was performed in MATLAB (Mathworks, Natick, MA, USA). Images from the Look-Locker series were used to reconstruct voxel-by-voxel signal relaxation curves which were fit to the equation $S(TI) = So^*(1-e^{-R1*TI})$, where S(t) represents the signal at a given inversion time (TI), So represents the steady-state signal at maximal TI, and R1 represents the longitudinal relaxation rate. Regions of interest (dentate gyrus [DG], cornu ammonis 1 [CA1], cornu ammonis 3 [CA3], and superior medial cortex [CTX]) were identified using the Allen Brain Mouse Atlas.

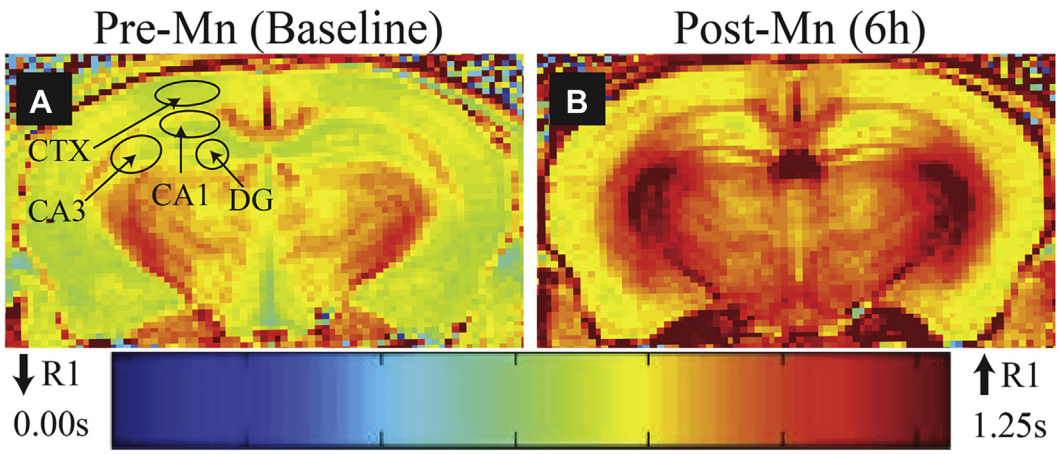

Fig. 1. Pre- and post-manganese parametric ΔR1 maps of a nontransgenic mouse. (A) High-resolution R1 mapping from baseline scans; regions of interest are denoted. (B) Same mouse, R1 maps from scan taken 6 hours after manganese injection. Abbreviations: CA1, cornu ammonis 1; CA3, cornu ammonis 3; CTX, superior medial cortex; DG, dentate gyrus; Mn, manganese.

Within each, the change in R1 relaxation rates (ΔR1) before and after $MnCl_2$ exposure was calculated as

$$\Delta R_1 = R1_{6h} - R1_{baseline}$$

2.3. Immunohistochemistry

Following MEMRI, mice were irreversibly anesthetized, exsanguinated, and transcardially perfused with saline followed by 4% phosphate-buffered paraformaldehyde (PFA, pH 7.4), a protocol mildly modified from Abisambra et al. (2010b). Brain samples were fixed in 4% paraformaldehyde for 24 hours, then cryoprotected by incubating in successive 24 hours increments with 10%, 20%, and 30% sucrose gradients as described previously (Jinwal et al., 2010). Brains were frozen on a temperature-controlled freezing stage, sectioned (25 μm) on a sliding microtome, and stored in a solution of PBS containing 0.02% sodium azide at 4 °C.

Free-floating immunohistochemistry was performed as described (Abisambra et al., 2010a). The following antibody dilutions were used: pS262 (Anaspec) 1; 10,000; pT231 (Invitrogen) 1:25,000; MC1 (kind gift from P. Davies) 1:2500. IHC sections were imaged using a Zeiss AxioScan (Zeiss, Germany). Image quantification was performed using ImageJ as follows: regions of interest (CA1, CA3, DG, and CTX) in 2–4 coronal sections per mouse were quantified. Then, all images were thresholded identically and intensity was measured for each region of interest. Quantifications shown are mean ± standard error of the mean.

2.4. Statistical analysis

All statistical analyses for MEMRI were performed using GraphPad Prism 6 (Graph Pad Software, Inc, La Jolla, CA, USA). Results are shown as the mean ± standard error. Data from Fig. 2 were analyzed using two-way ANOVA with a Bonferroni post-test. Data from Figs. 3 and 4 were analyzed using a student's unpaired *t*-test. A $p < 0.05$ was considered significant. For immunohistochemistry, any outliers to standard deviations from the mean were excluded. Two-way ANOVAs with multiple comparison post-hoc tests were performed to identify statistically significant differences using GraphPad Prism 6 software. A confidence interval of 95% ($p < 0.05$) was considered statistically significant.

3. Results

We first investigated MEMRI viability as a method to reveal age-related changes in wild-type mice. Since aging impacts calcium homeostasis, overall learning and memory, and neuronal connectivity (Gray and Johnston, 1987; Landfield, 1988; Sastry et al., 1986), we speculated that MEMRI could detect age-dependent alterations in brain regions where these functions are crucial. We first established a baseline model in control mice by performing MEMRI scans in groups of mice aged 2, 3, 6, and 10 months of age. Representative coronal sections of high-resolution R1 maps are shown for each age group (Fig. 2A–D). Quantification of ΔR1 revealed increased changes in relaxation rates (ΔR1, where R1 = 1/T1) in hippocampal regions CA1, CA3, and DG (Figs. 1A and 2E–G) as well as in the CTX (Fig. 2H). In all regions, there was an initial increase in ΔR1 values from 2 to 3 months, followed by a sharp decrease in ΔR1 values as animal age increases (Fig. 2E–H), suggesting manganese uptake decreases with age. These results suggest MEMRI is a sensitive and quantitative technique to distinguish age-related alterations in nontransgenic mice. We next sought to determine whether ΔR1 values could distinguish differences between age-related and neurodegenerative disease–associated alterations.

MEMRI successfully detected differences in AD mouse models overexpressing APP (Smith et al., 2007) and has been used to examine axonal transport rates in olfactory bulbs of rTg4510 (Majid et al., 2014). Because cognitive decline is closely associated with pathogenic tau accumulation, we used rTg4510 mice to identify whether MEMRI specifically detects changes in regions of the brain negatively impacted by tauopathy. Tau transgenic rTg4510 mice express very high levels of human tau with a pathogenic mutation associated with FTDL17 (Santacruz et al., 2005). Pretangle pathology matures into *bona fide* Alzheimer's-like tau tangles by 4 months of age (Ramsden et al., 2005; Santacruz et al., 2005). This pathological transition precedes moderate yet significant electrophysiological deficits and cognitive impairments, which become evident after 3.5 months and 4 months, respectively (Abisambra et al., 2010b, 2013; Ramsden et al., 2005). By 5.5 months, rTg4510 mice show overt tangle pathology along with significant cognitive decline and brain atrophy (Santacruz et al., 2005). These signs and symptoms are further potentiated with age: at 10 months, rTg4510 mice show larger tangles reminiscent of those present in frontotemporal lobar degeneration brains, ~20% reduction in brain weight, and more severe cognitive deficits than 5.5-month-old transgenic mice (Ramsden et al., 2005).

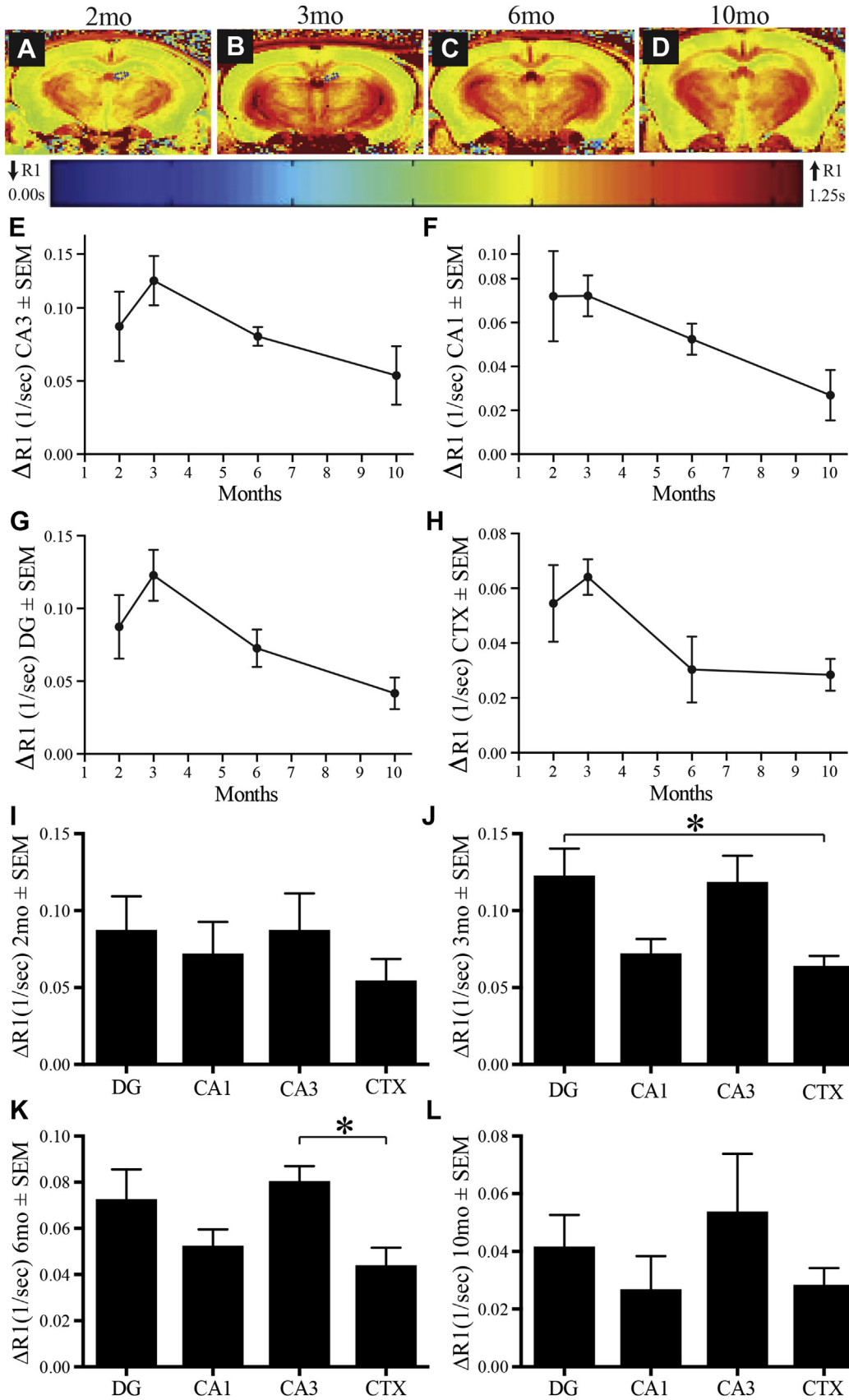

Fig. 2. MEMRI detects age-related changes in manganese uptake in nontransgenic mice. (A–D) Representative MEMRI-R1 map of non-transgenic mice at (A) 2 months, (B) 3 months, (C) 6 months, and (D) 10 months. Quantification of ΔR1 values in (E) CA3, (F) CA1, (G) dentate gyrus (DG), and (H) superior medial cortex (CTX). (I, J) ΔR1 and one-way ANOVA analysis using Tukey's multiple comparisons test of different brain regions (DG, CA1, CA3, and CTX) in (I) 2 months, (J) 3 months, (K) 6 months, and (L) 10 months control mice. All values are mean ± SEM, n = at least 6 per group. $^{*}p < 0.05$. Abbreviations: CA1, cornu ammonis 1; CA3, cornu ammonis 3; DG, dentate gyrus; MEMRI, manganese-enhanced magnetic resonance imaging.

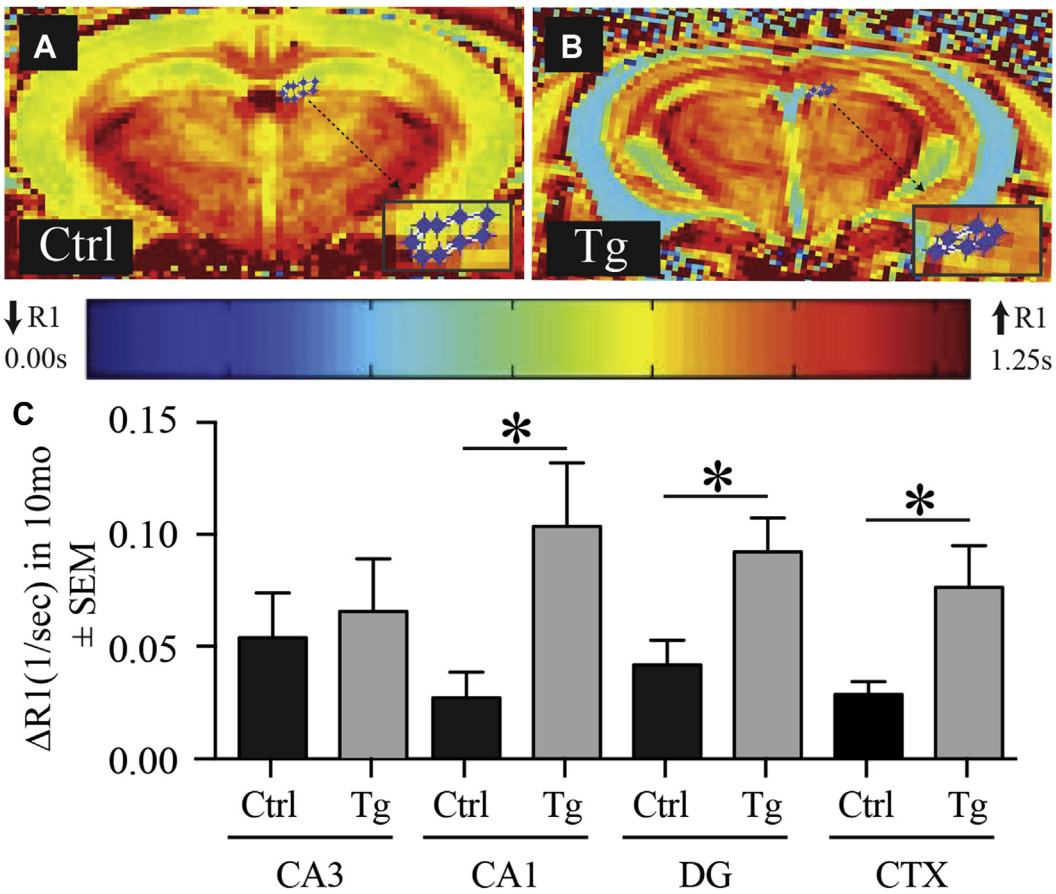

Fig. 3. Significant MEMRI changes in aged tauopathic mice. Representative R1 maps of MEMRI scans of 10-month littermate control (A) and 10-month rTg4510 (Tg) mice (B). (C) Quantification of ΔR1 values in CA3, CA1, dentate gyrus (DG), and superior medial cortex (CTX). All values are mean ± SEM, n = 6, $^{*}p < 0.05$.

We hypothesized that alterations in broad neuronal function caused by severe tau pathology would be detectable by MEMRI. We performed MEMRI ΔR1 analyses in 10-month rTg4510 transgenic mice, an advanced stage in the disease showing significant brain atrophy, tau pathology, and cognitive impairment. Indeed, MEMRI ΔR1 revealed gross abnormalities in rTg4510 brain morphology: cortical thinning (Fig. 3B) and accumulation of cerebrospinal fluid (blue color, Fig. 3B). Comparison of pre- and post-contrast R1 maps revealed that rTg4510 mice have significantly increased ΔR1 (Fig. 3B and C) in CA1, and DG regions of the hippocampus, as well as in the cortex compared with age-matched littermate control mice (Fig. 3A–C). There was no difference in any MEMRI signatures in the rTg4510 littermate controls (MAPT, tTA, or wt). These data suggest that rTg4510 mice have a much greater rate of manganese uptake and retention in the brain. Interestingly, we observed a significant decrease in ΔR1 from 3 month to 10 month of age (Fig. 3I). The only significant decrease between the different regions over time occurred in CA3.

We then tested the sensitivity of MEMRI to identify alterations in rTg4510 mice before the onset of cognitive decline. While deficits in synaptic plasticity are detected as early at 3.5 months in rTg4510 (Abisambra et al., 2013), robust deficits in cognition are readily detected in these animals at 4 months of age (Ramsden et al., 2005). We examined mice at 2 and 3 months of age, before the onset of severe cognitive damage. At 2 months, ΔR1 was unchanged between rTg4510 mice and littermate controls (Fig. 4). At 3 months, rTg4510 showed significant differences in ΔR1 in the CA1, CA3, DG, and cortical brain regions compared to 2-month-old rTg4510 mice (Fig. 4). Compared with littermate controls, R1 in the CA1 and CA3 region of the hippocampus was significantly increased (Fig. 4). Thus, specific tau-related changes in neuronal dysfunction are detectable by MEMRI as early as 3 months of age, before the onset of severe cognitive impairment in a transgenic tau animal model. These data suggest that MEMRI can detect changes in broad neuronal function before cognitive impairment.

To identify how closely MEMRI deficits are associated with increased pathogenic tau, we performed immunohistochemistry on 2- and 3-month-old rTg4510 mice. We first measured an early pathological tau conformation detected by the antibody MC1 (Weaver et al., 2000). As expected, MC1 immunoreactivity was present in hippocampal subregions and the cortex of both 2- and 3-month-old rTg4510 mice (Fig. 5). However, MC1 immunoreactivity was significantly increased in the CA3, DG, and the CTX regions of these 3-month-old tau transgenic mice (Fig. 5).

We next measured the presence of phosphorylated tau species present in pre-tangle pathology. Tau is phosphorylated at Ser262 and T231 early during in disease progression in AD and other diseases (Goedert et al., 1995; Hirano et al., 1968). Despite the appearance of pS262 and pT231 in pre-tangle pathology (Augustinack et al., 2002), we did not detect differences in the signal for these phospho-tau species between 2- and 3-month-old rTg4510 mice (Supplemental Fig. 1). Thus, these data suggest that presymptomatic detection of tau-related changes in neuronal function by MEMRI are associated with the accumulation of the earliest conformational markers of pathogenic tau, but not tau hyperphosphorylated at pS262 or pT231.

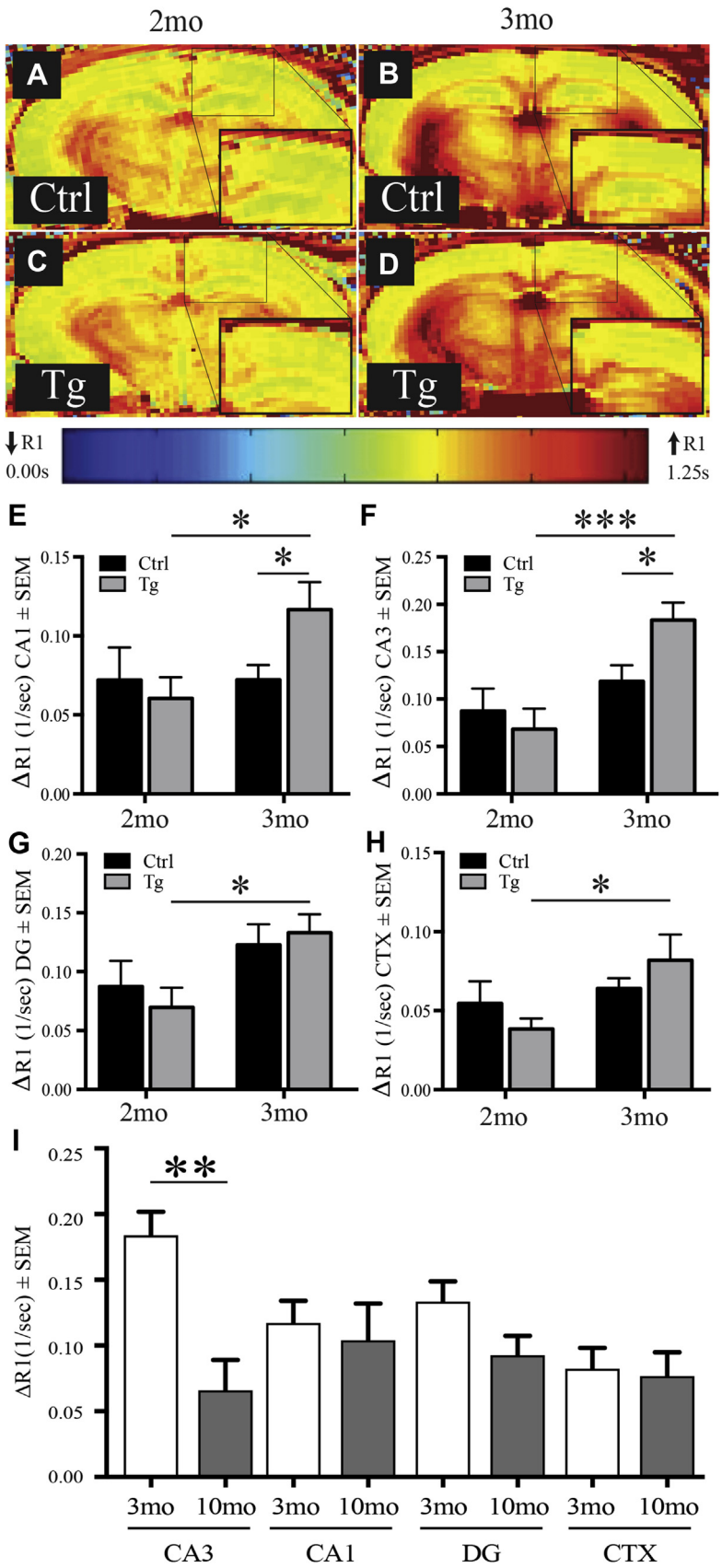

Fig. 4. MEMRI-R1 detects early signs of neuronal dysfunction in transgenic rTg4510 mice before the onset of cognitive deficits. (A–D) Representative R1 map of (A) 2-month littermate control, (B) 3-month littermate control, (C) 2-month rTg4510 mouse (Tg), and (D) 3-month rTg4510 mouse (Tg). Quantification of ΔR1 values in (E) CA1, (F) CA3, (G) dentate gyrus (DG), and (H) superior medial cortex (CTX). (I) ΔR1 comparison between different brain regions (CA3, CA1, DG, and CTX) in 3-month and 10-month rTg4510. All values are mean ± SEM, n = at least 4. $^{***}p < 0.001$, $^{**}p < 0.01$, $^{*}p < 0.05$. Abbreviations: CA1, cornu ammonis 1; CA3, cornu ammonis 3; CTX, cortex; DG, dentate gyrus; MEMRI, manganese-enhanced magnetic resonance imaging.

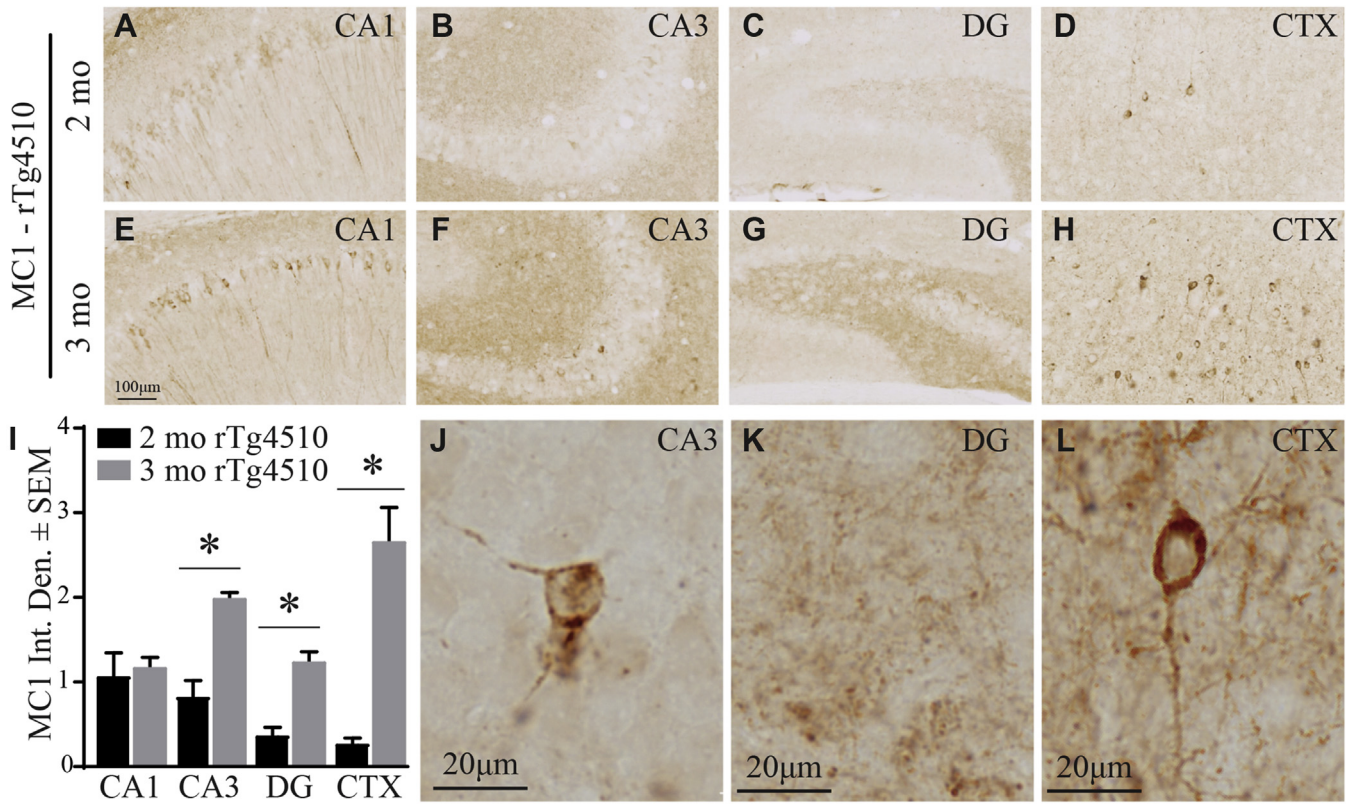

Fig. 5. MEMRI coincides with increased signal of an early marker of tau pathology. (A–H) Representative immunohistochemistry micrographs (20× objective) from 2- and 3-month rTg4510 stained with MC1 tau. (I) Quantification of MC1 levels in CA1, CA3, DG, and CTX. Data are mean ± SEM, n = 3 mice per group and 2–4 slices per mouse, $^{*}p < 0.05$. (J–L) Representative immunohistochemistry micrographs of 3-month rTg4510 mice in the regions denoted (CA3, DG, CTX) that were statistically significantly different and show tangle-bearing neurons and filaments (60× objective). Abbreviations: CA1, cornu ammonis 1; CA3, cornu ammonis 3; CTX, cortex; DG, dentate gyrus; MEMRI, manganese-enhanced magnetic resonance imaging.

4. Discussion

We used MEMRI coupled with high-resolution R1 mapping to measure broad neuronal function in mice. We identified longitudinal changes in small functional hippocampal regions (Fig. 2), significant neuronal changes in aged tau transgenic mice (Fig. 3), and the earliest sign of neuronal dysfunction in tauopathic hippocampus and cortex (Fig. 4). These latter changes coincide with the appearance of MC1-positive tau but not phospho-tau protein aggregates (Fig. 5). An important and critical finding of these studies is the identification of the earliest sign of brain alterations in a well-characterized tau mouse model, suggesting that MEMRI-R1 can be used to identify the beginning of a viable and potentially more effective therapeutic window in brains with neurodegeneration.

This is a highly sensitive approach to perform subregional analyses, which permits quantification of broad neuronal function in small areas of interest. The derived data offer unique insights into tauopathies by establishing areas most susceptible to tau-mediated neuronal damage. Future translational efforts could also use MEMRI-R1 to identify subtle changes in neuronal function in small regions of the brain in response to interventions.

The molecular mechanisms governing manganese uptake, retention, and clearance in brain cells remain incompletely understood. In 10-month-old transgenic mice, we detected significantly increased ΔR1 in all the regions analyzed except for the CA3 (Fig. 3). Similarly, ΔR1 of 3-month-old transgenic mice was significantly increased from age-matched nontransgenic controls in CA3 and CA1 but not in DG or CTX (Fig. 4). The presence of elevated changes in R1 values, correlating with heightened cellular levels of manganese, suggests that normal pathways for calcium homeostasis are impacted. Here, it is possible that MEMRI-ΔR1 detects calcium dysregulation, which is a major sign of neuronal dysfunction that has been previously described (Decker et al., 2015). These data also suggest that the mechanisms mediating calcium dysregulation in tauopathy also regulate evident manganese mis-sorting. Therefore, manganese is an effective calcium surrogate with tremendous potential to reveal changes in calcium dynamics, as an early sign of dysfunction in disease. In addition, using manganese to monitor calcium pathways would be a powerful means to measure quantitatively the effect of treatments on neuronal function. Data from Fig. 3F demonstrates that ΔR1 in CA3 decreases significantly over time. Together with the suggestion that CA3 plays an important role in disease progression of rTg4510 mice, our data suggest that the CA3 undergoes significant and early changes in rTg4510, which do not persist through 10 month compared with controls. Despite lack of persistence, these changes suggest that CA3 certainly plays a distinct and crucial role in disease progression worthy of further investigation.

Despite the ΔR1 aberrancies in tau transgenic mice, our approach revealed distinct ΔR1 patterns at 3 months of age in all imaged brains. In nontransgenic mice, ΔR1 values increased at 3 months (Fig. 2). This pattern was significantly increased in 3-month-old rTg4510 mice compared with 2-month-old rTg4510, and both 2- and 3-month-old littermate controls (Fig. 4). These data highlight important neurological processes at 3 months, which are altered in rTg4510 mice before the appearance of significant tau pathology and cognitive impairment.

Our approach builds on previous studies (Antkowiak et al., 2012; Lin and Koretsky, 1997; Pautler, 2004; Pautler et al., 1998; Vandsburger et al., 2012) to measure changes in the brain. MEMRI offers a powerful approach to quantitatively perform functional and minimally invasive measurements in the intact brain. Alternatives that reveal functional measurements, particularly in early stages of tauopathy, are terminal procedures such as electrophysiological measurements (Abisambra et al., 2013). Other studies employing MEMRI to measure changes in rTg4510 mice have also shown important differences. In one instance, MEMRI was used to measure transport rates and tract tracing in the olfactory bulb and showed that rTg4510 mice present transport deficits along olfactory axons (Majid et al., 2014). These data in the olfactory tract suggest and support our findings that there are neuronal deficits in the hippocampus of tau transgenic mice.

Another study by Perez and colleagues observed neuronal dysfunction in the CA3 of 5-month-old rTg4510 mice using MEMRI (Perez et al., 2013). Since tau pathology ensues well before 5 months in rTg4510 mice, it was reasonable to measure changes at earlier time points, which led us to identify MEMRI deficits as early as 3 months of age in rTg4510 mice (Fig. 4). Our approach expands on this finding by adding sensitivity to detect abnormal patterns of neuronal dysfunction in the transgenic mice in specific subregions (DG, CA1, CA3, and CTX) as well as significant differences in both the CA1 and CA3 when compared with nontransgenic mice. The ability to detect differences in neighboring subregions of the hippocampus suggests that MEMRI is highly sensitive. These data also foreshadow a mechanism of disease showing that CA1 and CA3 are the first regions to be affected by tau overexpression in the forebrain. Our results are supported by previous findings showing that rTg4510 mice present significant tau deposition in CA1 of 2-month-old mice, and that tau aggregation spreads to CA3; tau pathology finally reaches the DG by 8 months (Ramsden et al., 2005).

Despite the robust differences measured in CA1, DG, and CTX of 10-month-old rTg4510 mice, we were surprised to find that the CA3 did not show significant differences from controls. One possible explanation is that ΔR1 in CA3 is suppressed due to more neuronal atrophy in this region compared with other subregions of the hippocampus. This would lead to a reduction of voltage-gated calcium channels that would impair manganese influx (Lee and Koretsky, 2005). Interestingly, neuronal dysfunction is detected in rTg4510 mice at 3 months in the CA3 and CA1 regions of the hippocampus when compared with nontransgenic mice (Fig. 4).

An important consideration in this study is that the rTg4510 model is characterized by aggressive pathology (Ramsden et al., 2005; Santacruz et al., 2005). This is in part due to increased expression (approximately 13 times more) of human P301L tau, which is associated with onset of frontotemporal dementia (FTD). It would certainly be interesting to establish the effect of wild-type tau overexpression on ΔR1 changes. Since overexpression of wild-type tau leads to tauopathic aberrancies (Duff et al., 2000), and many other tauopathies are characterized by non-P301L tau tangles, we would expect to determine ΔR1 changes; however, the extent of these changes is unknown. On the other hand, the mechanisms of cell damage imparted by P301L and wild-type pathological tau could be different, and as a result ΔR1 might be normal in the latter condition. If this is the case, our approach would be more pertinent to FTD, and as such, it would be a unique approach to differentiate FTD from other non-P301L tauopathies AD.

Electrophysiological measurements show impaired long-term potentiation deficits as early as 3–3.5 months in rTg4510 mice suggesting circuitry malfunction in the CA1–CA3 (Abisambra et al., 2013). Other studies have indicated synaptic density deficits as well as spine loss in the rTg4510 mice at 7–9 months without calcium dysregulation (Kopeikina et al., 2013; Kuchibhotla et al., 2014). Therefore, compensatory mechanisms could be occurring in the circuitry at later time points to adapt to the changes occurring in CA3 at the early time point of 3 months where neuronal dysfunction is first detected in the hippocampus (Fig. 4). Electrophysiological approaches to measure calcium dysregulation in rTg4510 mice at 3 months of age are currently underway and could highlight a major molecular mechanism leading to neuronal dysfunction in early stages of the disease.

5. Conclusions

This study supports the use of MEMRI and R1 mapping as a sensitive and quantitative technique to identify changes in broad neuronal function as a consequence of development, aging, and disease. Moreover, the MEMRI application described herein has the potential to reveal early therapeutic windows for disease and monitor the impact of treatments in patients. A major step forward in the field will be translational efforts to use manganese-based FDA approved compounds in humans such as mangafodipir. Finally, these data demonstrate that neurological dysfunction coincides with the appearance of MC1 tau and before deposition of hyperphosporylated tau pathology.

Disclosure statement

The authors have no actual or potential conflicts of interests.

Acknowledgements

This study was funded by the University of Kentucky Alzheimer's Disease Center (UK-ADC), which is supported by NIH/NIA P30 AG028383. J. F. A., S. N. F., A. I., R. A. C., S. E. M., E. M., D. L., G. K. N., and E. M. were supported by NIH/NINDS 1R01 NS091329-01, Alzheimer's Association NIRG-14-322441, NIH/NCATS 5UL1TR000117-04, NIH/NIGMS 5P30GM110787, Department of Defense AZ140097, the University of Kentucky Epilepsy Center (EpiC), NIH/NIA P30 AG028383, and NIH/NIMHD L32 MD009205-01. The authors acknowledge Dr Donna Wilcock for use of the AxioScan, Dr Peter Davies for the MC1 antibody, and Dr Frederick Schmitt for comments on this manuscript and insights into these experiments. Author contributions are as follows: J. F. A. designed the study. S. N. F., A. I., S. E. M., E. M., and D. L. performed MRI. M. V. developed analysis program for MEMRI and M. V., D. L., S. E. M., and R. A. C. analyzed MEMRI data. A. I. and E. M. performed mouse husbandry and with S. N. F., tissue collection. S. N. F. performed all IHC and analysis. S. N. F., M. V., and J. F. A. interpreted data and wrote the paper. Data and materials will be made widely available on reasonable request to the corresponding author.

Appendix A. Supplementary data

Supplementary data associated with this article can be found, in the online version, at http://dx.doi.org/10.1016/j.neurobiolaging.2017.04.007.

References

Abisambra, J., Jinwal, U.K., Miyata, Y., Rogers, J., Blair, L., Li, X., Seguin, S.P., Wang, L., Jin, Y., Bacon, J., Brady, S., Cockman, M., Guidi, C., Zhang, J., Koren, J., Young, Z.T., Atkins, C.A., Zhang, B., Lawson, L.Y., Weeber, E.J., Brodsky, J.L., Gestwicki, J.E., Dickey, C.A., 2013. Allosteric heat shock protein 70 inhibitors rapidly rescue synaptic plasticity deficits by reducing aberrant tau. Biol. Psychiatry 74, 367–374.

Abisambra, J.F., Blair, L.J., Hill, S.E., Jones, J.R., Kraft, C., Rogers, J., Koren 3rd, J., Jinwal, U.K., Lawson, L., Johnson, A.G., Wilcock, D., O'Leary, J.C., Jansen-West, K., Muschol, M., Golde, T.E., Weeber, E.J., Banko, J., Dickey, C.A., 2010a.

Phosphorylation dynamics regulate Hsp27-mediated rescue of neuronal plasticity deficits in tau transgenic mice. J. Neurosci. 30, 15374–15382.
Abisambra, J.F., Fiorelli, T., Padmanabhan, J., Neame, P., Wefes, I., Potter, H., 2010b. LDLR expression and localization are altered in mouse and human cell culture models of Alzheimer's disease. PLoS One 5, e8556.
Alzheimer's Association, 2016. 2016 Alzheimer's disease facts and figures. Alzheimer's Demen. 12, 459–509.
Antkowiak, P.F., Vandsburger, M.H., Epstein, F.H., 2012. Quantitative pancreatic beta cell MRI using manganese-enhanced Look-Locker imaging and two-site water exchange analysis. Magn. Reson. Med. 67, 1730–1739.
Augustinack, J., Schneider, A., Mandelkow, E.-M., Hyman, B., 2002. Specific tau phosphorylation sites correlate with severity of neuronal cytopathology in Alzheimer's disease. Acta Neuropathol. 103, 26–35.
Bissig, D., Berkowitz, B.A., 2014. Testing the calcium hypothesis of aging in the rat hippocampus in vivo using manganese-enhanced MRI. Neurobiol. Aging 35, 1453–1458.
Carome, M., Wolfe, S., 2011. Florbetapir-PET imaging and postmortem beta-amyloid pathology. JAMA 305, 1857 author reply 1857–1858.
Chien, D.T., Szardenings, A.K., Bahri, S., Walsh, J.C., Mu, F., Xia, C., Shankle, W.R., Lerner, A.J., Su, M.Y., Elizarov, A., Kolb, H.C., 2014. Early clinical PET imaging results with the novel PHF-tau radioligand [F18]-T808. J. Alzheimer's Dis. 38, 171–184.
Choi, S.R., Golding, G., Zhuang, Z., Zhang, W., Lim, N., Hefti, F., Benedum, T.E., Kilbourn, M.R., Skovronsky, D., Kung, H.F., 2009. Preclinical properties of 18F-AV-45: a PET agent for Abeta plaques in the brain. J. Nucl. Med. 50, 1887–1894.
Decker, J.M., Kruger, L., Sydow, A., Zhao, S., Frotscher, M., Mandelkow, E., Mandelkow, E.M., 2015. Pro-aggregant Tau impairs mossy fiber plasticity due to structural changes and Ca(++) dysregulation. Acta Neuropathol. Commun. 3, 23.
Drapeau, P., Nachshen, D.A., 1984. Manganese fluxes and manganese-dependent neurotransmitter release in presynaptic nerve endings isolated from rat brain. J. Physiol. 348, 493–510.
Dubois, B., Hampel, H., Feldman, H.H., Scheltens, P., Aisen, P., Andrieu, S., Bakardjian, H., Benali, H., Bertram, L., Blennow, K., Broich, K., Cavedo, E., Crutch, S., Dartigues, J.F., Duyckaerts, C., Epelbaum, S., Frisoni, G.B., Gauthier, S., Genthon, R., Gouw, A.A., Habert, M.O., Holtzman, D.M., Kivipelto, M., Lista, S., Molinuevo, J.L., O'Bryant, S.E., Rabinovici, G.D., Rowe, C., Salloway, S., Schneider, L.S., Sperling, R., Teichmann, M., Carrillo, M.C., Cummings, J., Jack Jr., C.R. Proceedings of the Meeting of the International Working Group (IWG) and the American Alzheimer's Association on "The Preclinical State of AD"; July 23, 2015; Washington DC, USA, 2016. Preclinical Alzheimer's disease: definition, natural history, and diagnostic criteria. Alzheimer's Demen. 12, 292–323.
Duff, K., Knight, H., Refolo, L.M., Sanders, S., Yu, X., Picciano, M., Malester, B., Hutton, M., Adamson, J., Goedert, M., Burki, K., Davies, P., 2000. Characterization of pathology in transgenic mice over-expressing human genomic and cDNA tau transgenes. Neurobiol. Dis. 7, 87–98.
Goedert, M., Jakes, R., Vanmechelen, E., 1995. Monoclonal antibody AT8 recognises tau protein phosphorylated at both serine 202 and threonine 205. Neurosci. Lett. 189, 167–169.
Gray, R., Johnston, D., 1987. Noradrenaline and beta-adrenoceptor agonists increase activity of voltage-dependent calcium channels in hippocampal neurons. Nature 327, 620–622.
Hirano, A., Dembitzer, H.M., Kurland, L.T., Zimmerman, H.M., 1968. The fine structure of some intraganglionic alterations. Neurofibrillary tangles, granulovacuolar bodies and "rod-like" structures as seen in Guam amyotrophic lateral sclerosis and parkinsonism-dementia complex. J. Neuropathol. Exp. Neurol. 27, 167–182.
Jinwal, U.K., Koren 3rd, J., Borysov, S.I., Schmid, A.B., Abisambra, J.F., Blair, L.J., Johnson, A.G., Jones, J.R., Shults, C.L., O'Leary 3rd, J.C., Jin, Y., Buchner, J., Cox, M.B., Dickey, C.A., 2010. The Hsp90 cochaperone, FKBP51, increases Tau stability and polymerizes microtubules. J. Neurosci. 30, 591–599.
Johnson, K.A., Schultz, A., Betensky, R.A., Becker, J.A., Sepulcre, J., Rentz, D., Mormino, E., Chhatwal, J., Amariglio, R., Papp, K., Marshall, G., Albers, M., Mauro, S., Pepin, L., Alverio, J., Judge, K., Philiossaint, M., Shoup, T., Yokell, D., Dickerson, B., Gomez-Isla, T., Hyman, B., Vasdev, N., Sperling, R., 2016. Tau positron emission tomographic imaging in aging and early Alzheimer disease. Ann. Neurol. 79, 110–119.
Klunk, W.E., Engler, H., Nordberg, A., Wang, Y., Blomqvist, G., Holt, D.P., Bergstrom, M., Savitcheva, I., Huang, G.F., Estrada, S., Ausen, B., Debnath, M.L., Barletta, J., Price, J.C., Sandell, J., Lopresti, B.J., Wall, A., Koivisto, P., Antoni, G., Mathis, C.A., Langstrom, B., 2004. Imaging brain amyloid in Alzheimer's disease with Pittsburgh Compound-B. Ann. Neurol. 55, 306–319.
Kopeikina, K.J., Wegmann, S., Pitstick, R., Carlson, G.A., Bacskai, B.J., Betensky, R.A., Hyman, B.T., Spires-Jones, T.L., 2013. Tau causes synapse loss without disrupting calcium homeostasis in the rTg4510 model of tauopathy. PLoS One 8, e80834.
Koretsky, A.P., Silva, A.C., 2004. Manganese-enhanced magnetic resonance imaging (MEMRI). NMR Biomed. 17, 527–531.
Kuchibhotla, K.V., Wegmann, S., Kopeikina, K.J., Hawkes, J., Rudinskiy, N., Andermann, M.L., Spires-Jones, T.L., Bacskai, B.J., Hyman, B.T., 2014. Neurofibrillary tangle-bearing neurons are functionally integrated in cortical circuits in vivo. Proc. Natl. Acad. Sci. U. S. A. 111, 510–514.
Landfield, P.W., 1988. Hippocampal neurobiological mechanisms of age-related memory dysfunction. Neurobiol. Aging 9, 571–579.
Lee, J.H., Silva, A.C., Merkle, H., Koretsky, A.P., 2005. Manganese-enhanced magnetic resonance imaging of mouse brain after systemic administration of $MnCl_2$: dose-dependent and temporal evolution of T1 contrast. Man Reson Med 53, 640–648.
Lin, Y.J., Koretsky, A.P., 1997. Manganese ion enhances T1-weighted MRI during brain activation: an approach to direct imaging of brain function. Magn. Reson. Med. 38, 378–388.
Majid, T., Ali, Y.O., Venkitaramani, D.V., Jang, M.K., Lu, H.C., Pautler, R.G., 2014. In vivo axonal transport deficits in a mouse model of fronto-temporal dementia. Neuroimage. Clin. 4, 711–717.
Marquie, M., Normandin, M.D., Vanderburg, C.R., Costantino, I.M., Bien, E.A., Rycyna, L.G., Klunk, W.E., Mathis, C.A., Ikonomovic, M.D., Debnath, M.L., Vasdev, N., Dickerson, B.C., Gomperts, S.N., Growdon, J.H., Johnson, K.A., Frosch, M.P., Hyman, B.T., Gomez-Isla, T., 2015. Validating novel tau positron emission tomography tracer [F-18]-AV-1451 (T807) on postmortem brain tissue. Ann. Neurol. 78, 787–800.
Masumiya, H., Tsujikawa, H., Hino, N., Ochi, R., 2003. Modulation of manganese currents by 1, 4-dihydropyridines, isoproterenol and forskolin in rabbit ventricular cells. Pflugers Arch. 446, 695–701.
Mathis, C.A., Wang, Y., Klunk, W.E., 2004. Imaging beta-amyloid plaques and neurofibrillary tangles in the aging human brain. Curr. Pharm. Des. 10, 1469–1492.
Pautler, R.G., 2004. In vivo, trans-synaptic tract-tracing utilizing manganese-enhanced magnetic resonance imaging (MEMRI). NMR Biomed. 17, 595–601.
Pautler, R.G., Koretsky, A.P., 2002. Tracing odor-induced activation in the olfactory bulbs of mice using manganese-enhanced magnetic resonance imaging. NeuroImage 16, 441–448.
Pautler, R.G., Silva, A.C., Koretsky, A.P., 1998. In vivo neuronal tract tracing using manganese-enhanced magnetic resonance imaging. Magn. Reson. Med. 40, 740–748.
Perez, P.D., Hall, G., Kimura, T., Ren, Y., Bailey, R.M., Lewis, J., Febo, M., Sahara, N., 2013. In vivo functional brain mapping in a conditional mouse model of human tauopathy (tau(P301L)) reveals reduced neural activity in memory formation structures. Mol. Neurodegener. 8, 9.
Ramsden, M., Kotilinek, L., Forster, C., Paulson, J., McGowan, E., SantaCruz, K., Guimaraes, A., Yue, M., Lewis, J., Carlson, G., Hutton, M., Ashe, K.H., 2005. Age-dependent neurofibrillary tangle formation, neuron loss, and memory impairment in a mouse model of human tauopathy (P301L). J. Neurosci. 25, 10637–10647.
Santacruz, K., Lewis, J., Spires, T., Paulson, J., Kotilinek, L., Ingelsson, M., Guimaraes, A., DeTure, M., Ramsden, M., McGowan, E., Forster, C., Yue, M., Orne, J., Janus, C., Mariash, A., Kuskowski, M., Hyman, B., Hutton, M., Ashe, K.H., 2005. Tau suppression in a neurodegenerative mouse model improves memory function. Science 309, 476–481.
Sastry, B.R., Goh, J.W., Auyeung, A., 1986. Associative induction of posttetanic and long-term potentiation in CA1 neurons of rat hippocampus. Science 232, 988–990.
Shineman, D.W., Basi, G.S., Bizon, J.L., Colton, C.A., Greenberg, B.D., Hollister, B.A., Lincecum, J., Leblanc, G.G., Lee, L.B., Luo, F., Morgan, D., Morse, I., Refolo, L.M., Riddell, D.R., Scearce-Levie, K., Sweeney, P., Yrjanheikki, J., Fillit, H.M., 2011. Accelerating drug discovery for Alzheimer's disease: best practices for preclinical animal studies. Alzheimer's Res. Ther. 3, 28.
Smith, K.D., Kallhoff, V., Zheng, H., Pautler, R.G., 2007. In vivo axonal transport rates decrease in a mouse model of Alzheimer's disease. NeuroImage 35, 1401–1408.
Vandsburger, M.H., French, B.A., Kramer, C.M., Zhong, X., Epstein, F.H., 2012. Displacement-encoded and manganese-enhanced cardiac MRI reveal that nNOS, not eNOS, plays a dominant role in modulating contraction and calcium influx in the mammalian heart. American journal of physiology. Heart Circul. Physiol. 302, H412–H419.
Weaver, C.L., Espinoza, M., Kress, Y., Davies, P., 2000. Conformational change as one of the earliest alterations of tau in Alzheimer's disease. Neurobiol. Aging 21, 719–727.